Coherent-Mode Representations in Optics

Andrey S. Ostrovsky

SPIE
PRESS
Bellingham, Washington USA

Library of Congress Cataloging-in-Publication Data

Ostrovsky, Andrey S.
Coherent-mode representations in optics / Andrey S. Ostrovsky.
p. cm. -- (SPIE monograph ; pm 164)
Includes bibliographical references and index.
ISBN 0-8194-6350-7
1. Coherence (Optics). 2. Physical optics. I. Title. II. Series.

QC476.C6O77 2006
535'.2--dc22 2006011409

Published by

SPIE—The International Society for Optical Engineering
P.O. Box 10
Bellingham, Washington 98227-0010 USA
Phone: +1 360 676 3290
Fax: +1 360 647 1445
Email: spie@spie.org
Web: http://spie.org

Printed in the United States of America.

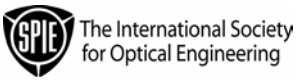

To the memory of my mother, Alla Burjinskaya Ostrovskaya,
and my father, Sergey Ostrovsky.

Contents

Preface

Everyone knows the fundamental role that the Fourier transform plays in optics, representing a monochromatic light field as a linear superposition of plane waves propagating in different directions. Perhaps, the coherent-mode representation of the optical field broached for the first time by H. Gamo in his *Matrix Treatment of Partial Coherence* (Progress in Optics III, E. Wolf, ed., North-Holland, Amsterdam, 1964), which was later developed by E. Wolf in his "New theory of partial coherence in the space-frequency domain" (*J. Opt. Soc. Am. A*, Vol. 72, No. 3, 1982, and Vol. 3, No. 1, 1986), plays a not less important role in contemporary optics. From a physical point of view, the coherent-mode representation describes an optical field of any state of coherence as a linear superposition of uncorrelated, completely coherent modes, a fact that gives new insight into the physics of generation, propagation, and transformation of optical radiation. From a mathematical standpoint, it expresses the cross-spectral density function of an optical field as a sum of terms that are separable in space, a fact that allows significant simplification of the analysis of statistical optical processes and systems. However, to my mind, the coherent-mode representation of optical fields, despite its power and attractiveness, has not yet found its due place in optical science and practice. This is affirmed, in particular, by a relatively small number of publications where the coherent-mode representation is treated. Even in a monumental treatise like *Optical Coherence and Quantum Optics* by L. Mandel and E. Wolf, less than two dozen pages are dedicated to this subject.

The present book represents a modest attempt to make up, to a certain extent, for a deficiency in possible applications of the coherent-mode representations in several areas of optics. This book is mainly based on the original results obtained by the author and his postgraduate students but, to ensure a thorough coverage of the total scope of the subject, it also contains some results of other authors, which are properly referenced. I tried to present this book in a brief recapitulative form, handy for both professionals and postgraduate students in physical optics. I hope that the book will be interesting for the reader and will stimulate the subsequent development of the coherent-mode representations in optics and their practical applications.

There are many people to whom I owe a special word of thanks for their help with the creation of this book. First of all, I consider it my pleasant duty to mention here the scientists whose publications had a decisive influence on the results presented in the book. Listed in alphabetical order, they are: G. S. Agarwal, W. Carter, J. Durnin, J. Duvernoy, J. T. Foley, A. T. Friberg, H. Gamo,

J. W. Goodman, F. Gory, G. Guattari, L. Mandel, E. W. Marchand, N. Mucunda, R. Martínez-Herrero, P. Mejías, M. Nieto-Vesperinas, C. Padovani, B. E. A. Saleh, R. Simon, K. Sundar, J. Turunen, J. van der Gracht, V. Vasara, A. Walther, and E. Wolf. I would also like to mention with gratitude my former postgraduate students, M. V. Rodríguez Solís, O. Ramos Romero, and J. C. Ramírez San-Juan, who are the coauthors of several of my papers used in this book. I am much indebted to Yulia Ostrovskaya and Philip J. Stabler for the excellent language redaction of the manuscript.

The main part of the writing was done at the Physics and Mathematics Department of the Autonomous University of Puebla, Mexico. I am grateful to M.Sc. E. Doger Guerrero, former rector of the university, M.Sc. E. Agüera Ibáñez, current rector, Dr. P. H. Hernández Tejeda, vice-rector, and Dr. C. Ramírez Romero, head of the department, for providing the excellent facilities for my work. Part of the text was prepared during my sabbatical leave at the National Institute of Astronomy, Optics, and Electronics, Mexico. I acknowledge my indebtedness to Dr. J. S. Guichard Romero, Director of the Institute, Dr. J. F. Soto Eguibar, Deputy Director, and G. Martínez Niconoff, former coordinator of the Optical Division, for their hospitality and fruitful collaboration. The work on the book was partially supported by the National Council for Science and Technology (CONACYT) of Mexico under the projects 3644-E, 25841-E, and 36875-E; this is much appreciated.

I acknowledge with thanks the excellent cooperation I received from the staff of SPIE Press at all stages of the production of this book. In particular, I wish to express my appreciation to Timothy Lamkins, Acquisitions Editor, and Sharon Streams, Press Manager, for their exceptional attention to my work.

Finally, I thank my wife, Marina, without whose patience, encouragement, and support this book would not have been possible.

Andrey S. Ostrovsky

Autonomous University of Puebla
Puebla, Mexico
May 2006

1

Coherent-Mode Representation of Optical Fields and Sources

1.1 Introduction

In the 1980s, E. Wolf proposed a new theory of partial coherence formulated in the space-frequency domain.[1,2] The fundamental result of this theory is the fact that a stationary optical field of any state of coherence may be represented as a superposition of coherent modes, i.e., elementary uncorrelated field oscillations that are spatially completely coherent.† The importance of this result can hardly be exaggerated since it opens a new perspective in understanding and interpreting the physics of generation, propagation, and transformation of optical radiation. In this chapter, using primarily the basic book by Mandel and Wolf,[4] we give an outline of the theory of optical coherence in the space-frequency domain and coherent-mode representations of an optical field. We also consider the concept of the effective number of modes needed for the coherent-mode representation of an optical field,[5] and give a brief survey of the known coherent-mode representations of some model sources, namely, the Gaussian Schell-model source ,[6–9] Bessel correlated source,[10] and the Lambertian source.[11]

1.2 Foundations of the Coherence Theory in the Space-Frequency Domain

Let us consider a scalar quasi-monochromatic optical field occupying some finite closed domain D. Let $V(\mathbf{r}, t)$ be the *complex analytic signal* associated with this field at a point specified by the position vector $\mathbf{r} = (x, y, z)$ and at time t. For any realistic optical field, $V(\mathbf{r}, t)$ is a fluctuating function of time, which may be regarded as a *sample realization* of some *random process*. Hence, in the general case, an optical field can only be described in statistical terms. Within the framework of the second-order moments theory of random processes, the statistical description of a fluctuating field is given by the *cross-correlation function* $\Gamma(\mathbf{r}_1, \mathbf{r}_2, t_1, t_2)$, defined as

$$\Gamma(\mathbf{r}_1, \mathbf{r}_2, t_1, t_2) = \left\langle V^*(\mathbf{r}_1, t_1)\, V(\mathbf{r}_2, t_2) \right\rangle, \tag{1.1}$$

†A similar result has been obtained in the past by H. Gamo in the framework of matrix treatment of partial coherence.[3]

where the asterisk denotes the complex conjugate and the angle brackets denote the average taken over an ensemble of all possible process realizations. The random field is said to be *stationary in the wide sense* if its cross-correlation function depends on the two time arguments only through their difference $\tau = t_2 - t_1$, i.e.,

$$\Gamma(\mathbf{r}_1, \mathbf{r}_2, \tau) = \left\langle V^*(\mathbf{r}_1, t)\, V(\mathbf{r}_2, t+\tau) \right\rangle. \tag{1.2}$$

The cross-correlation function $\Gamma(\mathbf{r}_1, \mathbf{r}_2, \tau)$ is known as the *mutual coherence function* and represents the central quantity of the *classical theory of optical coherence*. It may be noted that $\Gamma(\mathbf{r}_1, \mathbf{r}_2, \tau)$ describes an optical field in the *space-time domain*.

An alternative statistical description of an optical field may be obtained by assuming that $\Gamma(\mathbf{r}_1, \mathbf{r}_2, \tau)$ is absolutely integrable in the range $-\infty < \tau < \infty$ and, hence, may be represented by its Fourier transform

$$W(\mathbf{r}_1, \mathbf{r}_2, \nu) = \int_{-\infty}^{\infty} \Gamma(\mathbf{r}_1, \mathbf{r}_2, \tau) \exp(-\mathrm{i}2\pi\nu\tau)\, \mathrm{d}\tau, \tag{1.3}$$

where the Fourier variable ν has the meaning of frequency. The function $W(\mathbf{r}_1, \mathbf{r}_2, \nu)$ is known as the *cross-spectral density function* of the field and represents the central quantity of the *coherence theory in the space-frequency domain*.

We will now note a few important properties of the cross-spectral density function. In the first place, assuming that $W(\mathbf{r}_1, \mathbf{r}_2, \nu)$ is a continuous function of $\mathbf{r}_1$ and $\mathbf{r}_2$ bounded throughout the domain D, one necessarily finds that it is *square integrable in D*, i.e.,

$$\iint_D |W(\mathbf{r}_1, \mathbf{r}_2, \nu)|^2\, \mathrm{d}\mathbf{r}_1 \mathrm{d}\mathbf{r}_2 < \infty. \tag{1.4}$$

In the second place, $W(\mathbf{r}_1, \mathbf{r}_2, \nu)$ possesses *Hermitian symmetry*, i.e.,

$$W(\mathbf{r}_2, \mathbf{r}_1, \nu) = W^*(\mathbf{r}_1, \mathbf{r}_2, \nu), \tag{1.5}$$

which follows at once on taking the Fourier transform of both sides of the evident equality $\Gamma(\mathbf{r}_2, \mathbf{r}_1, -\tau) = \Gamma^*(\mathbf{r}_1, \mathbf{r}_2, \tau)$. In the third place, it may be shown (see Ref. 1, Appendix A) that $W(\mathbf{r}_1, \mathbf{r}_2, \nu)$ is a *nonnegative definite function*, i.e.,

$$\iint_D W(\mathbf{r}_1, \mathbf{r}_2, \nu)\, f^*(\mathbf{r}_1)\, f(\mathbf{r}_2)\, \mathrm{d}\mathbf{r}_1 \mathrm{d}\mathbf{r}_2 \geqslant 0, \tag{1.6}$$

where $f(\mathbf{r})$ is any square-integrable function.

In the particular case when $\mathbf{r}_1 = \mathbf{r}_2 = \mathbf{r}$, the cross-spectral density function becomes the *spectral density*

$$S(\mathbf{r}, \nu) = W(\mathbf{r}, \mathbf{r}, \nu). \tag{1.7}$$

Inequality (1.6), together with definition (1.7), implies that

$$S(\mathbf{r}, \nu) \geqslant 0 \tag{1.8}$$

and

$$|W(\mathbf{r}_1, \mathbf{r}_2, \nu)| \leqslant [S(\mathbf{r}_1, \nu)]^{1/2} [S(\mathbf{r}_2, \nu)]^{1/2}. \tag{1.9}$$

In view of inequality (1.9), the normalized cross-spectral density function may be defined as

$$\mu(\mathbf{r}_1, \mathbf{r}_2, \nu) = \frac{W(\mathbf{r}_1, \mathbf{r}_2, \nu)}{[S(\mathbf{r}_1, \nu)]^{1/2} [S(\mathbf{r}_2, \nu)]^{1/2}}, \tag{1.10}$$

known as the *spectral degree of coherence*. The following relation for $\mu(\mathbf{r}_1, \mathbf{r}_2, \nu)$ is obvious:

$$0 \leqslant |\mu(\mathbf{r}_1, \mathbf{r}_2, \nu)| \leqslant 1. \tag{1.11}$$

When $|\mu| = 0$ for each pair of different points $\mathbf{r}_1$ and $\mathbf{r}_2$, the field is referred to as *completely incoherent*; when $|\mu| = 1$, as *completely coherent*; and when $0 < |\mu| < 1$, as *partially coherent* in space.

We will now consider the propagation of the cross-spectral density in *free space*, i.e., in the space that does not contain any sources or absorbers. As is well known,[4] the mutual coherence function $\Gamma(\mathbf{r}_1, \mathbf{r}_2, \tau)$ satisfies, in free space, the two *wave equations*

$$\nabla_1^2 \Gamma(\mathbf{r}_1, \mathbf{r}_2, \tau) = \frac{1}{c^2} \frac{\partial^2}{\partial \tau^2} \Gamma(\mathbf{r}_1, \mathbf{r}_2, \tau), \tag{1.12a}$$

$$\nabla_2^2 \Gamma(\mathbf{r}_1, \mathbf{r}_2, \tau) = \frac{1}{c^2} \frac{\partial^2}{\partial \tau^2} \Gamma(\mathbf{r}_1, \mathbf{r}_2, \tau), \tag{1.12b}$$

where $\nabla_{1(2)}^2$ is the Laplacian operator taken with respect to the point $\mathbf{r}_{1(2)}$, and c is the speed of light in a vacuum. Then, taking the Fourier transform of Eqs. (1.12) with respect to variable τ, we find that the cross-spectral density $W(\mathbf{r}_1, \mathbf{r}_2, \nu)$ propagates in free space in accordance with the *coupled Helmholtz equations*

$$\nabla_1^2 W(\mathbf{r}_1, \mathbf{r}_2, \nu) + k^2 W(\mathbf{r}_1, \mathbf{r}_2, \nu) = 0, \tag{1.13a}$$

$$\nabla_2^2 W(\mathbf{r}_1, \mathbf{r}_2, \nu) + k^2 W(\mathbf{r}_1, \mathbf{r}_2, \nu) = 0, \tag{1.13b}$$

where $k = 2\pi\nu/c$ is the wave number. Furthermore, it will be useful to find the solution of these equations for the case when an optical field propagates into a half-space $z > 0$ with the known boundary values of cross-spectral density at all pairs of points $\mathbf{x}_1 = (x_1, y_1)$ and $\mathbf{x}_2 = (x_2, y_2)$ in the plane $z = 0$ (Fig. 1.1). The

solution of Eq. (1.13b) for fixed $\mathbf{r}_1$ is given by *Rayleigh's first diffraction formula*[4] as

$$W(\mathbf{r}_1, \mathbf{r}_2, \nu) = -\frac{1}{2\pi} \int_{(z=0)} W(\mathbf{r}_1, \mathbf{x}_2, \nu) \frac{\partial}{\partial z_2} \left[\frac{\exp(\mathrm{i}kR_2)}{R_2} \right] \mathrm{d}\mathbf{x}_2, \tag{1.14}$$

where $R_2 = |\mathbf{r}_2 - \mathbf{x}_2|$. The solution of Eq. (1.13a) for $\mathbf{r}_2 = \mathbf{x}_2$ is consequently given by

$$W(\mathbf{r}_1, \mathbf{x}_2, \nu) = -\frac{1}{2\pi} \int_{(z=0)} W(\mathbf{x}_1, \mathbf{x}_2, \nu) \frac{\partial}{\partial z_1} \left[\frac{\exp(-\mathrm{i}kR_1)}{R_1} \right] \mathrm{d}\mathbf{x}_1, \tag{1.15}$$

where $R_1 = |\mathbf{r}_1 - \mathbf{x}_1|$. On inserting Eq. (1.15) into Eq. (1.14), we obtain the following joint solution of Eqs. (1.13):

$$W(\mathbf{r}_1, \mathbf{r}_2, \nu) = \frac{1}{(2\pi)^2} \iint_{(z=0)} W(\mathbf{x}_1, \mathbf{x}_2, \nu) \times \frac{\partial}{\partial z_1} \left[\frac{\exp(-\mathrm{i}kR_1)}{R_1} \right] \frac{\partial}{\partial z_2} \left[\frac{\exp(\mathrm{i}kR_2)}{R_2} \right] \mathrm{d}\mathbf{x}_1 \mathrm{d}\mathbf{x}_2. \tag{1.16}$$

Calculating the derivatives in Eq. (1.16) and assuming that $(1/r_{1(2)}) \ll k$, one may readily find the following approximate expression for propagation of the cross-spectral density into the half-space:

$$W(\mathbf{r}_1, \mathbf{r}_2, \nu) = \left(\frac{k}{2\pi} \right)^2 \iint_{(z=0)} W(\mathbf{x}_1, \mathbf{x}_2, \nu) \times \frac{\exp[\mathrm{i}k(R_2 - R_1)]}{R_1 R_2} \cos\theta_1 \cos\theta_2 \mathrm{d}\mathbf{x}_1 \mathrm{d}\mathbf{x}_2. \tag{1.17}$$

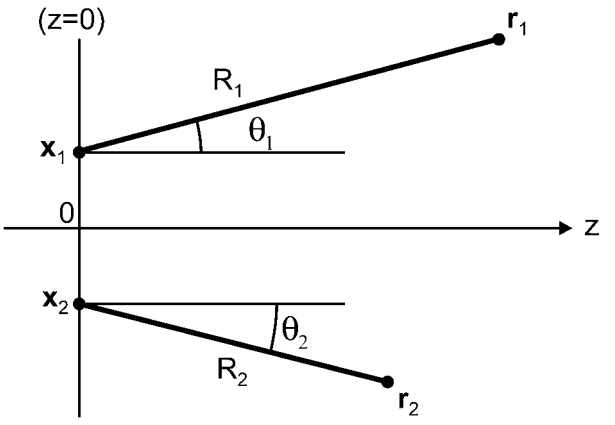

Figure 1.1 Notation relating to the propagation of the cross-spectral density function from the plane $z = 0$ into the half-space $z > 0$.

1.3 Coherent-Mode Structure of the Field

As is well known from the theory of integral equations, any continuous function that satisfies conditions (1.4)–(1.6) and, hence, the cross-spectral density $W(\mathbf{r}_1, \mathbf{r}_2, \nu)$, may be expressed in the form of *Mercer's expansion* as

$$W(\mathbf{r}_1, \mathbf{r}_2, \nu) = \sum_n \lambda_n(\nu)\, \varphi_n^*(\mathbf{r}_1, \nu)\, \varphi_n(\mathbf{r}_2, \nu), \tag{1.18}$$

where $\lambda_n(\nu)$ are the *eigenvalues* and $\varphi_n(\mathbf{r}, \nu)$ are the *eigenfunctions* of the *homogeneous Fredholm integral equation of the second kind*,

$$\int_D W(\mathbf{r}_1, \mathbf{r}_2, \nu)\, \varphi_n(\mathbf{r}_1, \nu)\, \mathrm{d}\mathbf{r}_1 = \lambda_n(\nu)\, \varphi_n(\mathbf{r}_2, \nu). \tag{1.19}$$

It is important to stress that all the eigenvalues $\lambda_n(\nu)$ are real and nonnegative, i.e.,

$$\lambda_n^*(\nu) = \lambda_n(\nu) \geqslant 0, \tag{1.20}$$

and the eigenfunctions $\varphi_n(\mathbf{r}, \nu)$ are mutually orthonormal in D (if it is not already so, this may be achieved using the Gram-Schmidt procedure), i.e.,

$$\int_D \varphi_n^*(\mathbf{r}, \nu)\, \varphi_m(\mathbf{r}, \nu)\, \mathrm{d}\mathbf{r} = \delta_{nm}, \tag{1.21}$$

where δ_{nm} is the Kronecker symbol. It is appropriate to ascertain one more property of the eigenfunctions $\varphi_n(\mathbf{r}, \nu)$. On inserting Eq. (1.18) into Eq. (1.13b), we obtain

$$\sum_n \lambda_n(\nu)\, \varphi_n^*(\mathbf{r}_1, \nu)\, \nabla_2^2 \varphi_n(\mathbf{r}_2, \nu) + k^2 \sum_n \lambda_n(\nu)\, \varphi_n^*(\mathbf{r}_1, \nu)\, \varphi_n(\mathbf{r}_2, \nu) = 0. \tag{1.22}$$

Next, multiplying Eq. (1.22) by $\varphi_m(\mathbf{r}_1, \nu)$, integrating the result with respect to $\mathbf{r}_1$ over the domain D, and making use of the orthonormality relation (1.21), we find that the eigenfunctions $\varphi_n(\mathbf{r}, \nu)$ satisfy the Helmholtz equation,

$$\nabla^2 \varphi_n(\mathbf{r}, \nu) + k^2 \varphi_n(\mathbf{r}, \nu) = 0. \tag{1.23}$$

To clear up the physical meaning of expansion (1.18), we rewrite it in the form

$$W(\mathbf{r}_1, \mathbf{r}_2, \nu) = \sum_n \lambda_n(\nu)\, W_n(\mathbf{r}_1, \mathbf{r}_2, \nu), \tag{1.24}$$

where

$$W_n(\mathbf{r}_1, \mathbf{r}_2, \nu) = \varphi_n^*(\mathbf{r}_1, \nu)\, \varphi_n(\mathbf{r}_2, \nu). \tag{1.25}$$

It follows directly from Eqs. (1.23) and (1.25) that the function $W_n(\mathbf{r}_1, \mathbf{r}_2, \nu)$ satisfies the equations

$$\nabla_1^2 W_n(\mathbf{r}_1, \mathbf{r}_2, \nu) + k^2 W_n(\mathbf{r}_1, \mathbf{r}_2, \nu) = 0, \tag{1.26a}$$

$$\nabla_2^2 W_n(\mathbf{r}_1, \mathbf{r}_2, \nu) + k^2 W_n(\mathbf{r}_1, \mathbf{r}_2, \nu) = 0, \tag{1.26b}$$

which are just the same as those governing the free-space propagation of the cross-spectral density $W(\mathbf{r}_1, \mathbf{r}_2, \nu)$. Hence, the function $W_n(\mathbf{r}_1, \mathbf{r}_2, \nu)$ may be regarded as the cross-spectral density associated with a *mode* of the field. Next, making use of Eqs. (1.10) and (1.25), we find that the spectral degree of coherence of each field mode is given by

$$\mu_n(\mathbf{r}_1, \mathbf{r}_2, \nu) = \frac{\varphi_n^*(\mathbf{r}_1, \nu)\, \varphi_n(\mathbf{r}_2, \nu)}{|\varphi_n(\mathbf{r}_1, \nu)|\, |\varphi_n(\mathbf{r}_2, \nu)|}. \tag{1.27}$$

It follows from Eq. (1.27) that

$$|\mu_n(\mathbf{r}_1, \mathbf{r}_2, \nu)| = 1, \tag{1.28}$$

i.e., that each field mode represents the spatially completely coherent contribution. Thus, *expansion (1.24) may be interpreted as representing the cross-spectral density of the field as a superposition of contributions from modes that are completely coherent in the space-frequency domain*. For this reason, we will refer to expansion (1.18) as the *coherent-mode representation of the field*. We will also refer to the set

$$\Lambda = \{\lambda_n(\nu), \varphi_n(\mathbf{r}, \nu)\} \tag{1.29}$$

as the *coherent-mode structure of the field*. In the special case when the integral equation (1.19) admits only one solution $\varphi(\mathbf{r}, \nu)$ associated with an eigenvalue $\lambda(\nu)$, Eq. (1.18) takes the form

$$W(\mathbf{r}_1, \mathbf{r}_2, \nu) = \lambda(\nu)\, \varphi^*(\mathbf{r}_1, \nu)\, \varphi(\mathbf{r}_2, \nu), \tag{1.30}$$

which implies that the field consists of the sole coherent mode, i.e., that it is spatially completely coherent at frequency ν.

Equation (1.18) allows us to obtain some other useful coherent-mode representations. Indeed, on making use of representation (1.18) in definition (1.7), we obtain the relation

$$S(\mathbf{r}, \nu) = \sum_n \lambda_n(\nu)\, |\varphi_n(\mathbf{r}, \nu)|^2. \tag{1.31}$$

On integrating Eq. (1.31) over D with due regard for Eq. (1.21), we come to the relation

$$\int_D S(\mathbf{r}, \nu)\, \mathrm{d}\mathbf{r} = \sum_n \lambda_n(\nu). \tag{1.32}$$

On making use of definition (1.25) and Eq. (1.21), we obtain the following orthonormality relation:

$$\iint_D W_n^* (\mathbf{r}_1, \mathbf{r}_2, \nu)\, W_m (\mathbf{r}_1, \mathbf{r}_2, \nu)\, \mathrm{d}\mathbf{r}_1 \mathrm{d}\mathbf{r}_2 = \delta_{nm}. \tag{1.33}$$

Finally, applying the relation

$$|W (\mathbf{r}_1, \mathbf{r}_2, \nu)|^2 = \sum_n \sum_m \lambda_n (\nu)\, \lambda_m (\nu)\, W_n^* (\mathbf{r}_1, \mathbf{r}_2, \nu)\, W_m (\mathbf{r}_1, \mathbf{r}_2, \nu)\,, \tag{1.34}$$

obtained directly from definition (1.25), and integrating its both sides twice over the domain D with due regard for relation (1.33), we find that

$$\iint_D |W (\mathbf{r}_1, \mathbf{r}_2, \nu)|^2\, \mathrm{d}\mathbf{r}_1 \mathrm{d}\mathbf{r}_2 = \sum_n \lambda_n^2 (\nu)\,. \tag{1.35}$$

The deduced modal relations (1.31), (1.32), and (1.35), as well as the basic coherent-mode representation (1.18), will be widely used in our subsequent considerations.

1.4 Ensemble Representation of the Cross-Spectral Density Function

On making use of the coherent-mode representation (1.18), one may deduce another useful representation of the cross-spectral density function expressed in terms of the ensemble of field realizations.

Let us construct a random function of the form

$$U (\mathbf{r}, \nu) = \sum_n a_n (\nu)\, \varphi_n (\mathbf{r}, \nu)\,, \tag{1.36}$$

where $\varphi_n(\mathbf{r}, \nu)$ are, as before, the eigenfunctions of Eq. (1.19) and $a_n(\nu)$ are some random variables that will be specified later. Since, as follows from Eq. (1.23), each term in expansion (1.36) satisfies the Helmholtz equation, the function $U(\mathbf{r}, \nu)$ does the same, i.e.,

$$\nabla^2 U (\mathbf{r}, \nu) + k^2 U (\mathbf{r}, \nu) = 0. \tag{1.37}$$

Hence, the function $U(\mathbf{r}, \nu)$ may be considered as an *optical signal*, i.e., the time-independent part of a monochromatic wave function

$$V (\mathbf{r}, t) = U (\mathbf{r}, \nu) \exp (-\mathrm{i}2\pi\nu t)\,. \tag{1.38}$$

The cross-correlation function of the optical signal (1.36) at two points $\mathbf{r}_1$ and $\mathbf{r}_2$ is given by

$$\left\langle U^*(\mathbf{r}_1,\nu)\,U(\mathbf{r}_2,\nu)\right\rangle = \sum_n \sum_m \left\langle a_n^*(\nu)\,a_m(\nu)\right\rangle \varphi^*(\mathbf{r}_1,\nu)\,\varphi(\mathbf{r}_2,\nu)\,, \tag{1.39}$$

where the angle brackets, unlike those used in Eq. (1.1), this time denote the statistical averaging over an ensemble of frequency-dependent (not time-dependent) realizations.

Let us now assume that the random variables $a_n(\nu)$ are chosen to satisfy the condition

$$\left\langle a_n^*(\nu)\,a_m(\nu)\right\rangle = \lambda_n(\nu)\,\delta_{nm}, \tag{1.40}$$

where $\lambda_n(\nu)$ are, as before, the eigenvalues of Eq. (1.19). The condition (1.40) can be satisfied, for example, by taking

$$a_n(\nu) = [\lambda_n(\nu)]^{1/2}\exp(\mathrm{i}\theta_n)\,, \tag{1.41}$$

where θ_n are statistically independent random variables uniformly distributed in the interval $[0, 2\pi]$. Applying condition (1.40) to Eq. (1.39), we obtain

$$\left\langle U^*(\mathbf{r}_1,\nu)\,U(\mathbf{r}_2,\nu)\right\rangle = \sum_n \lambda_n(\nu)\,\varphi_n^*(\mathbf{r}_1,\nu)\,\varphi_n(\mathbf{r}_2,\nu)\,. \tag{1.42}$$

Finally, comparing Eqs. (1.42) and (1.18), we come to a new representation of the cross-spectral density function in the form

$$W(\mathbf{r}_1,\mathbf{r}_2,\nu) = \left\langle U^*(\mathbf{r}_1,\nu)\,U(\mathbf{r}_2,\nu)\right\rangle. \tag{1.43}$$

This ensemble representation may be considered as *an alternative definition of the cross-spectral density function* $W(\mathbf{r}_1,\mathbf{r}_2,\nu)$ *in the form of the cross-correlation function of the optical signal given by* Eq. (1.36) *with condition* (1.40). Applying this definition, we may obtain a new representation of the spectral density $S(\mathbf{r},\nu)$,

$$S(\mathbf{r},\nu) = \left\langle |U(\mathbf{r},\nu)|^2\right\rangle. \tag{1.44}$$

This representation clearly shows that spectral density represents the spatial distribution of an average squared modulus of monochromatic oscillations and, hence, $S(\mathbf{r},\nu)$ may be referred to as the *power spectrum* of an optical field.

1.5 Effective Number of Coherent Modes

We will inquire now about the number of coherent modes needed to represent a random field in D. To do this, we use the concept of the *effective number of coherent modes* introduced in Ref. 5.

As follows from Section 1.3, the eigenvalues $\lambda_n(\nu)$ may be arranged in a non-increasing sequence as

$$\lambda_0(\nu) \geqslant \lambda_1(\nu) \geqslant \lambda_2(\nu) \geqslant \cdots \geqslant \lambda_n(\nu) \geqslant \cdots \geqslant 0. \tag{1.45}$$

Hence, one may equate each of the lowest-order eigenvalues in Eq. (1.32) with $\lambda_0(\nu)$, and take the rest to be equal to zero. This allows the following definition of the effective number $\mathcal{N}(\nu)$ of coherent modes needed to represent the field:

$$\mathcal{N}(\nu) \equiv \frac{1}{\lambda_0(\nu)} \sum_{n=0}^{\infty} \lambda_n(\nu). \tag{1.46}$$

As can be seen, the number $\mathcal{N}(\nu)$ is, in general, noninteger; but for convenience, in practice it may be approximated by its integer part. It is obvious that the number $\mathcal{N}(\nu)$ depends on the statistical properties of the field. To estimate its upper bound, we use the inequality

$$\sum_{n=0}^{\infty} \left(\frac{\lambda_n(\nu)}{\lambda_0(\nu)} \right)^2 \leqslant \sum_{n=0}^{\infty} \frac{\lambda_n(\nu)}{\lambda_0(\nu)}, \tag{1.47}$$

which is true in view of relation (1.45). From this inequality we obtain a lower bound on the value $\lambda_0(\nu)$ as

$$\lambda_0(\nu) \geqslant \frac{\sum_{n=0}^{\infty} \lambda_n^2(\nu)}{\sum_{n=0}^{\infty} \lambda_n(\nu)}. \tag{1.48}$$

On making use of Eqs. (1.48) and (1.46), we find the upper bound on the number $\mathcal{N}(\nu)$ to be

$$\mathcal{N}(\nu) \leqslant \frac{\left(\sum_{n=0}^{\infty} \lambda_n(\nu) \right)^2}{\sum_{n=0}^{\infty} \lambda_n^2(\nu)}. \tag{1.49}$$

Finally, to express the upper bound on the effective number of coherent modes needed to represent the field in terms of the cross-spectral density, we apply the

modal relations (1.32) and (1.35) into Eq. (1.49) to obtain

$$\mathcal{N}(\nu) \leqslant \frac{\left(\int_D S(\mathbf{r},\nu)\,\mathrm{d}\mathbf{r}\right)^2}{\iint_D |W(\mathbf{r}_1,\mathbf{r}_2,\nu)|^2\,\mathrm{d}\mathbf{r}_1\mathrm{d}\mathbf{r}_2}. \tag{1.50}$$

To clarify the physical meaning of the obtained result, in Ref. 5 the following definitions of the *effective volume of the field* and the *effective coherence volume* are introduced, respectively:

$$\mathcal{V}_{\mathrm{e}}(\nu) = \frac{1}{S_{\max}(\boldsymbol{\nu})}\int_D S(\mathbf{r},\nu)\,\mathrm{d}\mathbf{r}, \tag{1.51}$$

$$\mathcal{V}_{\mathrm{ce}}(\nu) = \frac{1}{\mathcal{V}_{\mathrm{e}}(\nu)S^2_{\max}(\boldsymbol{\nu})}\iint_D |W(\mathbf{r}_1,\mathbf{r}_2,\nu)|^2\,\mathrm{d}\mathbf{r}_1\mathrm{d}\mathbf{r}_2, \tag{1.52}$$

where

$$S_{\max}(\boldsymbol{\nu}) = \max_{\mathbf{r}\in D} S(\mathbf{r},\nu). \tag{1.53}$$

By applying definitions (1.51) and (1.52) into Eq. (1.50), we obtain

$$\mathcal{N}(\nu) \leqslant \frac{\mathcal{V}_{\mathrm{e}}(\nu)}{\mathcal{V}_{\mathrm{ce}}(\nu)}. \tag{1.54}$$

Thus, *the more incoherent is the field, the more coherent modes are needed for its representation*.

Concluding this section, we note that the effective number $\mathcal{N}(\nu)$ of coherent modes may be used in practice to establish an optimal point for truncating the modal representation (1.18).

1.6 Coherent-Mode Representations of Some Model Sources

The mode representation of the field considered in Section 1.3 may be applied without any changes for describing the optical source, which can be a primary or a secondary one. Furthermore, this representation may be used for many infinite sources. To find the coherent-mode structure of the source, it is necessary to solve the integral equation (1.19) with the kernel given by the cross-spectral density $W(\mathbf{r}_1,\mathbf{r}_2,\nu)$ of the true source distribution (in the case of a primary source) or the field distribution across the source (in the case of a secondary source). Unfortunately, the solutions of this equation in a closed form are obtained at present only for a very limited number of source models. A brief review of the main known solutions of the integral equation (1.19) is given below.

1.6.1 Gaussian Schell-model source

A partially coherent planar source is said to be of the *Schell-model class* if its cross-spectral density function has the form

$$W(\mathbf{x}_1, \mathbf{x}_2, \nu) = [S(\mathbf{x}_1, \nu)]^{1/2} [S(\mathbf{x}_2, \nu)]^{1/2} \mu(\mathbf{x}_1 - \mathbf{x}_2, \nu), \tag{1.55}$$

where, as can be seen, the spectral degree of coherence $\mu(\nu)$ depends on the difference of coordinates $\mathbf{x}_1$ and $\mathbf{x}_2$. If the power spectrum and the spectral degree of coherence have the form of Gaussian functions, i.e.,

$$S(\mathbf{x}, \nu) = S(0, \nu) \exp\left[-\frac{\mathbf{x}^2}{2\sigma_S^2(\nu)}\right], \tag{1.56}$$

$$\mu(\mathbf{x}_1 - \mathbf{x}_2, \nu) = \exp\left[-\frac{(\mathbf{x}_1 - \mathbf{x}_2)^2}{2\sigma_\mu^2(\nu)}\right], \tag{1.57}$$

where $\sigma_S(\nu)$ and $\sigma_\mu(\nu)$ are positive constants, such a source is referred to as the Gaussian Schell-model source. The parameters $\sigma_S(\nu)$ and $\sigma_\mu(\nu)$ may be interpreted as the rms width of the power spectrum distribution across the source and the rms width of the spectral degree of coherence, respectively. The ratio of rms widths

$$\gamma(\nu) = \frac{\sigma_\mu(\nu)}{\sigma_S(\nu)} \tag{1.58}$$

may be regarded as a measure of the *degree of global coherence* of the Gaussian Schell-model source.

The coherent-mode structure of 1D Gaussian Schell-model source has been constructed in Refs. 6 and 7 and has the following form:

$$\varphi_n(x, \nu) = \left(\frac{2c}{\pi}\right)^{1/4} \frac{1}{\sqrt{2^n n!}} H_n\left(x\sqrt{2c}\right) \exp\left(-cx^2\right), \tag{1.59}$$

$$\lambda_n(\nu) = S(0, \nu) \left(\frac{\pi}{a+b+c}\right)^{1/2} \left(\frac{b}{a+b+c}\right)^n, \tag{1.60}$$

where

$$a = \frac{1}{4\sigma_S^2(\nu)}, \qquad b = \frac{1}{2\sigma_\mu^2(\nu)}, \qquad c = \left(a^2 + 2ab\right)^{1/2}, \tag{1.61}$$

and H_n is the Hermite polynomial of order n. The upper bound on the effective number of coherent modes (1.50) needed to represent the 1D Gaussian Schell-model source has been calculated in Ref. 5 and is given by

$$\mathcal{N}(\nu) \leqslant \left[1 + \frac{4}{\gamma^2(\nu)}\right]^{1/2}. \tag{1.62}$$

In Ref. 8, the considered results are generalized for the case of a 2D Gaussian Schell-model source. In Ref. 9, the reader can find the coherent-mode structure for a special class of 2D Gaussian Schell-model sources with an additional new type of phase, the so-called *twist phase*, in their cross-spectral density function.

1.6.2 Bessel-correlated source

In Ref. 10 was introduced a new class of partially coherent sources described by the cross-spectral density function of the form

$$W(\mathbf{x}_1, \mathbf{x}_2, \nu) = [S(r_1, \nu)]^{1/2} [S(r_2, \nu)]^{1/2} \times J_0\left\{\beta(\nu)\left[r_1^2 + r_2^2 - 2r_1 r_2 \cos(\theta_1 - \theta_2)\right]^{1/2}\right\}, \tag{1.63}$$

where r and θ are the polar coordinates in the source plane, J_0 is the Bessel function of the first kind and of zero order, and β is a constant whose meaning will be discussed later. The source with $W(\mathbf{x}_1, \mathbf{x}_2, \nu)$, given by Eq. (1.63), belongs to the Schell-model class and may, for brevity, be referred to as the *Bessel-correlated source*. The coherent-mode structure of this source has the following form:

$$\varphi_n(r, \theta, \nu) = \frac{1}{\sqrt{\lambda_n}} [S(r, \nu)]^{1/2} \times \left\{a_n J_n[\beta(\nu) r] \exp(-\mathrm{i}n\theta) + b_n J_{-n}[\beta(\nu) r] \exp(\mathrm{i}n\theta)\right\}, \tag{1.64}$$

$$\lambda_n(\nu) = 2\pi \int_0^\infty S(r, \nu) J_0^2[\beta(\nu) r] r \mathrm{d}r, \tag{1.65}$$

where the ratio a_n/b_n is arbitrary. It is important to note that there is a twofold degeneracy for the eigenfunctions $\varphi_n(r, \theta, \nu)$, except for the case $n = 0$.

The preceding results hold, whatever the power spectrum $S(r, \nu)$ is. In the particular case when

$$S(r, \nu) = \begin{cases} S(0, \nu) & \text{for } 0 \leqslant r \leqslant R \\ 0 & \text{for } r > R \end{cases}, \tag{1.66}$$

the eigenvalues $\lambda_n(\nu)$ defined by Eq. (1.63) take the form

$$\lambda_n(\nu) = \pi R^2 S_0(\nu) \left\{ J_n^2[\beta(\nu) R] - J_{n-1}[\beta(\nu) R] J_{n+1}[\beta(\nu) R] \right\}. \quad (1.67)$$

In another particular case, when

$$S(r, \nu) = S(0, \nu) \exp\left[-\frac{2r^2}{\sigma_S^2(\nu)} \right], \quad (1.68)$$

the eigenvalues $\lambda_n(\nu)$ are

$$\lambda_n(\nu) = \frac{\pi \sigma_S^2(\nu)}{2} S(0, \nu) \exp\left[\frac{-\beta^2(\nu) \sigma_S^2(\nu)}{4} \right] I_n\left[\frac{\beta^2(\nu) \sigma_S^2(\nu)}{4} \right], \quad (1.69)$$

where I_n is the modified Bessel function of order n. It may be noted that in both cases the dimensionless parameters $\beta(\nu)R$ and $\beta(\nu)\sigma_S(\nu)$ have the meaning of a measure of the degree of global coherence of the Bessel-correlated source.

1.6.3 Lambertian source

As is well known, the *Lambertian source* is a planar source, which radiates the optical energy with angular density that follows a $\cos\theta$ law, where θ is the angle between the direction of observation and the normal to the source. According to Ref. 11, the cross-spectral density function of a 1D Lambertian source may be approximated by

$$W(x_1, x_2, \nu) = \frac{\pi C(\nu)}{L} J_0[k(x_1 - x_2)], \quad (1.70)$$

where $C(\nu)$ is a positive constant, L is the length of the source, and k is the wave number associated with frequency ν. It has been shown that the coherent-mode structure of such a source in the limit $kL \gg 1$ (the case of a large source) may be approximated by the following expressions:

$$\varphi_n(x, \nu) = \frac{1}{\sqrt{L}} \exp\left(\pm i n \frac{2\pi}{L} x \right), \quad (1.71)$$

$$\lambda_n(\nu) = \begin{cases} [2\pi C(\nu)/L] \left[k^2 - n^2 (2\pi/L)^2 \right]^{-1/2} & \text{for } n \leqslant kL/2\pi, \\ 0 & \text{for } n > kL/2\pi. \end{cases} \quad (1.72)$$

As can be seen, there is a twofold degeneracy for the eigenfunctions $\varphi_n(x, \nu)$, except for the case $n = 0$. The total number of coherent modes (not the effective

number $\mathcal{N}$, as previously discussed) needed to represent the 1D Lambertian source is seen to be given by

$$M \approx 2\left(\frac{kL}{2\pi}\right) + 1. \tag{1.73}$$

1.7 Concluding Remarks

The coherent-mode representation of cross-spectral density function gives a new insight into the physical nature of the partially coherent optical field as a superposition of completely spatially coherent and mutually uncorrelated modes. This brings a new understanding of the processes of generating, propagating, and transforming optical radiation. From a mathematical standpoint, coherent-mode representation expresses the cross-spectral density function of an optical field as a linear combination of terms that are separable in space, a fact that allows significant simplification of the analysis of statistical optical processes and systems. Both these facts make coherent-mode representation of optical fields and sources an essential tool in optical science and practice.

For the sake of simplicity, we limited our considerations to those within the framework of classical scalar electromagnetic theory because it is quite sufficient for many important applications and because vectorial mode analysis is still being developed. We have also restricted our considerations within the second-order coherence theory. Information on coherent-mode representations within higher-order coherence theory may be found in Ref. 2.

2

Coherent-Mode Representation of Optical Systems

2.1 Introduction

Linear system theory has been successfully employed for describing optical systems.[12,13] Within the framework of the linear system approach, the output of an optical system $g(\mathbf{x}')$ and its input $f(\mathbf{x})$ are related by a linear transformation of the general form

$$g\left(\mathbf{x}'\right) = \int_{-\infty}^{\infty} f\left(\mathbf{x}\right) h\left(\mathbf{x}', \mathbf{x}\right) \mathrm{d}\mathbf{x}, \tag{2.1}$$

where $h(\mathbf{x}, \mathbf{x}')$ is the so-called *impulse response* of the system, i.e., the output at $\mathbf{x}'$ resulting from the impulse input at point $\mathbf{x}$. Such a linear transformation describes an optical system with both completely coherent and completely incoherent illumination. In the first case, $f(\mathbf{x})$ and $g(\mathbf{x}')$ have the meaning of light intensities; while in the second case, they should be considered as the complex amplitudes of an optical field. At the same time, as it has been shown first by Gamo[3] and then by Thompson,[14] when partially coherent illumination is used, an optical system exhibits an essential nonlinear nature. In this case, to describe an optical system, one must apply the basic ideas from nonlinear system theory.

The output $g(\mathbf{x}')$ of any nonlinear system can be expressed as a functional of the input signal $f(\mathbf{x})$, which is represented by the Volterra series[15,16]

$$g\left(\mathbf{x}'\right) = q_0\left(\mathbf{x}'\right) + \sum_{n=1}^{\infty} \int \cdots \int_{-\infty}^{\infty} f\left(\mathbf{x}_1\right) \ldots f\left(\mathbf{x}_n\right) q_n\left(\mathbf{x}', \mathbf{x}_1, \ldots, \mathbf{x}_n\right) \mathrm{d}\mathbf{x}_1 \ldots \mathrm{d}\mathbf{x}_n, \tag{2.2}$$

where $q_n(\mathbf{x}'; \mathbf{x}_1, \ldots, \mathbf{x}_n)$ denotes the nth-order Volterra kernel of the system. Saleh[17] showed that many optical systems and processes can be represented either exactly or approximately by the third term of this series, i.e.,

$$g\left(\mathbf{x}'\right) = \iint_{-\infty}^{\infty} f^*\left(\mathbf{x}_1\right) f\left(\mathbf{x}_2\right) q_2\left(\mathbf{x}', \mathbf{x}_1, \mathbf{x}_2\right) \mathrm{d}\mathbf{x}_1 \mathrm{d}\mathbf{x}_2. \tag{2.3}$$

The transformation described by Eq. (2.3) is referred to as a *bilinear transform* and the corresponding nonlinear system is called a *bilinear system*. The second-order Volterra kernel $q_2(\mathbf{x}', \mathbf{x}_1, \mathbf{x}_2)$ represents the response of the system to two

impulses located at points $\mathbf{x}_1$ and $\mathbf{x}_2$ and, hence, may be referred to as a *double-impulse response*. A comprehensive analysis of the properties of a double-impulse response for various optical systems is given in Ref. 17.

The bilinear transform (2.3) can be successfully used to describe any optical system with partially coherent illumination,[18] but the complexity of the second-order Volterra kernel $q_2(\mathbf{x}, \mathbf{x}'_1, \mathbf{x}'_2)$, which is a 6D complex function, makes such a description too cumbersome. Several attempts have been made to reduce the description of an optical system with partially coherent illumination,[19–25] but the problem remained still far from its complete solution. Recently, employing the coherent-mode representation of the illumination field, we have succeeded in significantly reducing the description of a partially coherent optical system, and have proposed an effective technique for calculating the power spectrum at its output.[26–32] These results are presented in the subsequent sections.

2.2 Bilinear Systems in Optics

Let us consider an elementary optical system with a single positive lens, shown in Fig. 2.1. For an *object*, we will consider a thin plane transmitting screen, which affects the amplitude of the incident optical field in accordance with a complex function $t_o(\mathbf{x})$ referred to as an *amplitude transmittance*. We will assume that the object is illuminated by a stochastic quasi-monochromatic scalar field characterized by the cross-spectral density function $W(\mathbf{x}_1, \mathbf{x}_2)$ (for the sake of simplicity, here and further on, we suppress the explicit dependence of the considered quantities on frequency ν). Taking the amplitude transmittance $t_o(\mathbf{x})$ for the input of the system, we will find the output of the system as the power spectrum $S(\mathbf{x}') = W(\mathbf{x}', \mathbf{x}')$ of the field in the $\mathbf{x}'$ plane.

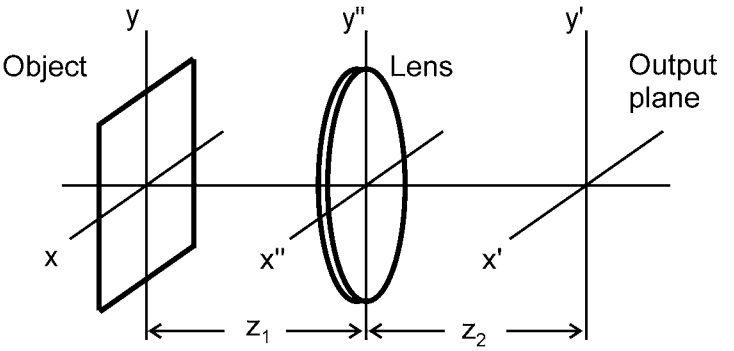

Figure 2.1 Single-lens optical system.

As the starting point of our calculations, we use an ensemble representation of the cross-spectral density function of the illumination field (see Section 1.4), i.e.,

$$W(\mathbf{x}_1, \mathbf{x}_2) = \left\langle U^*(\mathbf{x}_1)\, U(\mathbf{x}_2) \right\rangle, \tag{2.4}$$

where $U(\mathbf{x})$ is an optical signal associated with the illumination field, and the angular brackets denote, as always, an ensemble average. Taking into account that the optical signals on both sides of the object are related as

$$U'(\mathbf{x}) = t_o(\mathbf{x})\, U(\mathbf{x}), \tag{2.5}$$

one finds that the cross-spectral density function of the field just beyond the object is given by

$$W'(\mathbf{x}_1, \mathbf{x}_2) = \left\langle t_o^*(\mathbf{x}_1)\, t_o(\mathbf{x}_2)\, U^*(\mathbf{x}_1)\, U(\mathbf{x}_2) \right\rangle = t_o^*(\mathbf{x}_1)\, t_o(\mathbf{x}_2)\, W(\mathbf{x}_1, \mathbf{x}_2). \tag{2.6}$$

The cross-spectral density function of the field $W(\mathbf{x}_1'', \mathbf{x}_2'')$ just in front of the lens may be found by the use of Eq. (1.17) to be

$$W\left(\mathbf{x}_1'', \mathbf{x}_2''\right) = \left(\frac{k}{2\pi}\right)^2 \iint_{-\infty}^{\infty} W'(\mathbf{x}_1, \mathbf{x}_2) \times \frac{\exp\left[\mathrm{i}k(R_2 - R_1)\right]}{r_1 r_2} \cos\theta_1 \cos\theta_2 \mathrm{d}\mathbf{x}_1 \mathrm{d}\mathbf{x}_2, \tag{2.7}$$

where

$$R_{1(2)} = \left[\left(\mathbf{x}_{1(2)}'' - \mathbf{x}_{1(2)}\right)^2 + z_1^2\right]^{1/2}. \tag{2.8}$$

To simplify the following calculations, we will employ the so-called *paraxial approximation*, which is quite justifiable in our case (see, e.g., Ref. 24). Within a paraxial approximation, one can use the following relations for the parameters in Eq. (2.7):

$$\cos\theta_1 \approx \cos\theta_2 \approx 1, \tag{2.9}$$

$$R_{1(2)} \approx z_1 \tag{2.10}$$

in the denominator of the fraction under the integral, and

$$R_{1(2)} \approx z_1 \left[1 + \frac{\left(\mathbf{x}_{1(2)}'' - \mathbf{x}_{1(2)}\right)^2}{2z_1^2}\right] \tag{2.11}$$

in the exponential function, in view of the fact that here $R_{1(2)}$ is multiplied by a very large number k and that, besides, the small phase variations can change the

value of the exponential significantly. The result of such an approximation is

$$W\left(\mathbf{x}_1'', \mathbf{x}_2''\right) = \left(\frac{k}{2\pi z_1}\right)^2 \iint_{-\infty}^{\infty} W'\left(\mathbf{x}_1, \mathbf{x}_2\right) \times \exp\left\{\mathrm{i}\frac{k}{2z_1}\left[\left(\mathbf{x}_2'' - \mathbf{x}_2\right)^2 - \left(\mathbf{x}_1'' - \mathbf{x}_1\right)^2\right]\right\} \mathrm{d}\mathbf{x}_1 \mathrm{d}\mathbf{x}_2. \quad (2.12)$$

Under certain conditions (see, e.g., Ref. 24), the positive lens in the $\mathbf{x}''$ plane may be considered as a thin plane transmitting screen with an amplitude transmittance

$$t_l\left(\mathbf{x}''\right) = P\left(\mathbf{x}''\right) \exp\left[-\mathrm{i}\frac{k}{2f}\left(\mathbf{x}''\right)^2\right], \quad (2.13)$$

where f is the focal length of the lens and $P(\mathbf{x}'')$ is the so-called pupil function defined as

$$P\left(\mathbf{x}''\right) = \begin{cases} 1 & \text{inside the lens aperture} \\ 0 & \text{otherwise.} \end{cases} \quad (2.14)$$

Hence, the cross-spectral density function of the field just beyond the lens may be found by analogy with Eq. (2.6), i.e.,

$$W'\left(\mathbf{x}_1'', \mathbf{x}_2''\right) = t_l^*\left(\mathbf{x}_1''\right) t_l\left(\mathbf{x}_2''\right) W\left(\mathbf{x}_1'', \mathbf{x}_2''\right) = P\left(\mathbf{x}_1''\right) P\left(\mathbf{x}_2''\right) \exp\left\{-\mathrm{i}\frac{k}{2f}\left[\left(\mathbf{x}_2''\right)^2 - \left(\mathbf{x}_1''\right)^2\right]\right\} W\left(\mathbf{x}_1'', \mathbf{x}_2''\right). \quad (2.15)$$

Now, to find the cross-spectral density function of the field in the output $\mathbf{x}'$ plane, we again use the paraxial approximation of Eq. (1.17), which gives as a result

$$W\left(\mathbf{x}_1', \mathbf{x}_2'\right) = \left(\frac{k}{2\pi z_2}\right)^2 \iint_{-\infty}^{\infty} W'\left(\mathbf{x}_1'', \mathbf{x}_2''\right) \times \exp\left\{\mathrm{i}\frac{k}{2z_2}\left[\left(\mathbf{x}_2' - \mathbf{x}_2''\right)^2 - \left(\mathbf{x}_1' - \mathbf{x}_1''\right)^2\right]\right\} \mathrm{d}\mathbf{x}_1'' \mathrm{d}\mathbf{x}_2''. \quad (2.16)$$

On substituting consecutively for $W'(\mathbf{x}_1'', \mathbf{x}_2'')$ from Eqs. (2.15), (2.12), and (2.6) into Eq. (2.16) and taking $\mathbf{x}_1' = \mathbf{x}_2' = \mathbf{x}$, we find after straightforward calculations the following expression for the power spectrum of the field in the output plane:

$$S\left(\mathbf{x}'\right) = \iint_{-\infty}^{\infty} t_o^*\left(\mathbf{x}_1\right) t_o\left(\mathbf{x}_2\right) W\left(\mathbf{x}_1, \mathbf{x}_2\right) h^*\left(\mathbf{x}', \mathbf{x}_1\right) h\left(\mathbf{x}', \mathbf{x}_2\right) \mathrm{d}\mathbf{x}_1 \mathrm{d}\mathbf{x}_2, \quad (2.17)$$

where

$$h\left(\mathbf{x}',\mathbf{x}\right)=\left(\frac{k}{2\pi}\right)^2\frac{1}{z_1z_2}\exp\left[\mathrm{i}\frac{k}{2z_2}\left(\mathbf{x}'\right)^2\right]\exp\left[\mathrm{i}\frac{k}{2z_1}\mathbf{x}^2\right]$$
$$\times\int_{-\infty}^{\infty}P\left(\mathbf{x}''\right)\exp\left[\mathrm{i}\frac{k}{2}\left(\frac{1}{z_1}+\frac{1}{z_2}-\frac{1}{f}\right)\left(\mathbf{x}''\right)^2\right]$$
$$\times\exp\left[-\mathrm{i}\frac{k}{z_2}\mathbf{x}''\cdot\left(\mathbf{x}'+\frac{z_2}{z_1}\mathbf{x}\right)\right]\mathrm{d}\mathbf{x}''. \tag{2.18}$$

Finally, comparing Eqs. (2.18) and (2.3), we come to the conclusion that an elementary optical system as shown in Fig. 2.1 represents a bilinear system with the double-impulse response

$$q_2\left(\mathbf{x}',\mathbf{x}_1,\mathbf{x}_2\right)=W\left(\mathbf{x}_1,\mathbf{x}_2\right)h^*\left(\mathbf{x}',\mathbf{x}_1\right)h\left(\mathbf{x}',\mathbf{x}_2\right). \tag{2.19}$$

We will now consider two important particular cases, which are interesting from the standpoint of practice.

If the geometry in Fig. 2.1 satisfies the *lens law*, $1/z_1+1/z_2=1/f$, the double-impulse response of the system takes the same form as Eq. (2.19), but with

$$h\left(\mathbf{x}',\mathbf{x}\right)=\left(\frac{k}{2\pi}\right)^2\frac{1}{z_1z_2}\exp\left[\mathrm{i}\frac{k}{2z_2}\left(\mathbf{x}'\right)^2\right]\exp\left[\mathrm{i}\frac{k}{2z_1}\mathbf{x}^2\right]$$
$$\times\int_{-\infty}^{\infty}P\left(\mathbf{x}''\right)\exp\left[-\mathrm{i}\frac{k}{z_2}\mathbf{x}''\cdot\left(\mathbf{x}'+\frac{z_2}{z_1}\mathbf{x}\right)\right]\mathrm{d}\mathbf{x}'', \tag{2.20}$$

which is known as the *amplitude spread function* of the optical system. In this case, Eq. (2.17) may be interpreted as representing an *image of the object* with the scale defined by the factor z_2/z_1.

If the geometry in Fig. 2.1 satisfies the condition $z_1=z_2=f$, and the physical extent of the input is much smaller than the lens aperture, it may be readily shown (see, e.g., Ref. 13) that the double-impulse response of the system again takes the same form as Eq. (2.19), but with

$$h\left(\mathbf{x}',\mathbf{x}\right)=\frac{k}{\mathrm{i}2\pi f}\exp\left(-\mathrm{i}\frac{k}{f}\mathbf{x}'\cdot\mathbf{x}\right). \tag{2.21}$$

In this case, Eq. (2.17) may be interpreted as representing a 4D Fourier transform of the object with spatial frequencies defined by the vector $(k/2\pi f)\mathbf{x}'$.

2.3 Coherent-Mode Representations of a Bilinear System

It seems to be quite obvious that the coherent-mode representation of the illuminating field can considerably simplify the description of an optical system with

partially coherent illumination. Indeed, representing the illuminating field as the superposition of uncorrelated and completely coherent modes, we can expect that the power spectrum of the field in the output plane of an optical system will represent the superposition of fractional power spectra of the coherent system responces produced by these modes. In this way, the cumbersome problem of describing the optical system with partially coherent illumination can be traced back to the coherent case. The corresponding mathematical treatment is as follows.

Let us recall the coherent-mode representation of the cross-spectral density function (1.18) and rewrite it for the illuminating field at the input of the optical system shown in Fig. 2.1 as follows:

$$W(\mathbf{x}_1, \mathbf{x}_2) = \sum_n \lambda_n \varphi_n^*(\mathbf{x}_1)\, \varphi_n(\mathbf{x}_2), \tag{2.22}$$

where λ_n are the eigenvalues and $\varphi_n(\mathbf{x})$ are the eigenfunctions of the Fredholm integral equation

$$\int_D W(\mathbf{x}_1, \mathbf{x}_2)\, \varphi_n(\mathbf{x}_1)\, \mathrm{d}\mathbf{x}_1 = \lambda_n \varphi_n(\mathbf{x}_2). \tag{2.23}$$

As we remember, each term under the summation sign on the right-hand side of Eq. (2.22) may be regarded as being associated with a completely coherent mode of the illuminating field. Substituting for $W(\mathbf{x}_1, \mathbf{x}_2)$ from Eq. (2.22) into Eq. (2.17) and separating the integral operations, we obtain

$$S(\mathbf{x}') = \sum_n \lambda_n \left| \int_{-\infty}^{\infty} t_o(\mathbf{x})\, \varphi_n(\mathbf{x})\, h(\mathbf{x}', \mathbf{x})\, \mathrm{d}\mathbf{x} \right|^2. \tag{2.24}$$

Obviously, each term under the summation sign in Eq. (2.24) may be interpreted as a portion of the system output corresponding to the nth coherent mode of the illumination field or, for brevity, as a *modal output* of the system. Hence, the expansion given by Eq. (2.24) may be referred to as the *coherent-mode representation of an optical system with partially coherent illumination.*

To show the advantages of the coherent-mode representation of an optical system with partially coherent illumination, we will rewrite Eq. (2.24) in two different, but equivalent, forms. At first we write it as

$$S(\mathbf{x}') = \sum_n \left| \int_{-\infty}^{\infty} t_o(\mathbf{x})\, q_1^{(n)}(\mathbf{x}', \mathbf{x})\, \mathrm{d}\mathbf{x} \right|^2, \tag{2.25}$$

where

$$q_1^{(n)}(\mathbf{x}', \mathbf{x}) = \sqrt{\lambda_n}\, \varphi_n(\mathbf{x})\, h(\mathbf{x}', \mathbf{x}). \tag{2.26}$$

With due regard for the Volterra series (2.2), the function $q_1^{(n)}(\mathbf{x}', \mathbf{x})$ given by Eq. (2.26) represents the first-order Volterra kernel and hence the integral

$$\int_{-\infty}^{\infty} t_o(\mathbf{x})\, q_1^{(n)}(\mathbf{x}', \mathbf{x})\, \mathrm{d}\mathbf{x} \tag{2.27}$$

may be regarded as the output of the corresponding linear (coherent) optical system or, for brevity, the *modal system*. Thus, one can give the following physical interpretation of the expansion (2.25): *an optical system with partially coherent illumination may be represented as the parallel connection of modal coherent systems with the impulse responses* $q_1^{(n)}(\mathbf{x}', \mathbf{x})$*, each followed by a squarer, as shown in Fig. 2.2.*

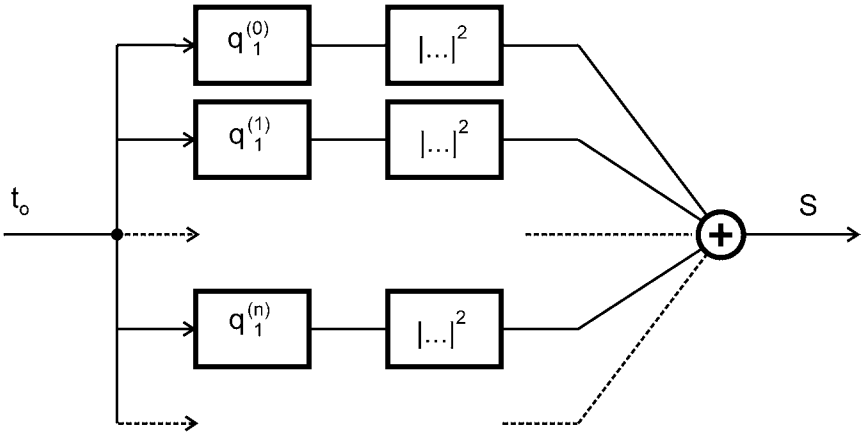

Figure 2.2 Modal representation (I) of partially coherent optical system.

Let us now rewrite Eq. (2.24) as

$$S(\mathbf{x}') = \sum_n \left| \int_{-\infty}^{\infty} t_o^{(n)}(\mathbf{x})\, q_1(\mathbf{x}', \mathbf{x})\, \mathrm{d}\mathbf{x} \right|^2, \tag{2.28}$$

where $q_1(\mathbf{x}', \mathbf{x}) = h(\mathbf{x}', \mathbf{x})$ and

$$t_o^{(n)}(\mathbf{x}) = \sqrt{\lambda_n}\, \varphi_n(\mathbf{x})\, t_o(\mathbf{x}). \tag{2.29}$$

The function $t_o^{(n)}(\mathbf{x})$ describes the result of the modulation of the field mode by the object and may be defined as a *modal object*. One can see that the integral in Eq. (2.28) represents the response of the completely coherent, linear in complex amplitude, system to the modal object $t_o^{(n)}(\mathbf{x})$. Thus, we can give the following physical interpretation of expansion (2.28): *an optical system with partially coherent illumination may be represented as the parallel connection of the coherent*

systems with the same impulse response $q_1(\mathbf{x}', \mathbf{x})$ and with the modal objects $t_o^{(n)}(\mathbf{x})$ at their inputs, each followed by a squarer, as shown in Fig. 2.3.

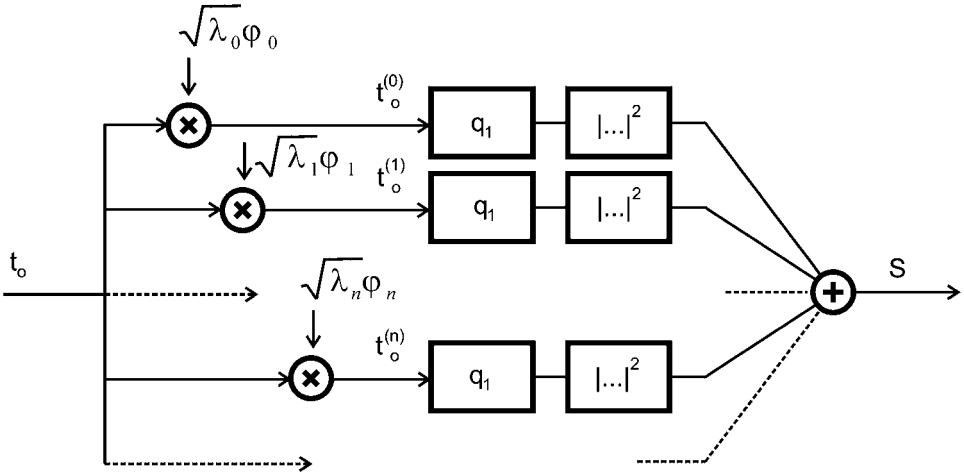

Figure 2.3 Modal representation (II) of partially coherent optical system.

The coherent-mode representations of an optical system, given by Eqs. (2.25) and (2.28), are equivalent from the point of view of the final result, but express the effect of partial coherence of illumination in two different ways. Indeed, when using representation (2.25), one attributes the effect of partial coherence to the transfer characteristic of the optical system, while in representation (2.28) this effect is attributed to the transfer characteristic of the object. Therefore, when we need to describe an optical system with a definite type of illumination, the preference should be given to representation (2.25), whereas when needed for an optical system with variable illumination, it is more convenient to use representation (2.28).

2.4 Fast Algorithm for Bilinear Transforms in Optics

In this section, we compare the computational complexity of calculating the power spectrum $S(\mathbf{x}')$ with the use of the bilinear transform representation (2.17) and the coherent-mode representation (2.24).

Using $K \times K$ sampling points in each plane, $\mathbf{x}$ and $\mathbf{x}'$, Eq. (2.17) can be written in the discrete form

$$S(i,j) = \sum_{k=1}^{K}\sum_{l=1}^{K}\sum_{m=1}^{K}\sum_{n=1}^{K} t_o^*(k,l)\, t_o(m,n)\, W(k,l,m,n) \times h^*(i,j,k,l)\, h(i,j,m,n)\,, \tag{2.30}$$

where the distances between samples $\triangle x$ and $\triangle y$ are assumed, without loss of generality, to have the value of one. The dominant portion of the calculations of power

spectrum $S(i, j)$ in accordance with Eq. (2.30) is the multiplication of the complex values t_o^*, t_o, W, h^*, and h, taken for all possible combinations of sampling points (k, l), (m, n), and (i, j). The number of the needed complex multiplications in this case is

$$C = \left(K^2\right)^3 = K^6. \tag{2.31}$$

The magnitude of this number can easily result in an unacceptably long computation time. Thus, for example, when $K = 100$ and the computational speed is 10^6 operations per second, the computer run time needed to calculate $S(i, j)$ makes up about 300 hours.

Now, let us evaluate the computational complexity of the calculation of power spectrum $S(\mathbf{x}')$ using the coherent-mode representation (2.24). Assuming that the summation in the coherent mode representation (2.22) is truncated by the effective number of coherent modes $\mathcal{N}$ (see Section 1.5), we can write the discrete version of Eq. (2.24) as

$$\begin{aligned} S(i, j) = \sum_{n=0}^{\mathcal{N}-1} \left[\sum_{k=1}^{K} \sum_{l=1}^{K} t_o(k, l) \sqrt{\lambda_n} \varphi_n(k, l) h^*(i, j, k, l) \right] \\ \times \left[\sum_{k=1}^{K} \sum_{l=1}^{K} t_o(k, l) \sqrt{\lambda_n} \varphi_n(k, l) h^*(i, j, k, l) \right]^*. \end{aligned} \tag{2.32}$$

It may be readily seen that this time the number of complex multiplications needed to calculate $S(i, j)$ is

$$C = \mathcal{N}\left[\left(K^2\right)^2 + K^2\right] = \mathcal{N}K^2\left(K^2 + 1\right), \tag{2.33}$$

or, for sufficiently large K,

$$C \approx \mathcal{N}K^4. \tag{2.34}$$

To compare this result to the one given by Eq. (2.31), we first discuss the range of possible values of $\mathcal{N}$. As shown in Section 1.5, the value of $\mathcal{N}$ increases with decreasing the degree of coherence of the illumination field. For completely coherent illumination, $\mathcal{N} = 1$, and the computational effort C decreases to K^4. For partially coherent illumination, C increases linearly with $\mathcal{N}$, i.e., the computational effort is lager the more incoherent the illumination. For sufficiently large values of $\mathcal{N}$, say $\mathcal{N} \geqslant K$, the illumination may be generally considered to be completely incoherent. In this case, the cross-spectral density function $W(\mathbf{x}_1, \mathbf{x}_2)$ may be approximated by the Dirac function,[18] i.e.,

$$W(\mathbf{x}_1, \mathbf{x}_2) = S_0 \delta(\mathbf{x}_1 - \mathbf{x}_2), \tag{2.35}$$

and the bilinear transform (2.17) is reduced to

$$S\left(\mathbf{x}'\right) = S_0 \int_{-\infty}^{\infty} |t_o\left(\mathbf{x}\right)|^2 \left|h\left(\mathbf{x}';\mathbf{x}\right)\right|^2 \mathrm{d}\mathbf{x}, \tag{2.36}$$

where S_0 is a constant. Hence, the number of operations needed to compute $S(i, j)$ again reduces to K^4.

The comparison of the computational efficiency of the direct calculation of bilinear transform (2.30) and its coherent-mode representation (2.32), for different values of $\mathcal{N}$, is illustrated by a schematic picture in Fig 2.4. It is evident from this figure that the coherent-mode representation (2.32) can be efficiently employed to calculate the power spectrum $S(\mathbf{x}')$ when $\mathcal{N} \leqslant K$. For the same values of K and computational speed used in the previous example, the computer run time needed to calculate $S(i, j)$ from Eq. (2.32) takes from two minutes to three hours, depending on the degree of illumination coherence. By analogy with the well known algorithm of fast Fourier transform (FFT), we will refer to the algorithm for the calculation of bilinear transform (2.17) on the basis of Eq. (2.32) as a *fast bilinear transform (FBLT) algorithm*.

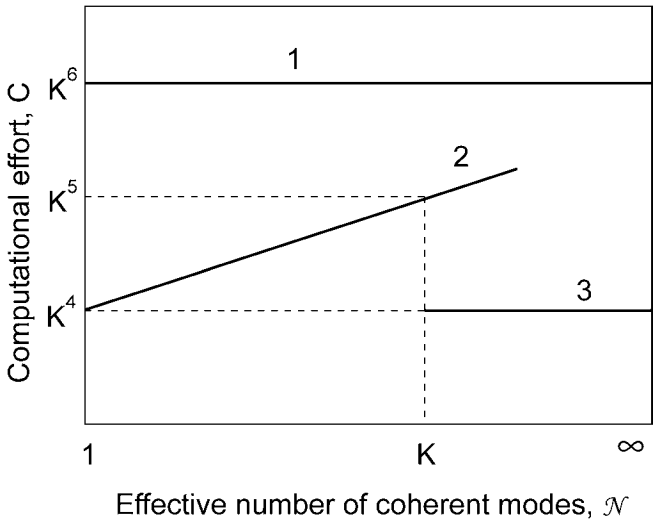

Figure 2.4 Estimation of the computational effort C as a function of the effective number $\mathcal{N}$ of coherent modes of ilumination: 1 computation in accordance with Eq. (2.30); 2 computation in accordance with Eq. (2.32); 3 computation in accordance with Eq. (2.35).

2.5 Numerical Simulation

To illustrate the application of the FBLT algorithm, let us consider two examples of calculating the power spectrum (2.17) in the output plane of the optical system shown in Fig 2.1.

For an object, we choose the 1D *Dirac comb function*, i.e.,

$$t(x) = \sum_m \delta(x - mx_0). \tag{2.37}$$

This object was studied for the following two reasons. First, both the ideal image and the exact Fourier spectrum of such an object have the same form of the Dirac comb function. Secondly, the choice of this object allows the result of integration in Eq. (2.17) to be obtained in an explicit analytic form, a fact that gives us a chance to evaluate the accuracy of the FBLT algorithm. Taking into account the 1D character of our object, and for the sake of simplicity, for the illumination field we consider the secondary 1D Gaussian Schell-model source (see Section 1.6.1) with the cross-spectral density function defined by Eqs. (1.55)–(1.57) and the coherent mode structure given by Eqs. (1.58)–(1.61). Finally, assuming that the pupil function of the lens has a circular form of radius R, we accept the amplitude spread function of the optical system, calculated in accordance with Eq. (2.20) as

$$h(\rho) = \exp\left(\mathrm{i}\frac{k}{2z_2}\rho^2\right)\frac{J_1(kR\rho/2f)}{kR\rho/2f}, \tag{2.38}$$

where $\rho = (u^2 + v^2)^{1/2}$ and J_1 denotes the Bessel function of the first kind and of the first order.

At first, we suppose that the optical system forms the image of an object without magnification ($z_1 = z_2 = 2f$). Then, substituting for $t(x)$, $W(x_1, x_2)$, and $h(u; x)$ from Eqs. (2.37), (1.55), and (2.38), respectively, into the 1D version of Eq. (2.17) and making use of the sifting property of the Dirac function, it is a straightforward matter to obtain the following expression for power spectrum $S(x')$:

$$S\left(x'\right) = S(0)\sum_{m,l} A_{ml}\frac{J_1\left[kR\left(u + mx_0\right)/2f\right]}{kR\left(u + mx_0\right)/2f}\frac{J_1\left[kR\left(u + lx_0\right)/2f\right]}{kR\left(u + lx_0\right)/2f}, \tag{2.39}$$

where

$$A_{ml} = \exp\left[-\frac{x_0^2}{4\sigma_S^2}\left(m^2 + l^2\right)\right]\exp\left[-\frac{x_0^2}{2\sigma_\mu^2}(m - l)^2\right]. \tag{2.40}$$

By analogy, but this time using the 1D version of Eq. (2.24) with due regard for the truncation of summation by N terms, we obtain the following approximation of power spectrum $S(x')$:

$$\widehat{S}\left(x'\right) = S(0)\sum_{n=0}^{N-1} B_n\left[\sum_m C_{nk}\frac{J_1\left[kR\left(u + mx_0\right)/2f\right]}{kR\left(u + mx_0\right)/2f}\right]^2, \tag{2.41}$$

where

$$B_n = \frac{1}{2^n n!}\left(\frac{b}{a+b+c}\right)^n, \tag{2.42}$$

and

$$C_{nm} = H_n\left(mx_0\sqrt{2c}\right)\exp\left(-cm^2x_0^2\right) \tag{2.43}$$

with H_n, as before, denoting the Hermite polynomial of order n.

Now, we suppose that the optical system performs the Fourier transform of an object ($z_1 = z_2 = f$). In this case, making use of Eqs. (2.21), (1.55), and (2.37), by analogy with the foregoing, one can find that power spectrum $S(x')$ takes the form

$$S\left(x'\right) = S_0\left\{A_0 + \sum_{m\neq l} A_{ml}\cos\left[\frac{k}{2f}x'x_0\left(m-l\right)\right]\right\}, \tag{2.44}$$

where

$$A_0 = \sum_m \exp\left(-\frac{x_0^2}{2\sigma_I^2}m^2\right) \tag{2.45}$$

and A_{ml} are the same as in Eq. (2.39).

Using the FBLT algorithm, we obtain the following approximation of the power spectrum (2.44):

$$\widehat{S}\left(x'\right) = S_0\sum_{n=0}^{N-1} B_n\left\{C_{n0} + 2\sum_{m\neq l} C_{nml}\cos\left[\frac{k}{2f}x'x_0\left(m-l\right)\right]\right\}, \tag{2.46}$$

where

$$C_{n0} = \sum_m H_n^2\left(mx_0\sqrt{2c}\right)\exp\left(-2cm^2x_0^2\right), \tag{2.47}$$

$$C_{nml} = H_n\left(mx_0\sqrt{2c}\right)H_n\left(lx_0\sqrt{2c}\right)\exp\left[-cx_0^2\left(m^2+l^2\right)\right], \tag{2.48}$$

and B_n are the same as in Eq. (2.41).

To evaluate the quality of our approximation, we realized numerical calculations of power spectrum $S(x')$ in accordance with Eqs. (2.39), (2.41), (2.44), and (2.46). When calculating, we put $x_0 = 2.44\,(2\pi f/kR)$, which is twice greater than the Rayleigh limit of resolution for our optical system, and $\sigma_I = 2\sigma_\mu = 10x_0$,

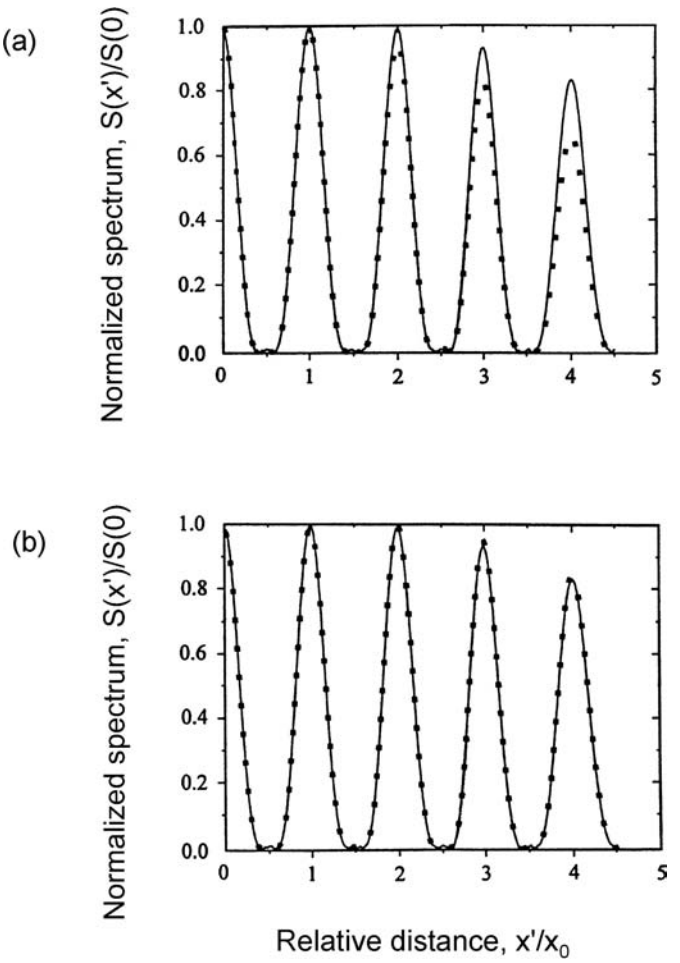

Figure 2.5 Results of calculating $S(x')$ in accordance with Eq. (2.41) for: (a) $N = 1$; (b) $N = 4$. Theoretical values of $S(x')$, obtained according to Eq. (2.39), are shown by solid curves.

which corresponds to the case of true partial coherence ($\gamma = 0.5$). We truncated the summation over indexes k, m, l to nine central Dirac impulses in the object, and varied the number N of the terms in the modal expansion.

The results of calculations are shown in Figs. 2.5 and 2.6. As can be seen from these figures, with the increase of the number N, the approximate power spectra distributions come closer to the theoretical curves. When the number N is equal to the effective number $\mathcal{N}$ of coherent modes of illumination (in our example $\mathcal{N} = 4$), the relative error of the FBLT algorithm constitutes approximately 1%, and when $N = 2\mathcal{N}$, it becomes negligible.

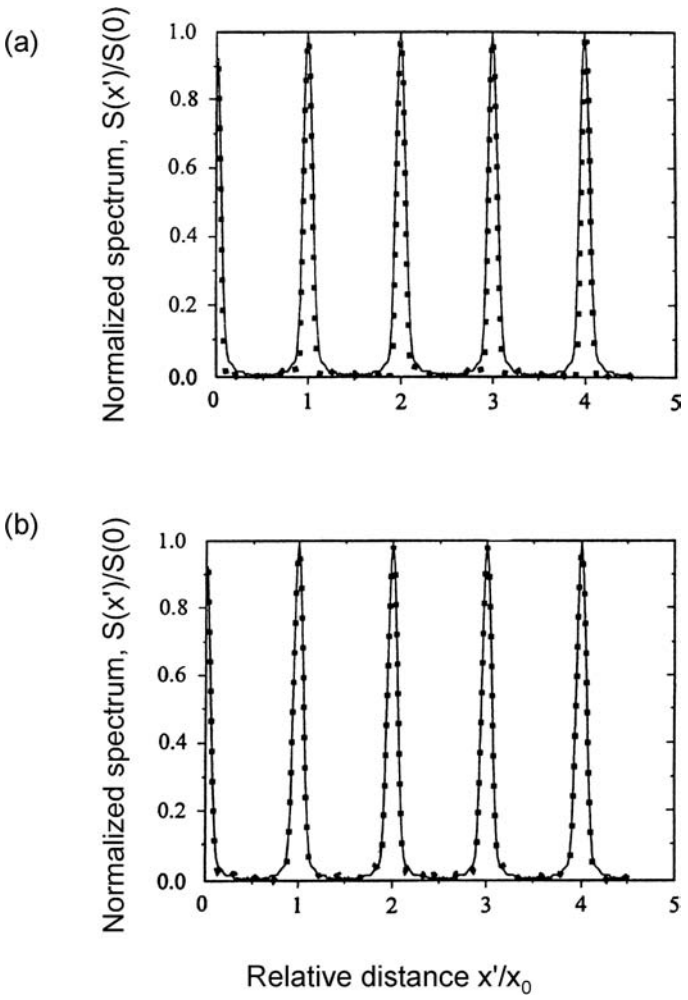

Figure 2.6 Results of calculating $S(x')$ in accordance with Eq. (2.46) for: (a) $N = 1$; (b) $N = 4$. Theoretical values of $S(x')$, obtained according to Eq. (2.44), are shown by solid curves.

2.6 Concluding Remarks

The coherent-mode representation of a partially coherent optical system may be interpreted as a replacement of the original system by an appropriate parallel combination of completely coherent modal systems; this gives a new insight into the physics of image formation under conditions of partially coherent illumination. From a practical standpoint, such a representation results in an effective algorithm for computing the power spectrum distribution at the output of an optical system with the illumination of any state of coherence. The proposed FBLT algorithm allows a significant reduction (by a factor of several orders) of the computational effort needed for calculating the power spectrum at the system output. However, it should be noted that the application of this algorithm requires knowledge of the

coherent-mode structure of the illumination field (eigenvalues λ_n and eigenfunctions φ_n). Unfortunately, such a coherent-mode structure can be deduced in closed form for a small number of known model sources (see Section 1.6). In the general case, evaluation of the coherent-mode structure entails the necessity of a numerical solution of the integral equation (2.23); this is not an easier computational task than the proper calculation of the output power spectrum. Nevertheless, it should be taken into account that once $\varphi_n(\mathbf{x})$ and λ_n have been calculated for a given illumination, they can be stored and applied to the calculation of the output power spectrum for any object and any optical system. Thus, the FBLT algorithm can be considered as an indispensable tool for the analysis and computer simulation of optical systems with partially coherent illumination.

3

Coherent-Mode Representation of Propagation-Invariant Fields

3.1 Introduction

As is well known, a bounded optical field propagating in free space undergoes diffractive spreading that changes its transverse intensity distribution. Nevertheless, it is not always the case if the field has an infinite extent. Almost two decades ago, Durnin[33] found an exact solution for the wave propagation equation that describes a whole class of so-called nondiffracting fields. It has been shown that any nondiffracting field represents the superposition of plane waves with wave vectors lying on a cone. In this case, all the wave vectors possess the same projection along, say, the z-axis and the constituent plane waves suffer one and the same phase change on propagation. Accordingly, they interfere in the same way at any constant z plane. The simplest member of the class of nondiffracting fields is the fundamental Bessel beam. The sharply peaked intensity profile of this beam, together with its propagation-invariant property, has generated wide interest to nondiffracting beams. The new models of nondiffracting beams have been studied and compared,[34–49] the possibility of their physical generation has been demonstrated in experiments,[50–56] and their potential practical applications have been discussed.[57–59] It is not out of place to mention here that nondiffracting beams have also received attention in acoustic science (see, e.g., Ref. 60).

The nondiffracting beams defined by Durnin's solution represent completely coherent optical fields. At the same time, as has been shown by Ohtsuka et al.[61,62] and Gori et al.,[9] some partially coherent fields can also exhibit propagation-invariant properties. Turunen et al.[63] have generalized the concept of diffraction-free propagation into a domain of partially coherent fields, and have deduced the general expression for the cross-spectral density function, which defines a wide class of partially coherent propagation-invariant fields.

In spite of a great number of published results, the theory of propagation-invariant fields is still far from completion. Recently, Ostrovsky et al.,[64–70] while trying to describe all the possible classes of propagation-invariant fields, have deduced the coherent-mode structure of propagation-invariant fields that allowed, in particular, predicting the existence of new peculiar propagation-invariant optical beams. Below, we consider this representation and the results obtained on its basis.

3.2 Propagation-Invariant Fields

Let us consider the propagation of a scalar quasi-monochromatic optical field in free space from the plane $z = 0$ toward the plane $z = z_0$ (Fig. 1.1), and let $W(\mathbf{x}_1, \mathbf{x}_2; 0)$ be the cross-spectral density function of this field in the plane $z = 0$ (from now on, we omit the explicit dependence of the considered quantities on the frequency ν). The cross-spectral density of the field in the plane $z = z_0$ may be found as a particular case of Eq. (1.17), i.e.,

$$W\left(\mathbf{x}_1', \mathbf{x}_2'\right) = \left(\frac{k}{2\pi}\right)^2 \iint_{(z=0)} W\left(\mathbf{x}_1, \mathbf{x}_2; 0\right) \times \frac{\exp\left[\mathrm{i}k(R_2 - R_1)\right]}{r_1 r_2} \cos\theta_1 \cos\theta_2 \mathrm{d}\mathbf{x}_1 \mathrm{d}\mathbf{x}_2, \tag{3.1}$$

where

$$R_{1(2)} = \left[\left(\mathbf{x}_{1(2)}' - \mathbf{x}_{1(2)}\right)^2 + z_0^2\right]^{1/2}. \tag{3.2}$$

As can be seen from Eq. (3.1), in the general case, the cross-spectral density function suffers changes of its form when propagating in free space. An optical field is said to be a *propagation-invariant field* if its cross-spectral density function remains the same in every plane normal to the z-axis, i.e.,

$$W\left(\mathbf{x}_1, \mathbf{x}_2; z_0\right) = W\left(\mathbf{x}_1, \mathbf{x}_2; 0\right). \tag{3.3}$$

It is obvious that the power spectrum of the propagation-invariant field possesses the same property as follows:

$$S\left(\mathbf{x}; z_0\right) = S\left(\mathbf{x}; 0\right). \tag{3.4}$$

To find the form of cross-spectral density function of a propagation-invariant field, we will employ the paraxial approximation (see Section 2.2), which is justifiable when the field propagates within a narrow solid angle around the z-axis, and thus, taking into account Eq. (3.4), in our case. In the paraxial approximation, one can use the following relations for the parameters in Eq. (3.1):

$$\cos\theta_1 \approx \cos\theta_2 \approx 1, \tag{3.5}$$

$$R_{1(2)} \approx z_0 \tag{3.6}$$

in the denominator of the fraction under the integral, and

$$R_{1(2)} \approx z_0 \left[1 + \frac{\left(\mathbf{x}_{1(2)}' - \mathbf{x}_{1(2)}\right)^2}{2z_0^2}\right] \tag{3.7}$$

in the exponential function. The resulting expression for the cross-spectral density function in the plane $z = z_0$ becomes

$$W\left(\mathbf{x}_1', \mathbf{x}_2'\right) = \left(\frac{k}{2\pi z_0}\right)^2 \iint_{(z=0)} W\left(\mathbf{x}_1, \mathbf{x}_2; 0\right) \times \exp\left\{\mathrm{i}\frac{k}{2z_0}\left[\left(\mathbf{x}_2' - \mathbf{x}_2\right)^2 - \left(\mathbf{x}_1' - \mathbf{x}_1\right)^2\right]\right\} \mathrm{d}\mathbf{x}_1 \mathrm{d}\mathbf{x}_2. \quad (3.8)$$

Now, we express $W(\mathbf{x}_1, \mathbf{x}_2; 0)$ through its 4D Fourier transform $\widetilde{W}(\mathbf{u}_1, \mathbf{u}_2; 0)$ as

$$W\left(\mathbf{x}_1, \mathbf{x}_2; 0\right) = \iint_{-\infty}^{\infty} \widetilde{W}\left(\mathbf{u}_1, \mathbf{u}_2; 0\right) \exp\left[\mathrm{i}2\pi\left(\mathbf{u}_2 \cdot \mathbf{x}_2 - \mathbf{u}_1 \cdot \mathbf{x}_1\right)\right] \mathrm{d}\mathbf{u}_1 \mathrm{d}\mathbf{u}_2. \quad (3.9)$$

Substituting from Eq. (3.9) into Eq. (3.8), interchanging the order of integration, and making use of the relation[71]

$$\int_{-\infty}^{\infty} \exp\left(\mathrm{i}\pi a^2 \mathbf{x}^2\right) \exp\left(\mathrm{i}2\pi \mathbf{u} \cdot \mathbf{x}\right) \mathrm{d}\mathbf{x} = \frac{1}{a^2} \exp\left(-\mathrm{i}\pi \frac{\mathbf{u}^2}{a^2}\right), \quad (3.10)$$

we obtain

$$W\left(\mathbf{x}_1', \mathbf{x}_2'\right) = \iint_{-\infty}^{\infty} \widetilde{W}\left(\mathbf{u}_1, \mathbf{u}_2; 0\right) \exp\left[-\mathrm{i}\frac{2\pi^2}{k} z_0 \left(\mathbf{u}_1^2 - \mathbf{u}_2^2\right)\right] \times \exp\left[\mathrm{i}2\pi\left(\mathbf{u}_2 \cdot \mathbf{x}_2' - \mathbf{u}_1 \cdot \mathbf{x}_1'\right)\right] \mathrm{d}\mathbf{u}_1 \mathrm{d}\mathbf{u}_2. \quad (3.11)$$

Furthermore, it will be appropriate to express Eq. (3.11) through the polar coordinates (r, ϕ) in the $\mathbf{u}$ plane as

$$W\left(\mathbf{x}_1', \mathbf{x}_2'\right) = \iint_0^{2\pi} \iint_0^{\infty} \widetilde{W}\left(r_1, r_2, \phi_1, \phi_2; 0\right) \exp\left[-\mathrm{i}\frac{2\pi^2}{k} z_0 \left(r_1^2 - r_2^2\right)\right] \times \exp\big[\mathrm{i}2\pi(x_2' r_2 \cos\phi_2 + y_2' r_2 \sin\phi_2 - x_1' r_1 \cos\phi_1 - y_1' r_1 \sin\phi_1)\big] r_1 r_2 \mathrm{d}r_1 \mathrm{d}r_2 \mathrm{d}\phi_1 \mathrm{d}\phi_2. \quad (3.12)$$

Finally, we recall the condition of the invariant propagation (3.3) and apply to it Eq. (3.12):

$$\iint_0^{2\pi} \iint_0^{\infty} \widetilde{W}\left(r_1, r_2, \phi_1, \phi_2; 0\right) \exp\left[-\mathrm{i}\frac{2\pi^2}{k} z_0 \left(r_1^2 - r_2^2\right)\right] \times \exp\left[\mathrm{i}2\pi(x_2 r_2 \cos\phi_2 + y_2 r_2 \sin\phi_2 - x_1 r_1 \cos\phi_1 - y_1 r_1 \sin\phi_1)\right] \times r_1 r_2 \mathrm{d}r_1 \mathrm{d}r_2 \mathrm{d}\phi_1 \mathrm{d}\phi_2$$

$$= \int\!\!\int_0^{2\pi} \int\!\!\int_0^{\infty} \widetilde{W}\,(r_1, r_2, \phi_1, \phi_2; 0) \exp\big[\mathrm{i}2\pi(x_2 r_2 \cos\phi_2 + y_2 r_2 \sin\phi_2 - x_1 r_1 \cos\phi_1 - y_1 r_1 \sin\phi_1)\big] r_1 r_2 \mathrm{d}r_1 \mathrm{d}r_2 \mathrm{d}\phi_1 \mathrm{d}\phi_2. \tag{3.13}$$

Equality (3.13) shows that $\widetilde{W}(r, \phi; 0)$ must be the vanishing function for all r_1 and r_2 except when $r_1 = r_2$, i.e.,

$$\widetilde{W}\,(r_1, r_2, \phi_1, \phi_2; 0) = Q\,(r_1, \phi_1, \phi_2)\,\delta\,(r_1 - r_2)\,, \tag{3.14}$$

where δ is the Dirac function. Thus, finally, on substituting for $\widetilde{W}(r_1, r_2, \phi_1, \phi_2; 0)$ from Eq. (3.14) into Eq. (3.12) and making use of the sifting property of the Dirac function, we obtain the following expression for the transverse cross-spectral density function, which describes the whole class of propagation-invariant fields:

$$W\,(\mathbf{x}_1, \mathbf{x}_2; z_0) = \int\!\!\int_0^{2\pi} \int_0^{\infty} Q\,(r, \phi_1, \phi_2; 0) \exp\big[\mathrm{i}2\pi r\,(x_2 \cos\phi_2 + y_2 \sin\phi_2 - x_1 \cos\phi_1 - y_1 \sin\phi_1)\big] r^2 \mathrm{d}r \mathrm{d}\phi_1 \mathrm{d}\phi_2. \tag{3.15}$$

To clarify the physical meaning of the obtained result, we note that the exponential function $\exp[\mathrm{i}2\pi r(x\cos\phi + y\sin\phi)]$ appearing in Eq. (3.15) may be regarded as a plane wave propagating with direction cosines $\alpha = (2\pi/k)r\cos\phi$, $\beta = (2\pi/k)r\sin\phi$ and $\gamma = (1 - \alpha^2 - \beta^2)^{1/2}$. Hence, Eq. (3.15), together with requirement (3.14), shows that *the propagation-invariant field represents the superposition of plane waves, which are uncorrelated in the radial direction and have an arbitrary correlation in the azimuthal direction.*

3.3 Coherent-Mode Structure of the Propagation-Invariant Field

We will now find the coherent-mode structure Λ [see Eq. (1.29)] of the propagation-invariant field. Instead of trying to solve the Fredholm integral equation (1.19) with the kernel given by Eq. (3.15), we will recall that the cross-spectral density function $W_n(\mathbf{x}_1, \mathbf{x}_2; z_0)$ of each mode satisfies the same propagation equations as does the cross-spectral density function $W(\mathbf{x}_1, \mathbf{x}_2; z_0)$ of the field, and will repeat the treatment realized in the previous section [Eqs. (3.8)–(3.12)] for

$$W_n\,(\mathbf{x}_1, \mathbf{x}_2; z_0) = \varphi_n^*\,(\mathbf{x}_1; z_0)\,\varphi_n\,(\mathbf{x}_2; z_0) \tag{3.16}$$

and, hence, for

$$\widetilde{W}\,(\mathbf{u}_1, \mathbf{u}_2; 0) = \widetilde{\varphi}_n^*\,(\mathbf{u}_1; 0)\,\widetilde{\varphi}_n\,(\mathbf{u}_2; 0)\,, \tag{3.17}$$

where

$$\widetilde{\varphi}_n\,(\mathbf{u}; 0) = \int_{-\infty}^{\infty} \varphi_n\,(\mathbf{x}; 0) \exp\,(-\mathrm{i}2\pi\mathbf{u}\cdot\mathbf{x})\,\mathrm{d}\mathbf{x}. \tag{3.18}$$

The result will obviously be

$$W_n(\mathbf{x}_1, \mathbf{x}_2; z_0) = \int\!\!\int_0^{2\pi} \int\!\!\int_0^{\infty} \widetilde{\varphi}_n^*(r_1, \phi_1; 0)\, \widetilde{\varphi}_n(r_2, \phi_2; 0) \times \exp\left[-\mathrm{i}\frac{2\pi^2}{k} z_0 \left(r_1^2 - r_2^2\right)\right] \times \exp\left[-\mathrm{i}2\pi(x_1 r_1 \cos\phi_1 + y_1 r_1 \sin\phi_1)\right] \times \exp\left[\mathrm{i}2\pi(x_2 r_2 \cos\phi_2 + y_2 r_2 \sin\phi_2)\right] r_1 r_2 \mathrm{d}r_1 \mathrm{d}r_2 \mathrm{d}\phi_1 \mathrm{d}\phi_2. \tag{3.19}$$

The simplest way to satisfy the requirement of the invariant propagation (3.14) this time is to choose

$$\widetilde{\varphi}_n(r, \phi; 0) = Q_n(r, \phi)\, \delta(r - r_{0n}), \tag{3.20}$$

where r_{0n} is a positive constant. With this choice, Eq. (3.19) assumes the form

$$W_n(\mathbf{x}_1, \mathbf{x}_2; z_0) = r_{0n}^2 \int\!\!\int_0^{2\pi} Q_n^*(r_{0n}, \phi_1)\, Q_n(r_{0n}, \phi_2) \times \exp\left[-\mathrm{i}2\pi r_{0n}(x_1 \cos\phi_1 + y_1 \sin\phi_1)\right] \times \exp\left[\mathrm{i}2\pi r_{0n}(x_2 \cos\phi_2 + y_2 \sin\phi_2)\right] \mathrm{d}\phi_1 \mathrm{d}\phi_2, \tag{3.21}$$

whence it follows immediately that

$$\varphi_n(\mathbf{x}; z_0) = r_{0n} \int_0^{2\pi} Q_n(r_{0n}, \phi) \exp\left[\mathrm{i}2\pi r_{0n}(x \cos\phi + y \sin\phi)\right] \mathrm{d}\phi. \tag{3.22}$$

Using the polar coordinates (ρ, θ) in the $\mathbf{x}$ plane, we can rewrite (3.22) as

$$\varphi_n(\rho, \theta; z_0) = r_{0n} \int_0^{2\pi} Q_n(r_{0n}, \phi) \exp\left[\mathrm{i}2\pi r_{0n} \rho \cos(\phi - \theta)\right] \mathrm{d}\phi. \tag{3.23}$$

Now, we note that function $Q_n(r_{0n}, \phi)$ may be expanded into a Fourier series as

$$Q_n(r_{0n}, \phi) = \sum_{p=-\infty}^{\infty} q_{np} \exp(\mathrm{i}p\phi), \tag{3.24}$$

where

$$q_{np} = \frac{1}{2\pi} \int_0^{2\pi} Q_n(r_{0n}, \phi) \exp(-\mathrm{i}p\phi)\, \mathrm{d}\phi. \tag{3.25}$$

On substituting from Eq. (3.24) into Eq. (3.23) and changing the order of summation and integration, we obtain

$$\varphi_n(\rho, \theta; z_0) = r_{0n} \sum_{p=-\infty}^{\infty} q_{np} \int_0^{2\pi} \exp(\mathrm{i}p\phi) \exp\left[\mathrm{i}2\pi r_{0n} \rho \cos(\phi - \theta)\right] \mathrm{d}\phi. \quad (3.26)$$

Finally, recalling the integral representation of the Bessel function,[72] we can rewrite Eq. (3.26) as follows:

$$\varphi_n(\rho, \theta; z_0) = 2\pi r_{0n} \sum_{p=-\infty}^{\infty} \mathrm{i}^p q_{np} \exp(\mathrm{i}p\theta)\, J_p(2\pi r_{0n}\rho), \quad (3.27)$$

where J_p denotes the Bessel function of the first kind and of the order p.

It is necessary to stress here that the functions $\varphi_n(\mathbf{x}; z_0)$ given by Eq. (3.27) still do not define the coherent-mode structure of the propagation-invariant field because of the uncertainty of coefficients q_{np}, caused by the arbitrariness of the choice of the function $Q_n(r_{0n}, \phi)$, as well as the arbitrariness of the choice of the parameter r_{0n}. To remove this uncertainty, we will recall that the modal functions $\varphi_n(\mathbf{x}; z_0)$ must be mutually orthonormal, i.e.,

$$\int_0^{2\pi} \int_0^{R} \varphi_n^*(\rho, \theta; z_0)\, \varphi_m(\rho, \theta; z_0)\, \rho \mathrm{d}\rho \mathrm{d}\theta = \delta_{nm}, \quad (3.28)$$

where δ_{nm} is the Kronecker symbol, and the radial integration is performed within the finite domain D of radius R. On substituting for $\varphi_n(\mathbf{x}; z_0)$ from Eq. (3.27) into Eq. (3.28) and making use of the obvious relation

$$\int_0^{2\pi} \exp\left[\mathrm{i}(s - p)\theta\right] \mathrm{d}\theta = 2\pi\delta_{ps}, \quad (3.29)$$

we obtain

$$(2\pi)^3 r_{0n} r_{0m} \sum_{p=-\infty}^{\infty} q_{np}^* q_{mp} \int_0^{R} J_p(2\pi r_{0n}\rho)\, J_p(2\pi r_{0m}\rho)\, \rho \mathrm{d}\rho = \delta_{nm}. \quad (3.30)$$

Thus, we have shown that the functions $\varphi_n(\mathbf{x}; z_0)$ given by Eq. (3.27) with the parameters q_{np} and r_{0n} determined by the orthonormality condition (3.30), describe the coherent-mode structure of any propagation-invariant field. Furthermore, we will show that there are three different possibilities to choose the parameters q_{np} and r_{0n} as they satisfy condition (3.30). We will refer to the corresponding classes of the fields as *the propagation-invariant fields of the first, second,* and *third kind.*

3.4 Special Classes of Propagation-Invariant Fields

3.4.1 Propagation-invariant fields of the first kind

We start with the simplest case, which is when the propagation-invariant field is completely coherent. As it has been shown in Section 1.2, in this case, the field consists of a single mode. This can be taken into account by choosing the parameters q_{np} and r_{0n} in Eq. (3.27) as follows:

$$q_{np} = \begin{cases} q_{0p} & \text{for } n = 0, \\ 0 & \text{for } n \neq 0, \end{cases} \tag{3.31a}$$

$$r_{0n} = r_{0.} \tag{3.31b}$$

Since condition (3.30) in this case makes no sense, the values q_{0p} and r_0 can be taken arbitrarily. Hence, with due regard for Eq. (3.27), the coherent-mode structure of the propagation-invariant field of the first kind is described by only one modal function,

$$\varphi_0(\rho, \theta) = 2\pi r_0 \sum_{p=-\infty}^{\infty} \mathrm{i}^p q_{0p} \exp(\mathrm{i}p\theta)\, J_p(2\pi r_0 \rho), \tag{3.32}$$

which is the well-known general solution for so-called *nondiffracting beams*.[36] In the particular case when

$$q_{0p} = \begin{cases} q_0 & \text{for } p = 0, \\ 0 & \text{for } p \neq 0, \end{cases} \tag{3.33}$$

this solution takes the form

$$\varphi_0(\rho, \theta) = 2\pi r_0 q_0 J_0(2\pi r_0 \rho), \tag{3.34}$$

known as the *fundamental Bessel beam*.[33]

Now, we will clear up the physical nature of the propagation-invariant fields of the first kind using the example of the fundamental Bessel beam. With this purpose, we calculate the Fourier spectrum (3.18) for function (3.34) using the Fourier-Bessel transform,[13]

$$\widetilde{\varphi}_0(r, \phi) = (2\pi)^2 r_0 q_0 \int_0^R \rho J_0(2\pi r_0 \rho)\, J_0(2\pi r \rho)\, \mathrm{d}\rho. \tag{3.35}$$

Taking into account the property of the Bessel function,[72]

$$a\int_0^R \rho J_\mu(a\rho)\, J_\mu\left(a'\rho\right) d\rho = \delta\left(a-a'\right), \tag{3.36}$$

we obtain

$$\widetilde{\varphi}_0(r,\phi) = q_0\delta(r-r_0). \tag{3.37}$$

Then, in accordance with the physical meaning of the Fourier spectrum (3.37) as a superposition of the plane waves propagating with the direction cosines $\alpha = (2\pi/k)r_0\cos\theta$ and $\beta = (2\pi/k)r_0\sin\theta$ (see Section 3.1), one may conclude that *the fundamental Bessel beam represents the superposition of plane waves whose wave vectors lie on the conical surface with the vertex angle* $\gamma = \tan^{-1}[(k/2\pi r_0)^2 - 1]^{-1/2}$.

3.4.2 Propagation-invariant fields of the second kind

Now, we choose

$$q_{np} = \begin{cases} q_{nn} & for\, p = n, \\ q_{nn}^* & \text{for } p = -n, \\ 0 & \text{for } p \neq \pm n, \end{cases} \tag{3.38}$$

allowing the parameter r_{0n} to take arbitrary values. It is a straightforward matter to make sure that this choice, with the value q_{nn} taken so that

$$|q_{nn}|^2 = \left[16\pi^3 r_{0n}^2 \int_0^R J_n^2(2\pi r_{0n}\rho)\,\rho d\rho\right]^{-1}, \tag{3.39}$$

satisfies the orthonormality condition (3.30). Then, substituting for q_{np} from Eq. (3.38) into Eq. (3.27), we find that the coherent-mode structure of the propagation-invariant field of the second kind is described by a set of modal functions,

$$\begin{aligned}\varphi_n(\rho,\theta) = 2\pi r_{0n}\big[&\mathrm{i}^n q_{nn}\exp(\mathrm{i}n\theta)\, J_n(2\pi r_{0n}\rho) \\ &+ \mathrm{i}^{-n} q_{nn}^*\exp(-\mathrm{i}n\theta)\, J_{-n}(2\pi r_{0n}\rho)\big].\end{aligned} \tag{3.40}$$

It is obvious that a field with such a structure is partially coherent.

We will now find the cross-spectral density of the propagation-invariant field of the second kind. First of all, we note that there is a twofold degeneracy for the modal functions given by Eq. (3.40) (except for the case $n = 0$), considered as the

solutions (eigenfunctions) of the Fredholm integral equation (1.19). Indeed, if the function (3.40) satisfies Eq. (1.19) with an eigenvalue λ_n, the functions

$$\varphi'_n(\rho, \theta) = \mathrm{i}^n 2\pi r_{0n} q_{nn} \exp(\mathrm{i}n\theta)\, J_n(2\pi r_{0n}\rho), \tag{3.41}$$

and

$$\varphi''_n(\rho, \theta) = \mathrm{i}^{-n} 2\pi r_{0n} q^*_{nn} \exp(-\mathrm{i}n\theta)\, J_{-n}(2\pi r_{0n}\rho) \tag{3.42}$$

do the same. Then, substituting for φ_n from Eqs. (3.41) and (3.42) into Eq. (1.18) and taking into account relation (3.39), we find that the cross-spectral density function of any propagation field of the second kind is

$$\begin{aligned} W_{\mathrm{II}}(\rho_1, \theta_1, \rho_2, \theta_2) = {} & \lambda_0 4\pi^2 r_{00}^2 |q_{00}|^2 J_0(2\pi r_{00}\rho_1) J_0(2\pi r_{00}\rho_2) \\ & + 2\sum_{n=1}^{\infty} \lambda_n 4\pi^2 r_{0n}^2 |q_{nn}|^2 \cos[n(\theta_1 - \theta_2)] \\ & \times J_n(2\pi r_{0n}\rho_1) J_n(2\pi r_{0n}\rho_2). \end{aligned} \tag{3.43}$$

An interesting particular case of Eq. (3.43) may be obtained if we put $r_{0n} = r_0$ and choose $\lambda_n = 1/4\pi^2 r_{0n}^2 |q_{nn}|^2$. In this case, in accordance with the summation theorem of Bessel functions,[71]

$$J_0\left[a(\rho_1^2 + \rho_2^2 - 2\rho_1\rho_2\cos\alpha)^{1/2}\right] = \sum_{\mu=-\infty}^{\infty} J_\mu(a\rho_1 x)\, J_\mu(a\rho_2) \exp(i\mu\alpha), \tag{3.44}$$

we obtain

$$W_{\mathrm{II}}(\rho_1, \theta_1, \rho_2, \theta_2) = J_0\left\{2\pi r_0\left[\rho_1^2 + \rho_2^2 - 2\rho_1\rho_2\cos(\theta_1 - \theta_2)\right]^{1/2}\right\}. \tag{3.45}$$

As we have already seen (see Section 1.6.3), the field with the cross-spectral density function given by Eq. (3.45) is the well-known Bessel-correlated secondary source or, what is more appropriate in our case, the *Bessel-correlated beam*.[9]

To clarify the physical nature of the propagation-invariant fields of the second kind, we calculate the 4D Fourier transform of Eq. (3.45). It may be readily shown that

$$\widetilde{W}_{\mathrm{II}}(r_1, \phi_1, r_2, \phi_2) = \delta(r_1 - r_0)\,\delta(r_2 - r_0)\,\delta(\phi_1 - \phi_2). \tag{3.46}$$

Hence, we come to the following conclusion: *the Bessel-correlated beam represents the superposition of the plane waves, whose wave vectors lie on the conical surface with the vertex angle* $\gamma = \tan^{-1}[(k/2\pi r_0)^2 - 1]^{-1/2}$*; these waves are completely uncorrelated in the azimuthal direction.*

3.4.3 Propagation-invariant fields of the third kind

Our third choice for the parameters q_{np} and r_{0n} is

$$q_{np} = \begin{cases} q_{n\mu} & \text{for } p = \mu, \\ q^*_{n\mu} & \text{for } p = -\mu, \\ 0 & \text{for } p \neq \pm\mu, \end{cases} \tag{3.47a}$$

$$r_{0n} = \frac{\alpha_{\mu,n+1}}{2\pi R}, \tag{3.47b}$$

where μ is any positive integer, which will be further referred to as the *order* of the propagation-invariant field of the third kind, and $\alpha_{\mu,n+1}$ is the $(n+1)$th zero of the Bessel function J_μ. Using the orthonormality relation for the Bessel function,[72]

$$\int_0^R J_\mu\left(\alpha_{\mu,n+1}\frac{\rho}{R}\right) J_\mu\left(\alpha_{\mu,m+1}\frac{\rho}{R}\right) \rho \mathrm{d}\rho = \delta_{nm}\frac{R^2}{2} J^2_{\mu+1}\left(\alpha_{\mu,n+1}\right), \tag{3.48}$$

and taking q_{np} so that

$$\left|q_{n\mu}\right|^2 = \left[\pi\alpha^2_{\mu,n+1} J^2_{\mu+1}\left(\alpha_{\mu,n+1}\right)\right]^{-1}, \tag{3.49}$$

one may readily verify that the choice (3.47) also satisfies the orthonormality condition (3.30). Then, substituting for q_{np} and r_{0n} from Eq. (3.47) into Eq. (3.27), we find that the coherent-mode structure of a propagation-invariant field of the third kind and of the order μ is described by the set of modal functions

$$\varphi^{(\mu)}_n(\rho,\theta) = \frac{\alpha_{\mu,n+1}}{R}\left[\mathrm{i}^{\mu} q_{n\mu} \exp\left(\mathrm{i}\mu\theta\right) J_\mu\left(\alpha_{\mu,n+1}\frac{\rho}{R}\right) + \mathrm{i}^{-\mu} q^*_{n\mu} \exp\left(-\mathrm{i}\mu\theta\right) J_{-\mu}\left(\alpha_{\mu,n+1}\frac{\rho}{R}\right)\right]. \tag{3.50}$$

As may be seen, the propagation-invariant fields of the third kind are also partially coherent. Reasoning in respect of functions (3.50) as done in the previous case (with the only difference that, in this case, there is a twofold degeneracy for all n), it may be readily shown that the cross-spectral density function of any propagation-invariant field of the third kind and of the order μ is

$$W^{(\mu)}_{\mathrm{III}}(\rho_1,\theta_1,\rho_2,\theta_2) = \cos\left[\mu(\theta_1-\theta_2)\right] \sum_{n=0}^{\infty} \lambda^{(\mu)}_n \left(\frac{\alpha_{\mu,n+1}}{R}\right)^2 \left|q_{n\mu}\right|^2 \times J_\mu\left(\alpha_{\mu,n+1}\frac{\rho_1}{R}\right) J_\mu\left(\alpha_{\mu,n+1}\frac{\rho_2}{R}\right). \tag{3.51}$$

Interesting examples of propagation-invariant fields of the third kind may be given by choosing $\lambda_n^{(\mu)} = R^2/\alpha_{\mu,n+1}^2 |q_{n\mu}|^2$. In this case, Eq. (3.51) takes the form

$$W_{\mathrm{III}}^{(\mu)}(\rho_1, \theta_1, \rho_2, \theta_2) = \cos[\mu(\theta_1 - \theta_2)] \sum_{n=0}^{\infty} J_\mu\left(\alpha_{\mu,n+1}\frac{\rho_1}{R}\right) J_\mu\left(\alpha_{\mu,n+1}\frac{\rho_2}{R}\right), \tag{3.52}$$

and the corresponding power spectrum is

$$S_{\mathrm{III}}^{(\mu)}(\rho, \theta) = \sum_{n=0}^{\infty} J_\mu^2\left(\alpha_{\mu,n+1}\frac{\rho_1}{R}\right). \tag{3.53}$$

In order to have a clear view of the optical fields represented by Eq. (3.52), we performed the numerical calculation of the power spectrum distribution given by Eq. (3.53) for the first two orders μ, truncating the summation with respect to the index n by different values of the number N of zeros of the Bessel function taken from Ref. 73. The results of this calculation are shown in Fig. 3.1. As one may conclude from this figure, when N tends to infinity, the propagation-invariant field with the power spectrum $S_{\mathrm{III}}^{(0)}$ represents an infinitely thin light beam, and the propagation-invariant field with the power spectrum $S_{\mathrm{III}}^{(1)}$ represents an infinitely thin light tube. In this sense, we term these fields as the *light string beam* and the *light capillary beam*, respectively.

To clarify the physical nature of the light string and light capillary beams, we consider the 4D Fourier transform of Eq. (3.52). It can be readily shown that

$$\widetilde{W}_{\mathrm{III}}^{(0)}(r_1, \phi_1, r_2, \phi_2) = \sum_{n=0}^{\infty} \left(\frac{R}{\alpha_{0,n+1}}\right)^2 \delta\left(r_1 - \frac{\alpha_{0,n+1}}{2\pi R}\right) \delta\left(r_2 - \frac{\alpha_{0,n+1}}{2\pi R}\right) \tag{3.54}$$

and

$$\widetilde{W}_{\mathrm{III}}^{(1)}(r_1, \phi_1, r_2, \phi_2) = \cos(\phi_1 - \phi_2) \sum_{n=0}^{\infty} \left(\frac{R}{\alpha_{1,n+1}}\right)^2 \delta\left(r_1 - \frac{\alpha_{1,n+1}}{2\pi R}\right)$$

$$\times \delta\left(r_2 - \frac{\alpha_{1,n+1}}{2\pi R}\right). \tag{3.55}$$

Hence, we come to the following conclusions: (i) *the light string beam represents the superposition of the plane waves whose wave vectors lie on the conical surfaces with the vertex angles* $\gamma_n = \tan^{-1}[(kR/\alpha_{0,n+1})^2 - 1]^{-1/2}$, and *these waves are completely uncorrelated in the radial direction, i.e., for different cones, but are completely correlated in the azimuthal direction within each cone*; (ii) *the light capillary beam represents the superposition of the plane*

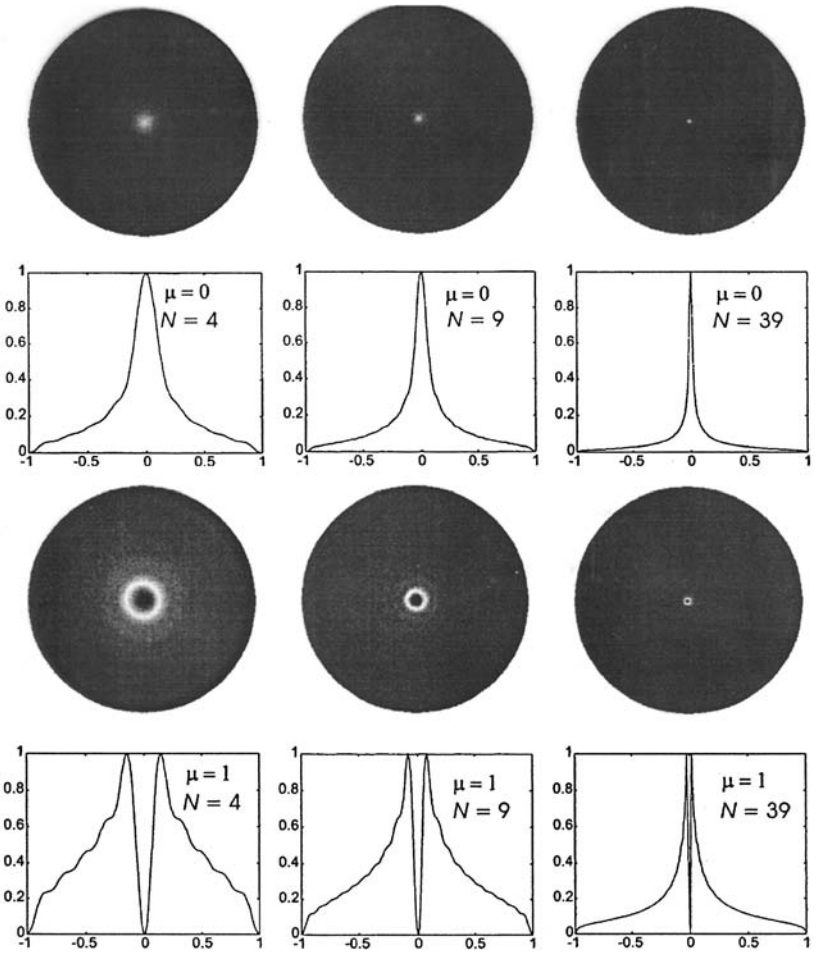

Figure 3.1 Power spectrums and their cross sections calculated in accordance with Eq. (3.53) for different orders μ and different values of truncating parameter N.

waves whose wave vectors lie on the conical surfaces with the vertex angles $\gamma_n = \tan^{-1}[(kR/\alpha_{1,n+1})^2 - 1]^{-1/2}$ *and these waves are completely uncorrelated in the radial direction, i.e., for different cones, but are partially correlated in the azimuthal direction within each cone in accordance with the* $\cos\phi$ *law.*

3.5 Generation of Propagation-Invariant Fields

Let us consider an optical system with a single positive lens, shown in Fig. 3.2, and let $W(\mathbf{x}_1, \mathbf{x}_2)$ be the cross-spectral density function of the field in the input plane of the system. Repeating the analysis made in Section 2.2 for z_1 and z_2 equal to the focal length f of the lens, one may readily find that the cross-spectral density

function in the output plane of this system is described by the expression

$$W\left(\mathbf{x}_1', \mathbf{x}_2'\right) = \iint_{-\infty}^{\infty} W\left(\mathbf{x}_1, \mathbf{x}_2\right) \exp\left[-\mathrm{i}\frac{k}{f}\left(\mathbf{x}_1' \cdot \mathbf{x}_1 - \mathbf{x}_2' \cdot \mathbf{x}_2\right)\right] \mathrm{d}\mathbf{x}_1 \mathrm{d}\mathbf{x}_2, \tag{3.56}$$

which is the 4D Fourier transform of the cross-spectral density function $W(\mathbf{x}_1, \mathbf{x}_2)$. On the other hand, as can be seen from Section 3.1, the propagation-invariant field is characterized by the specific form of the function $\widetilde{W}$, which is a 4D Fourier transform of the corresponding cross-spectral density function. Both of these facts can be used to generate a propagation-invariant field by producing a secondary planar source with a cross-spectral density function $W_S = \widetilde{W}$ in the front focal plane of the Fourier-transforming lens. Below we show how it may be done in order to generate the special propagation-invariant fields considered in the previous section, and discuss the possibility of physical realization of the desired secondary sources as well as the physical limitations of the techniques of generating the propagation-invariant fields.

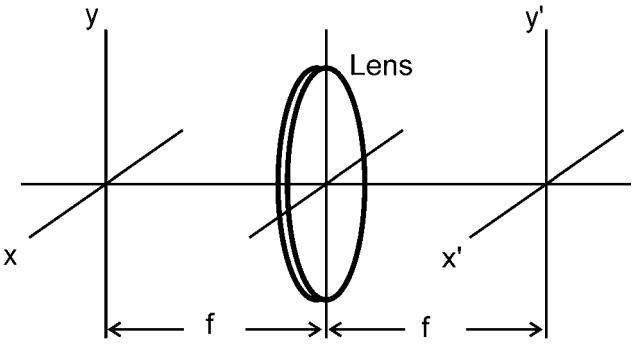

Figure 3.2 Fourier-transforming optical system.

In order to produce a secondary source with a cross-spectral density function $W_S = \widetilde{W}_{III}^{(0)}$, one may use a spatial light modulator with a complex amplitude transmittance that can be approximated as follows:

$$T(r, \phi) = T_0 \sum_{n=0}^{N-1} \frac{1}{\alpha_{0,n+1}} \delta\left(r - \alpha_{0,n+1} r_0\right) \exp\left(\mathrm{i}\Psi_n\right), \tag{3.57}$$

where (r, ϕ), this time, are the polar coordinates in the front focal plane of a Fourier-transforming lens, T_0 and r_0 are positive constants, and Ψ_n are statistically independent random variables that are uniformly distributed in the interval $[0, 2\pi]$. When illuminating this modulator by a homogeneous plane wave with an amplitude U_0, the cross-spectral density function at the output of the modulator is given by (see Section 2.2)

$$W_S(r_1, \phi_1, r_2, \phi_2) = U_0^2 \left\langle T^*(r_1, \phi_1)\, T(r_2, \phi_2) \right\rangle, \tag{3.58}$$

where the angle brackets denote the statistical average. Substituting for $T(r, \phi)$ from Eq. (3.57) into Eq. (3.58) and taking into account that, in accordance with the accepted statistical properties of random variables Ψ_n,

$$\langle \exp(-i\Psi_n) \exp(i\Psi_m) \rangle = \delta_{nm}, \tag{3.59}$$

we obtain

$$W_S(r_1, \phi_1, r_2, \phi_2) = U_0^2 T_0^2 \sum_{n=0}^{N-1} \frac{1}{\alpha_{0,n+1}^2} \delta\left(r_1 - \alpha_{0,n+1} r_0\right) \delta\left(r_2 - \alpha_{0,n+1} r_0\right). \tag{3.60}$$

Hence, the cross-spectral density function in the back focal plane of the Fourier-transforming lens will be of the form

$$W(\rho_1, \theta_1, \rho_2, \theta_2) = U_0^2 T_0^2 \left(\frac{r_0}{2\pi}\right)^2 \sum_{n=0}^{N-1} J_0\left(\alpha_{0,n+1} \frac{k r_0}{f} \rho_1\right) J_0\left(\alpha_{0,n+1} \frac{k r_0}{f} \rho_2\right). \tag{3.61}$$

As can be readily seen, Eq. (3.61) represents the finite sum approximation of Eq. (3.52) with $\mu = 0$, i.e., of the cross-spectral density function of the light string beam. It is obvious that the described technique can be used equally well for generating the fundamental Bessel beam. For this purpose, one must retain only one term of a sum in Eq. (3.57), say one with $n = 0$, and suppress the exponential factor.

In order to produce a secondary source with a cross-spectral density function $W_S = \widetilde{W}_{II}$, one may use a spatial light modulator with a complex amplitude transmittance that can be approximated as

$$T(r, \phi) = T_0 \delta(r - r_0) \exp[i\Psi(\phi)], \tag{3.62}$$

where, this time, the function $\Psi(\phi)$ for each value ϕ represents a random variable that is uniformly distributed in the interval $[0, 2\pi]$; the variables $\Psi(\phi_p)$ and $\Psi(\phi_s)$ are statistically independent for $p \neq s$. In this case, the cross-spectral density function of a secondary source will be exactly the same as given by Eq. (3.46) and, hence, the field with the cross-spectral density given by Eq. (3.45), i.e., the Bessel-correlated beam, will be generated in the back focal plane of the Fourier-transforming lens.

Finally, to produce the secondary source with a cross-spectral density $W_S = \widetilde{W}_{III}^{(1)}$, one may use a spatial light modulator with a complex amplitude transmittance that can be approximated as follows:

$$T(r, \phi) = T_0 \sum_{n=0}^{N-1} \frac{1}{\alpha_{1,n+1}} \delta\left(r - \alpha_{1,n+1} r_0\right) \{\exp[i\Phi_n(\phi)] + \exp[-i\Phi_n(\phi)]\}, \tag{3.63}$$

where

$$\Phi_n(\phi) = \begin{cases} 2\pi + \phi - \Psi_n & \text{for } 0 \leqslant \phi \leqslant \Psi_n, \\ \phi - \Psi_n & \text{for } \Psi_n \leqslant \phi \leqslant 2\pi, \end{cases} \tag{3.64}$$

and Ψ_n has the same meaning as in Eq. (3.57). Substituting for $T(r, \phi)$ from Eq. (3.63) into Eq. (3.58) and taking into account that

$$\left\langle \cos(\phi_1 + \Psi_n) \cos(\phi_2 + \Psi_m) \right\rangle = \delta_{nm} \cos(\phi_1 - \phi_2), \tag{3.65}$$

we come to the result

$$W_S(r_1, \phi_1, r_2, \phi_2) = U_0^2 T_0^2 \cos(\phi_1 - \phi_2) \sum_{n=0}^{N-1} \frac{1}{\alpha_{1,n+1}^2} \delta\left(r_1 - \alpha_{1,n+1} r_0\right) \times \delta\left(r_2 - \alpha_{1,n+1} r_0\right). \tag{3.66}$$

Hence, the cross-spectral density function in the back focal plane of the Fourier-transforming lens will be of the form

$$W(\rho_1, \theta_1, \rho_2, \theta_2) = U_0^2 T_0^2 \left(\frac{r_0}{2\pi}\right)^2 \cos(\theta_1 - \theta_2) \sum_{n=0}^{N-1} J_1\left(\alpha_{0,n+1} \frac{k r_0}{f} \rho_1\right) \times J_1\left(\alpha_{1,n+1} \frac{k r_0}{f} \rho_2\right). \tag{3.67}$$

As can be readily seen, Eq. (3.67) represents the finite sum approximation of Eq. (3.52) with $\mu = 1$, i.e., of the cross-spectral density function of the light capillary beam.

Now, we will briefly discuss the possibility of physical realization of space light modulators with the complex amplitude transmittance given by Eq. (3.57) or Eq. (3.63) (for more details see the next section). It is obvious that each of these modulators may be realized as a combination of a static amplitude-only modulator and a dynamic phase-only modulator with appropriate transmittance functions. The static amplitude-only modulator may be realized in a good approximation as a binary mask in the form of the transparent rings with the required radii and the widths proportional to the weight coefficients attached to the delta functions in Eqs. (3.57) and (3.63) (Fig. 3.3). Such a mask may be easily manufactured by means of a standard photolithographic technique. The dynamic phase-only modulator must represent a transparent plane screen that introduces the required azimuthal phase delays in the annular zones corresponding to the transparent rings of the binary mask that are changed randomly and independently in discrete moments of time (Fig. 3.4). As such a random phase screen, a liquid crystal display controlled by a computer may be used successfully.[74]

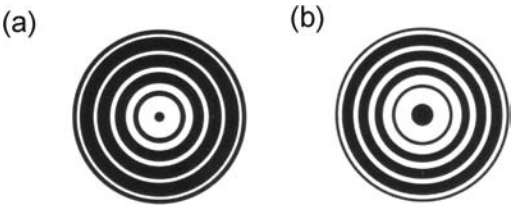

Figure 3.3 Binary masks for generating the (a) light string and (b) light capillary beams.

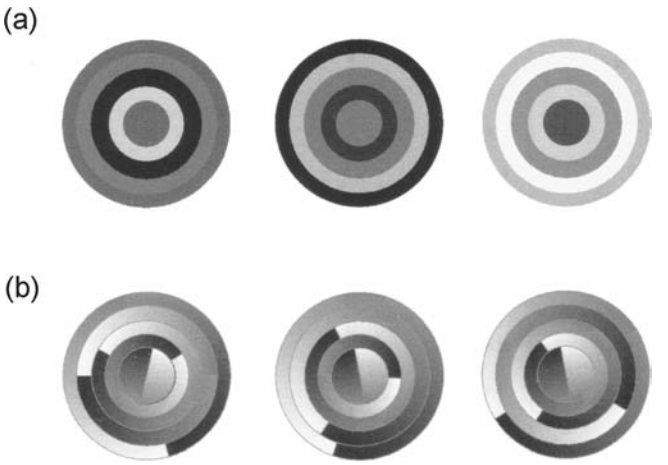

Figure 3.4 Different states of a ramdom phase screen for generating the (a) light string and (b) light capillay beams. The phase delay is presented by the gray level.

It is necessary to be aware that, in consequence of the finite aperture of a Fourier-transforming lens, the described techniques provide the propagation-invariant property of generated fields only in a finite range of distances z. This may be easily shown by the example of generating the fundamental Bessel beam sketched schematically in Fig. 3.5. As can be seen from this figure, the plane waves generated by each pair of points of the ring source overlap only within the dark shaded region. The depth of this region and, hence, the maximum range of the invariant propagation of the generated beam may be found by simple geometrical calculations as

$$z_{\max} = f\frac{R_0}{r_0}. \tag{3.68}$$

There are also other physical factors that affect the expected results. Thus, the finite thickness of transparent rings, used to produce the needed secondary source, violates the propagation-invariant condition, and a finite number of these rings results in an enlargement of the cross section of the light string and light capillary beams. Surely, the instrumental errors also affect the quality of fields to be generated.

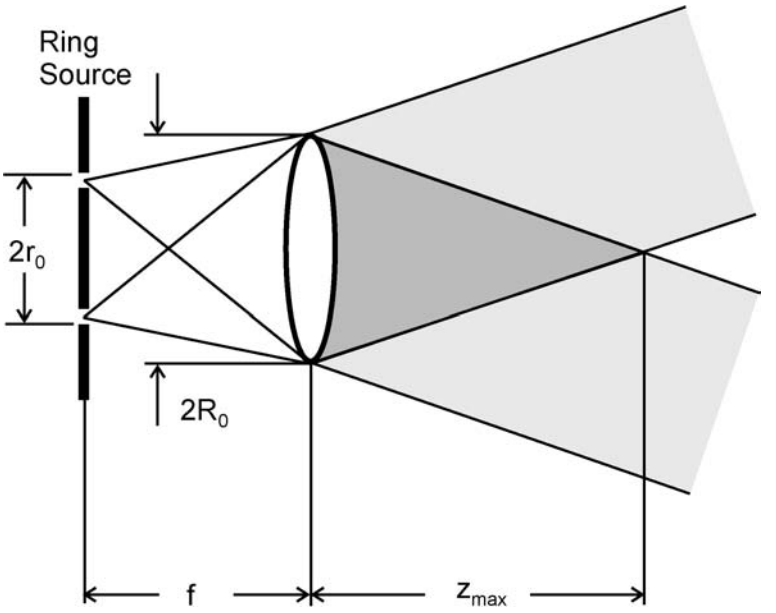

Figure 3.5 Invariant propagation region (dark shaded area) of generated propagation-invariant field.

3.6 Physical Simulation

In order to verify the practical feasibility of the techniques described in the previous section, we carried out two optical experiments on generating the light string and the light capillary beams. In these experiments, we used as a primary source an argon laser with linearly polarized radiation characterized by the wave length of 532 nm. To produce the needed secondary sources, we used binary masks with a finite number of transparent rings of variable width, which were specially manufactured by means of photolithographic technique. Taking into account a very fast decrease of the values $1/\alpha^2_{0,n+1}$ and $1/\alpha^2_{1,n+1}$ with n, to simplify our experiments, we limited the number of transparent rings to $N = 5$. As a dynamic phase modulator, we had available the commercial computer-controlled spatial light modulator HoloEye LC2002 constructed on the basis of a twisted nematic liquid crystal. This device has an active area of 26.2×20.0 mm, a spatial resolution of 832×624 pixels, and a frame frequency of 60 Hz in the SVGA mode. The configuration and control of the modulator were carried out with the aid of the included software. To provide the phase-only mode of modulation, we placed the liquid-crystal modulator between two polarizers with the orientation of the main axes recommended by the manufacturer as 44 deg and -54 deg, respectively. When doing this, we achieved approximately phase-only modulation of the optical field with a good linearity over the dynamic range of 1.8π. As can be seen from the analysis given in the previous section, the slight deviation of this range from the 2π value needed for the full-scaled phase modulation does not affect the expected results. At the same

time, the intensity distortions coupled with the phase modulation may violate the purity of the experiments. To reduce the factor of this undesirable intensity modulation up to the least possible value of 5%, we optimized the control parameters ("brightness" and "contrast") of the modulator.

In the first experiment, sketched schematically in Fig. 3.6, we tried to generate the light string beam. In this experiment, together with the liquid-crystal light modulator, we used a binary mask [Fig. 3.3(a)] with the geometric parameters given in Table 3.1. To control the liquid-crystal light modulator, we formed periodically changing with frequency of 60 Hz random video patterns of the form shown in Fig. 3.4(a). For a Fourier-transforming lens, we used a high-quality single lens with a 50-mm diameter and a focal length of 300 mm. We registered the transverse intensity distribution of the generated beam at different distances z behind the back focal plane of the Fourier-transforming lens. To provide a solid statistical average of the registered data, we used an exposure time of several seconds. The results of the experiment are shown in Fig. 3.7. As one can see from this figure, the generated beam may be approximately identified as the light string beam. The expansion of this beam, observed from a certain distance z, and its rather large diameter can be explained through reasons discussed at the end of the previous section.

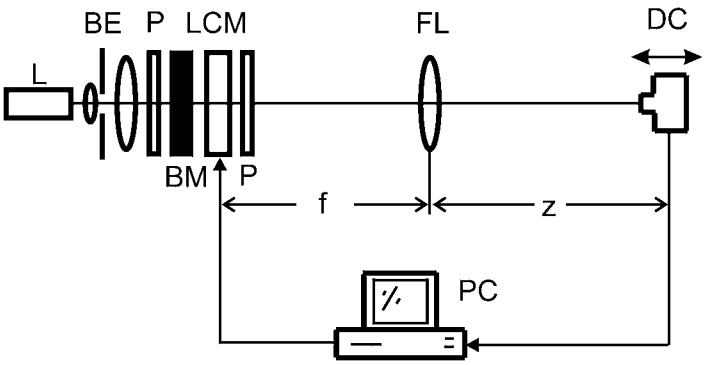

Figure 3.6 Experimental setup used for generating the light string beam: L laser; BE beam expander; P polarizer; BM binary mask; LCM liquid crystal modulator; FL Fourier-transforming lens; DC digital camera; PC personal computer.

Table 3.1 Parameters of binary mask I.

Ring number n	J_0 zero $\alpha_{0,n}$	Ring radius $r_{0,n}$ (mm)	Ring width $\Delta r_{0,n}$ (mm)
1	2.404	0.805	1.000
2	5.520	1.848	0.436
3	8.653	2.898	0.278
4	11.791	3.949	0.204
5	14.930	5.000	0.161

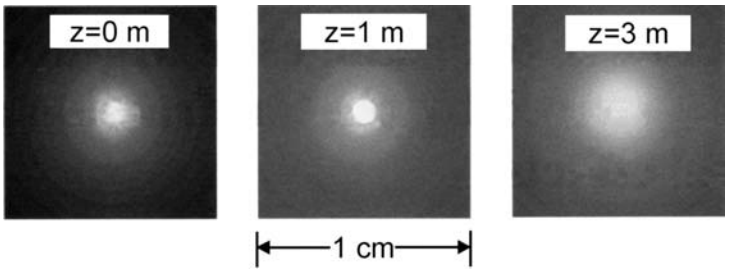

Figure 3.7 Results of the experiment on generating the light string beam.

In the second experiment, sketched schematically in Fig. 3.8, we tried to generate the light capillary beam. This time, we used a binary mask [Fig. 3.3(b)] with the geometric parameters given in Table 3.2, and controlled the liquid-crystal modulator by applying random video patterns of the form shown in Fig. 3.4(b). To provide a phase conjugation of the modulator transmittance in accordance with Eq. (3.63), we used a Mach-Zehnder interferometer with a Dove prism in one of its arms and a phase compensator in the other. In other respects, the experiment did not differ from the previous one. The results of the experiment are shown in Fig. 3.9. Notice that these results are somewhat worse than the previous ones; this can be explained by substantial difficulties of aligning the interferometric setup. Nevertheless, the beam generated in this experiment may be confidently identified as a certain approximation of the light capillary beam.

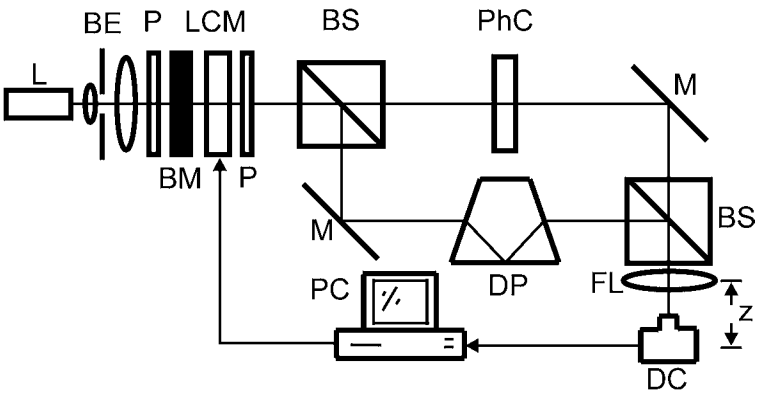

Figure 3.8 Experimental setup used for generating the light capillary beam: L laser; BE beam expander; P polarizer; BM binary mask; LCM liquid crystal modulator; BS beam splitter; M mirror; PhC phase compensator; DP Dove prism; FL Fourier-transforming lens; DC digital camera; PC personal computer.

Table 3.2 Parameters of binary mask II.

Ring number n	J_1 zero $\alpha_{1,n}$	Ring radius $r_{1,n}$ (mm)	Ring width $\Delta r_{1,n}$ (mm)
1	3.831	1.163	1.000
2	7.015	2.129	0.546
3	10.173	3.088	0.377
4	13.323	4.044	0.287
5	16.470	5.000	0.232

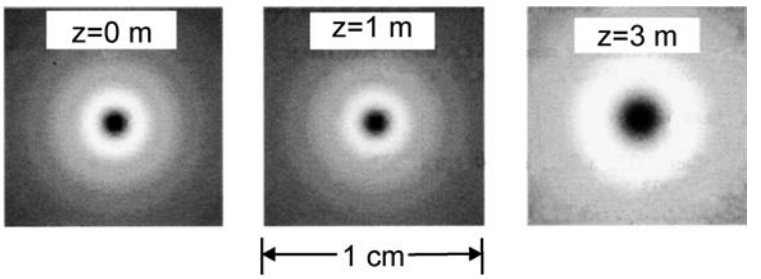

Figure 3.9 Results of the experiment on generating the light capillary beam.

3.7 Concluding Remarks

We have found the coherent-mode structure of the propagation-invariant field as a solution of the differential equation for propagation of the coherent modes of the field. Analyzing this solution, we have shown that three different kinds of propagation-invariant fields exist. Propagation-invariant fields of the first kind represent completely coherent fields, namely, nondiffracting Bessel beams or their linear combinations. Propagation-invariant fields of the second and the third kind are partially coherent fields with different coherent-mode structures. As a particular representative of the propagation-invariant fields of the second kind, the well-known Bessel-correlated beam with uniform power spectrum may be mentioned. Propagation-invariant fields of the third kind represent a new class of optical fields unknown before in the literature. We have deduced two interesting examples of such fields, termed by us light string and light capillary beams in view of a peculiar extremely sharply localized distribution of light energy in their transverse sections. It has been shown in theory and experimentally that light string and light capillary beams are physically realizable, at least in a good practical approximation. The extremely sharp transverse distribution of energy, coupled with a great depth of invariant propagation, allows us to expect that these beams could find many useful practical applications, for example, in optical communication, optical measurements, laser microtechnology, and microsurgery.

4

Coherent-Mode Representations in Radiometry

4.1 Introduction

During the last three decades, several attempts have been made to establish a relation between radiometry and physical optics.[75–123] These attempts have marked the beginning of a new theory that can be denominated as *modern radiometry*. The present state of this theory may be summarized as follows.

The fundamental primary quantity in *classical radiometry* is the *spectral radiant flux* $F(\nu)$ defined as the total power of radiation per unit frequency interval at frequency ν transported through some reference surface. The other radiometric quantities are defined as the corresponding spatial densities of the radiant flux on the basis of the *fundamental law of radiometry*, which, in the case of a planar source, may be written in the following form:[124]

$$F(\nu) = \int_{(2\pi)} \mathrm{d}\Omega \cos\theta \int_{(\sigma)} B(\mathbf{x}, \mathbf{s}, \nu)\, \mathrm{d}\mathbf{x} \tag{4.1a}$$

$$= \int_{(2\pi)} J(\mathbf{s}, \nu)\, \mathrm{d}\Omega \tag{4.1b}$$

$$= \int_{(\sigma)} E(\mathbf{x}, \nu)\, \mathrm{d}\mathbf{x}, \tag{4.1c}$$

where

$$B(\mathbf{x}, \mathbf{s}, \nu) = \frac{\mathrm{d}^2 F(\nu)}{\cos\theta \mathrm{d}\mathbf{x}\mathrm{d}\Omega} \tag{4.2}$$

is the surface-angular density of the radiant flux or the *radiance*,

$$J(\mathbf{s}, \nu) = \frac{\mathrm{d}F(\nu)}{\mathrm{d}\Omega} = \cos\theta \int_{(\sigma)} B(\mathbf{x}, \mathbf{s}, \nu)\, \mathrm{d}\mathbf{x} \tag{4.3}$$

is the angular density of the radiant flux or the *radiant intensity*, and

$$E(\mathbf{x}, \nu) = \frac{\mathrm{d}F(\nu)}{\mathrm{d}\mathbf{x}} = \int_{(2\pi)} B(\mathbf{x}, \mathbf{s}, \nu) \cos\theta \mathrm{d}\Omega \tag{4.4}$$

is the surface density of the radiant flux or the *radiant emittance*. In Eqs. (4.1)–(4.4), $\mathrm{d}\mathbf{x}$ is a source element at a point specified by the position vector $\mathbf{x}$, $\mathrm{d}\Omega$ is

an element of the solid angle around a direction specified by unit vector **s**, θ is the angle that the **s** direction makes with the unit normal **n** to the source plane, and the integrations extend over all source area σ and over the 2π solid angle formed by all the **s** directions that point into the hemisphere into which the radiation is propagating (Fig. 4.1). As one may see from these equations, radiance is the central quantity of the classical radiometry: all the other radiometric quantities are obtained by appropriate integration of the radiance. At the same time, as we already know, in physical optics the basic quantity of radiation is the cross-spectral density function defined alternatively (see Section 1.4) as

$$W(\mathbf{x}_1\mathbf{x}_2, \nu) = \left\langle U^*(\mathbf{x}_1, \nu)\, U(\mathbf{x}_2, \nu) \right\rangle, \tag{4.5}$$

where U is an optical signal associated with the field in the source plane, the asterisk denotes the complex conjugate, and the angle brackets denote an ensemble average.

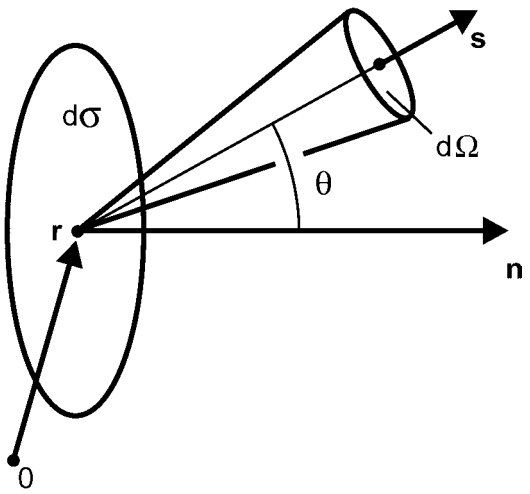

Figure 4.1 Notation relating to the definition of radiometric quantities.

It is evident that in order to connect classical radiometry with physical optics, it is necessary to establish the relation between the radiance $B(\mathbf{x}, \mathbf{s}, \nu)$, on one hand, and the cross-spectral density function $W(\mathbf{x}_1\mathbf{x}_2, \nu)$, on the other. The radiance $\widehat{B}(\mathbf{x}, \mathbf{s}, \nu)$ represented in terms of physical optics, i.e., expressed through $W(\mathbf{x}_1\mathbf{x}_2, \nu)$, received the denomination of *generalized radiance*. Surely, it may also be considered the *generalized radiant intensity* $\widehat{J}(\mathbf{s}, \nu)$, *generalized emittance* $\widehat{E}(\mathbf{x}, \nu)$, and *generalized flux* $\widehat{F}(\nu)$. The expression for the generalized radiance of a planar source has been obtained for the first time by Walther[75,80] in the following

form:

$$\widehat{B}(\mathbf{x},\mathbf{s},\nu)=\left(\frac{k}{2\pi}\right)^2\cos\theta\int_{(z=0)}W\left(\mathbf{x}+\frac{\mathbf{x}'}{2},\mathbf{x}-\frac{\mathbf{x}'}{2},\nu\right)\exp\left(-\mathrm{i}k\mathbf{s}_\perp\cdot\mathbf{x}'\right)\mathrm{d}\mathbf{x}', \tag{4.6}$$

where k is the wave number associated with the frequency ν, and $\mathbf{s}_\perp$ is the 2D vector obtained by projecting the 3D unit vector $\mathbf{s}$ onto the source plane. Somewhat later, Marchand and Wolf, making use of an analogous representation, derived the corresponding formulas for the generalized radiant emittance and generalized radiance intensity,[82]

$$\widehat{E}(\mathbf{x},\nu)=\frac{k^2}{2\sqrt{2\pi}}\int_{(z=0)}W\left(\mathbf{x}+\frac{\mathbf{x}'}{2},\mathbf{x}-\frac{\mathbf{x}'}{2},\nu\right)\frac{J_{3/2}\left(k\left|\mathbf{x}'\right|\right)}{\left(k\left|\mathbf{x}'\right|\right)^{3/2}}\mathrm{d}\mathbf{x}' \tag{4.7}$$

and

$$\widehat{J}(\mathbf{s},\nu)=\left(\frac{k}{2\pi}\right)^2\cos^2\theta\iint_{(z=0)}W(\mathbf{x}_1\mathbf{x}_2,\nu)\exp[-\mathrm{i}k(\mathbf{s}_\perp\cdot\mathbf{x}_1'-\mathbf{s}_\perp\cdot\mathbf{x}_1')]\mathrm{d}\mathbf{x}_1'\mathrm{d}\mathbf{x}_2', \tag{4.8}$$

where $J_{3/2}$ denotes the Bessel function of the first kind and of the order $3/2$. Unfortunately, as it can readily be shown, the generalized radiance and generalized emittance given by Eqs. (4.6) and (4.7), in the general case, may take on negative values, a result that is in contradiction to the physical meaning attributed to these quantities as the corresponding densities of the total power of radiation.[82] On these grounds, Wolf comes to the conclusion that both the generalized radiance (4.6) and the generalized radiant emittance (4.7) do not represent physically measurable quantities.[91] It is quite natural that such a conclusion leaves a certain doubt about the practical value of these results in the context of experimental radiometry (see, e.g., Ref. 110). To complete the statement Friberg[96] has proved a theorem that states, in particular, that there is no generalized radiance $\widehat{B}(\mathbf{x},\mathbf{s},\nu)$ that depends linearly on $W(\mathbf{x}_1\mathbf{x}_2,\nu)$ and simultaneously satisfies the condition of nonnegativeness for all $\mathbf{x}$ and $\mathbf{s}$.

The situation has been improved by Martínez-Herrero and Mejías,[102,106] and partially by the author,[122] who proposed a new generalized radiance that is expressed in terms of the coherent-mode representation of the cross-spectral density function and satisfies the nonnegativeness condition. The author has also shown[123] that such a radiance, under certain conditions, obeys the fundamental radiative transfer law. These results are given below.

4.2 Generalized Radiant Flux

Let us consider a stationary quasi-monochromatic planar source occupying a finite domain D in the plane $z=0$ and radiating into the free half-space $z>0$.

Let $W(\mathbf{x}_1, \mathbf{x}_2)$ be the transverse cross-spectral density function of this source in the plane $z = 0$ (from now on, we omit the explicit dependence of the considered quantities on the frequency ν). Then the cross-spectral density function of the radiated field is given by Eq. (1.17), which, for the sake of convenience, we reproduce here again as

$$W(\mathbf{r}_1, \mathbf{r}_2) = \left(\frac{k}{2\pi}\right)^2 \iint_D W(\mathbf{x}_1, \mathbf{x}_2) \frac{\exp[\mathrm{i}k(R_2 - R_1)]}{R_1 R_2} \cos\theta_1 \cos\theta_2 \mathrm{d}\mathbf{x}_1 \mathrm{d}\mathbf{x}_2, \tag{4.9}$$

where the meaning of parameters R_1, R_2, θ_1, and θ_2 becomes clear from the geometry shown in Fig. 1.1. Hence, the power spectrum of the radiated field is

$$\begin{aligned} S(\mathbf{r}) &= W(\mathbf{r}, \mathbf{r}) \\ &= \left(\frac{k}{2\pi}\right)^2 \iint_D W(\mathbf{x}_1, \mathbf{x}_2) \frac{\exp[\mathrm{i}k(R_2' - R_1')]}{R_1' R_2'} \cos\theta_1' \cos\theta_2' \mathrm{d}\mathbf{x}_1 \mathrm{d}\mathbf{x}_2, \end{aligned} \tag{4.10}$$

where R_1', R_2', and θ differ from the parameters in Eq. (4.9) in accordance with the new geometry shown in Fig. 4.2.

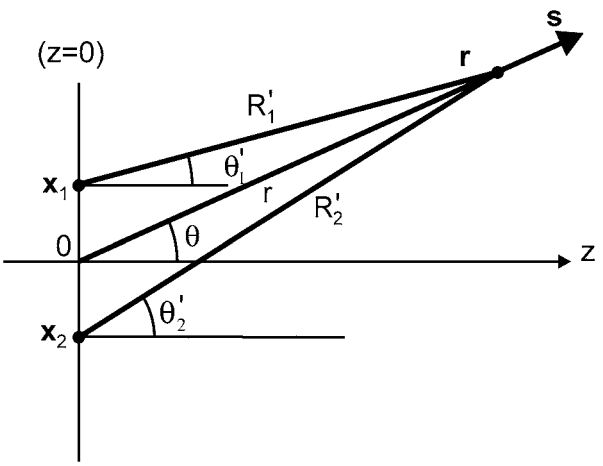

Figure 4.2 Notation relating to Eq. (4.10).

We suppose now that the point $\mathbf{r}$ is moved away from the source plane at a sufficiently large distance. Then the following approximations may be accepted:

$$R_1' \approx r - \mathbf{x}_1 \cdot \mathbf{s}_\perp, \qquad R_2' \approx r - \mathbf{x}_2 \cdot \mathbf{s}_\perp \tag{4.11}$$

in the exponential function of Eq. (4.10);

$$R_1' \approx R_2' \approx r \tag{4.12}$$

in the denominator under the integral of Eq. (4.10) (for the difference of these approximations, see the details of paraxial approximation in Section 2.2). In Eqs. (4.11) and (4.12), $r = |\mathbf{r}|$ and $\mathbf{s}_\perp$ is the 2D projection of the unit vector $\mathbf{s}$ onto the source plane. The so-called *far-zone approximation* $S^{(\infty)}(\mathbf{r})$ of the power spectrum (4.10) is given by

$$S^{(\infty)}(r\mathbf{s}) = \left(\frac{k}{2\pi}\right)^2 \frac{\cos^2\theta}{r^2} \iint_D W(\mathbf{x}_1, \mathbf{x}_2) \exp[-\mathrm{i}k\mathbf{s}_\perp \cdot (\mathbf{x}_2 - \mathbf{x}_1)] \mathrm{d}\mathbf{x}_1 \mathrm{d}\mathbf{x}_2, \tag{4.13}$$

where the vector $\mathbf{r}$ in the argument of function $S^{(\infty)}$, for clarity, is changed for $r\mathbf{s}$.

In accordance with the physical meaning of the radiant flux on one hand and the physical meaning of the power spectrum on the other, it is natural to accept as the definition of generalized radiant flux the far-zone spectrum $S^{(\infty)}(r\mathbf{s})$ integrated over a spherical surface in the solid angle of 2π, i.e.,

$$\widehat{F} = \int_{(2\pi)} r^2 S^{(\infty)}(r\mathbf{s}) \, \mathrm{d}\Omega. \tag{4.14}$$

On substituting for $S^{(\infty)}(r\mathbf{s})$ from Eq. (4.13) into definition (4.14), we obtain the following formula for the generalized radiant flux:

$$\widehat{F} = \left(\frac{k}{2\pi}\right)^2 \int_{(2\pi)} \mathrm{d}\Omega \cos^2\theta \iint_{(z=0)} W(\mathbf{x}_1, \mathbf{x}_2) \exp[-\mathrm{i}k\mathbf{s}_\perp \cdot (\mathbf{x}_2 - \mathbf{x}_1)] \mathrm{d}\mathbf{x}_1 \mathrm{d}\mathbf{x}_2, \tag{4.15}$$

where the integration over the coordinates $\mathbf{x}_1$ and $\mathbf{x}_2$ is formally extended to the whole plane $z = 0$, since function $W(\mathbf{x}_1, \mathbf{x}_2)$ has zero values for points located outside the source region. This formula will be used in the next section when constructing the coherent-mode representation of the generalized radiance.

4.3 Coherent-Mode Representation of Radiometric Quantities

In order to construct the coherent-mode representation of radiometric quantities, we recall at first the coherent-mode representation of the cross-spectral density function (1.18) and rewrite it for a planar secondary source as

$$W(\mathbf{x}_1, \mathbf{x}_2) = \sum_n \lambda_n \varphi_n^*(\mathbf{x}_1) \, \varphi_n(\mathbf{x}_2), \tag{4.16}$$

where λ_n are the eigenvalues and $\varphi_n(\mathbf{x})$ are the eigenfunctions of the Fredholm integral equation

$$\int_D W(\mathbf{x}_1, \mathbf{x}_2) \, \varphi_n(\mathbf{x}_1) \, \mathrm{d}\mathbf{x}_1 = \lambda_n \varphi_n(\mathbf{x}_2), \tag{4.17}$$

furthermore,

$$\lambda_n^* = \lambda_n \geqslant 0 \tag{4.18}$$

and

$$\int_D \varphi_n^*(\mathbf{x})\varphi_m(\mathbf{x})\mathrm{d}\mathbf{x} = \delta_{nm}. \tag{4.19}$$

It is obvious that Eq. (4.16) may be formally written in the form

$$W(\mathbf{x}_1, \mathbf{x}_2) = \int_{(z=0)} \chi(\mathbf{x}) \sum_n \lambda_n \varphi_n^*(\mathbf{x}_1)\, \varphi_n(\mathbf{x}_2)\, |\psi_n(\mathbf{x})|^2\, \mathrm{d}\mathbf{x}, \tag{4.20}$$

where $\chi(\mathbf{x})$ is a *characteristic function of the source*, defined as

$$\chi(\mathbf{x}) = \begin{cases} 1 & \text{for } \mathbf{x} \in D, \\ 0 & \text{for } \mathbf{x} \notin D, \end{cases} \tag{4.21}$$

and $\psi_n(\mathbf{x})$ are some arbitrary functions that form an orthonormal set in the domain D, i.e.,

$$\int_D \psi_n^*(\mathbf{x})\psi_m(\mathbf{x})\,\mathrm{d}\mathbf{x} = \delta_{nm}. \tag{4.22}$$

Then, substituting for $W(\mathbf{x}_1, \mathbf{x}_2)$ from Eq. (4.20) into Eq. (4.15), we obtain

$$\widehat{F} = \left(\frac{k}{2\pi}\right)^2 \int_{(2\pi)} \mathrm{d}\Omega \cos^2\theta \iiint_{(z=0)} \chi(\mathbf{x}) \sum_n \lambda_n \varphi_n^*(\mathbf{x}_1)\, \varphi_n(\mathbf{x}_2)\, |\psi_n(\mathbf{x})|^2 \times \exp[-\mathrm{i}k\mathbf{s}_\perp \cdot (\mathbf{x}_2 - \mathbf{x}_1)]\mathrm{d}\mathbf{x}\mathrm{d}\mathbf{x}_1\mathrm{d}\mathbf{x}_2. \tag{4.23}$$

Finally, changing the order of summation and integration and calculating the integrals with respect to $\mathbf{x}_1$and $\mathbf{x}_2$, we find

$$\widehat{F} = \left(\frac{k}{2\pi}\right)^2 \int_{(2\pi)} \mathrm{d}\Omega \cos^2\theta \int_{(z=0)} \chi(\mathbf{x}) \sum_n \lambda_n |\psi_n(\mathbf{x})|^2 \left|\widetilde{\varphi}_n\left(\frac{k}{2\pi}\mathbf{s}_\perp\right)\right|^2 \mathrm{d}\mathbf{x}, \tag{4.24}$$

where

$$\widetilde{\varphi}_n(\mathbf{u}) = \int_{-\infty}^{\infty} \varphi_n(\mathbf{x}) \exp(-\mathrm{i}2\pi\mathbf{u}\cdot\mathbf{x})\,\mathrm{d}\mathbf{x} \tag{4.25}$$

is the 2D Fourier transform of function $\varphi_n(\mathbf{x})$. As can be easily seen, Eq. (4.24) represents the general flux as the sum of the elementary contributions

$$\widehat{F}_n = \left(\frac{k}{2\pi}\right)^2 \int_{(2\pi)} \mathrm{d}\Omega \cos^2\theta \int_{(z=0)} \chi(\mathbf{x})\, \lambda_n |\psi_n(\mathbf{x})|^2 \left|\widetilde{\varphi}_n\left(\frac{k}{2\pi}\mathbf{s}_\perp\right)\right|^2 \mathrm{d}\mathbf{x}. \tag{4.26}$$

In order to attribute certain physical sense to these contributions, one may choose

$$\psi_n(\mathbf{x}) \equiv \varphi_n(\mathbf{x}). \tag{4.27}$$

In this case, Eq. (4.26) takes the form

$$\widehat{F} = \left(\frac{k}{2\pi}\right)^2 \int_{(2\pi)} \mathrm{d}\Omega \cos^2\theta \int_{(z=0)} \chi(\mathbf{x}) \sum_n \lambda_n |\varphi_n(\mathbf{x})|^2 \left|\widetilde{\varphi}_n\left(\frac{k}{2\pi}\mathbf{s}_\perp\right)\right|^2 \mathrm{d}\mathbf{x}, \tag{4.28}$$

which may be interpreted as representing the general radiance flux as a superposition of elementary radiant fluxes produced by the coherent modes of the source. In this sense, we will refer to Eq. (4.28) as the *coherent-mode representation of radiance flux*.

Now, we note that the generalized radiometric quantities must satisfy the same fundamental law of radiometry as do the radiometric quantities of the classical theory. Then, comparing consecutively Eq. (4.28) with Eqs. (4.1a)–(4.1c), we obtain the following *coherent-mode representations of radiance*, *radiant intensity*, and *radiant emittance*, respectively:

$$\widehat{\widehat{B}}(\mathbf{x}, \mathbf{s}) = \left(\frac{k}{2\pi}\right)^2 \cos\theta\chi(\mathbf{x}) \sum_n \lambda_n |\varphi_n(\mathbf{x})|^2 \left|\widetilde{\varphi}_n\left(\frac{k}{2\pi}\mathbf{s}_\perp\right)\right|^2; \tag{4.29}$$

$$\widehat{\widehat{J}}(\mathbf{s}) = \left(\frac{k}{2\pi}\right)^2 \cos^2\theta \sum_n \lambda_n \left|\widetilde{\varphi}_n\left(\frac{k}{2\pi}\mathbf{s}_\perp\right)\right|^2; \tag{4.30}$$

$$\widehat{\widehat{E}}(\mathbf{x}) = \left(\frac{k}{2\pi}\right)^2 \chi(\mathbf{x}) \sum_n \lambda_n Q_n |\varphi_n(\mathbf{x})|^2, \tag{4.31}$$

where

$$Q_n = \int_{(2\pi)} \cos^2\theta \left|\widetilde{\varphi}_n\left(\frac{k}{2\pi}\mathbf{s}_\perp\right)\right|^2 \mathrm{d}\Omega \tag{4.32}$$

and the double caret is used here to distinguish these representations from the corresponding generalized radiometric quantities given by Eqs. (4.6)–(4.8). For brevity, further on we will refer to the coherent-mode representations (4.29)–(4.31) as *modal radiometric characteristics* of the source. In conclusion, it is necessary to note that the modal radiometric characteristics defined by Eqs. (4.28)–(4.31) are always real and nonnegative and, hence, are true physically measurable quantities.

4.4 Free-Space Propagation of Modal Radiance

As is well known,[125] in a uniform medium that does not contain radiative sources or absorbers, the traditional radiance $B(\mathbf{x}, \mathbf{s}; z)$ of classical radiometry remains constant along straight lines, i.e., it obeys the *fundamental radiative transfer law* given by

$$\frac{\mathrm{d}}{\mathrm{d}s} B(\mathbf{x}, \mathbf{s}; z) = 0, \tag{4.33}$$

where $\mathrm{d}/\mathrm{d}s$ denotes the directional derivative. The question is: *does the modal radiance (4.29) obey the propagation law (4.33) for the traditional radiance of classical radiometry?* Here, we try to answer this question by deriving the equation for free-space propagation of the generalized radiance defined by Eq. (4.29).

As the starting point of our derivation, we use the following free-space propagation equation for the cross-spectral density $W(\mathbf{x}_1, \mathbf{x}_2; z)$ of a stationary field, obtained in Ref. 4 within the accuracy of the paraxial approximation:

$$\left(\nabla_{1\perp}^2 - \nabla_{2\perp}^2 + \mathrm{i}2k\frac{\partial}{\partial z}\right) W(\mathbf{x}_1, \mathbf{x}_2; z) = 0, \tag{4.34}$$

where $\nabla_{1\perp}^2$ and $\nabla_{2\perp}^2$ are the transverse Laplacian operators acting on coordinates $\mathbf{x}_1$ and $\mathbf{x}_2$, respectively. We recall that the cross-spectral density function $W_n(\mathbf{x}_1, \mathbf{x}_2; z)$ of each mode satisfies the same propagation equations, as does the cross-spectral density function $W(\mathbf{x}_1, \mathbf{x}_2; z)$ and, hence, we may write

$$\left(\nabla_{1\perp}^2 - \nabla_{2\perp}^2 + \mathrm{i}2k\frac{\partial}{\partial z}\right) \varphi_n^*(\mathbf{x}_1; z)\, \varphi_n(\mathbf{x}_2; z) = 0. \tag{4.35}$$

On formally inverting the Fourier relationship (4.25) with respect to $\mathbf{x} = \mathbf{x}_2$ and $\mathbf{u} = k\mathbf{s}_\perp/2\pi$, and interchanging the orders of differentiation and integration, we may rewrite Eq. (4.35) as

$$\int \left(\nabla_{1\perp}^2 - \nabla_{2\perp}^2 + \mathrm{i}2k\frac{\partial}{\partial z}\right) \varphi_n^*(\mathbf{x}_1; z)\, \widetilde{\varphi}_n\left(\frac{k}{2\pi}\mathbf{s}_\perp; z\right) \exp(\mathrm{i}k\mathbf{s}_\perp \cdot \mathbf{x}_2)\mathrm{d}\mathbf{s}_\perp = 0, \tag{4.36}$$

where the integration is taken effectively over the $\mathbf{s}_\perp$ domain in which $|\mathbf{s}_\perp| \ll 1$. After straightforward application of the operator $\nabla_{2\perp}^2$ to Eq. (4.36), we obtain

$$\int \left(\nabla_{1\perp}^2 + k^2\mathbf{s}_\perp^2 + \mathrm{i}2k\frac{\partial}{\partial z}\right) \varphi_n^*(\mathbf{x}_1; z)\, \widetilde{\varphi}_n\left(\frac{k}{2\pi}\mathbf{s}_\perp; z\right) \exp(\mathrm{i}k\mathbf{s}_\perp \cdot \mathbf{x}_2)\mathrm{d}\mathbf{s}_\perp = 0. \tag{4.37}$$

Since Eq. (4.37) must hold for all $\mathbf{x}_2$, it follows that

$$\left(\nabla_\perp^2 + k^2\mathbf{s}_\perp^2 + \mathrm{i}2k\frac{\partial}{\partial z}\right) \varphi_n^*(\mathbf{x}; z)\, \widetilde{\varphi}_n\left(\frac{k}{2\pi}\mathbf{s}_\perp; z\right) = 0 \tag{4.38}$$

or, passing on to the conjugate expression,

$$\left(\nabla_{\perp}^{2}+k^{2}\mathbf{s}_{\perp}^{2}-\mathrm{i}2k\frac{\partial}{\partial z}\right)\varphi_{n}\left(\mathbf{x};z\right)\widetilde{\varphi}_{n}^{*}\left(\frac{k}{2\pi}\mathbf{s}_{\perp};z\right)=0. \tag{4.39}$$

Multiplying Eq. (4.38) by $\varphi_n(\mathbf{x};z)\widetilde{\varphi}_n^*(\frac{k}{2\pi}\mathbf{s}_\perp;z)$ and Eq. (4.39) by $\varphi_n^*(\mathbf{x};z)\widetilde{\varphi}_n(\frac{k}{2\pi}\mathbf{s}_\perp;z)$ and taking the difference of the results with due regard for

$$f^{*}\left(u\right)\frac{\mathrm{d}}{\mathrm{d}u}f\left(u\right)+f\left(u\right)\frac{\mathrm{d}}{\mathrm{d}u}f^{*}\left(u\right)=\frac{\mathrm{d}}{\mathrm{d}u}\left|f\left(u\right)\right|^{2} \tag{4.40}$$

and

$$f\left(\mathbf{u}\right)\nabla_{\perp}^{2}f^{*}\left(\mathbf{u}\right)-f^{*}\left(\mathbf{u}\right)\nabla_{\perp}^{2}f\left(\mathbf{u}\right)=\mathrm{i}2\mathrm{Im}\left[f\left(\mathbf{u}\right)\nabla_{\perp}^{2}f^{*}\left(\mathbf{u}\right)\right], \tag{4.41}$$

we come to the following equation:

$$\frac{\partial}{\partial z}\left|\varphi_{n}\left(\mathbf{x};z\right)\right|^{2}\left|\widetilde{\varphi}_{n}\left(\mathbf{s}_{\perp};z\right)\right|^{2}+\frac{1}{k}\left|\widetilde{\varphi}_{n}\left(\frac{k}{2\pi}\mathbf{s}_{\perp};z\right)\right|^{2}\mathrm{Im}\left[\varphi_{n}\left(\mathbf{x};z\right)\nabla_{\perp}^{2}\varphi_{n}^{*}\left(\mathbf{x};z\right)\right]=0. \tag{4.42}$$

Equation (4.42) holds for each coherent mode and, hence, multiplying it by $\lambda_n(k/2\pi)^2$ and then summing up the results with respect to the index n, we obtain, with due regard for definition (4.16),

$$\frac{\partial}{\partial z}\widehat{\widehat{B}}\left(\mathbf{x},\mathbf{s};z\right)+\frac{1}{k}Q\left(\mathbf{x},\mathbf{s};z\right)=0, \tag{4.43}$$

where

$$Q\left(\mathbf{x},\mathbf{s};z\right)=\left(\frac{k}{2\pi}\right)^{2}\sum_{n}\lambda_{n}\left|\widetilde{\varphi}_{n}\left(\frac{k}{2\pi}\mathbf{s}_{\perp};z\right)\right|^{2}\mathrm{Im}\left[\varphi_{n}\left(\mathbf{x};z\right)\nabla_{\perp}^{2}\varphi_{n}^{*}\left(\mathbf{x};z\right)\right]. \tag{4.44}$$

Within the accuracy of the paraxial approximation, we may set $s_z \approx 1$ and write the following operator relation:

$$\frac{\mathrm{d}}{\mathrm{d}s}\approx\mathbf{s}_{\perp}\cdot\nabla_{\perp}+\frac{\partial}{\partial z}. \tag{4.45}$$

In addition, it seems to be quite justifiable for any $z > 0$ within the used approximation to regard $\widehat{\widehat{B}}(\mathbf{x},\mathbf{s};z)$ as being a sufficiently smooth function of $\mathbf{x}$. Then, taking into account that $|\mathbf{s}_\perp| \ll 1$, Eq. (4.43) may be rewritten in a good approximation as

$$\frac{\mathrm{d}}{\mathrm{d}s}\widehat{\widehat{B}}\left(\mathbf{x},\mathbf{s};z\right)+\frac{1}{k}Q\left(\mathbf{x},\mathbf{s};z\right)=0, \tag{4.46}$$

which is the free-space propagation equation for the generalized radiance (4.29).

As can be seen, Eq. (4.46) differs by its form from the analogous Eq. (4.33) for the traditional radiance of classical radiometry. But it is necessary to keep in mind that classical radiometry deals with highly incoherent thermal sources that generate radiation, whose effective wavelengths λ are very small, compared to their linear dimensions.[125] Therefore, let us now examine the behavior of expression (4.46) in a *short-wavelength limit*, i.e., when $k \to \infty$.

Functions $\hat{\hat{B}}(\mathbf{x}, \mathbf{s}; z)$ and $Q(\mathbf{x}, \mathbf{s}; z)$ depend on k explicitly via factor $(k/2\pi)^2$ and implicitly via frequency-dependent quantities λ_n, $\varphi_n(\mathbf{x}_1; z)$, $\widetilde{\varphi}_n^*(\frac{k}{2\pi}\mathbf{s}_\perp; z)$. Let us assume that they admit the expansion into powers of $1/k$, viz.,

$$\hat{\hat{B}}(\mathbf{x}, \mathbf{s}; z) = \hat{\hat{B}}(\mathbf{x}, \mathbf{s}; z)\Big|_{1/k=0} + \sum_{m=1}^{\infty} \left[\frac{\mathrm{d}^m}{\mathrm{d}(1/k)^m} \hat{\hat{B}}(\mathbf{x}, \mathbf{s}; z)\right]\Bigg|_{1/k=0} \left(\frac{1}{k}\right)^m, \quad (4.47)$$

$$Q(\mathbf{x}, \mathbf{s}; z) = Q(\mathbf{x}, \mathbf{s}; z)|_{1/k=0} + \sum_{m=1}^{\infty} \left[\frac{\mathrm{d}^m}{\mathrm{d}(1/k)^m} Q(\mathbf{x}, \mathbf{s}; z)\right]\Bigg|_{1/k=0} \left(\frac{1}{k}\right)^m. \quad (4.48)$$

Then, inserting (4.47) and (4.48) into Eq. (4.46) and equating terms of the same power in $1/k$, we obtain, in the limit of large k,

$$\frac{\mathrm{d}}{\mathrm{d}s} \hat{\hat{B}}_0(\mathbf{x}, \mathbf{s}; z) = 0, \quad (4.49)$$

where

$$\hat{\hat{B}}_0(\mathbf{x}, \mathbf{s}; z) \equiv \hat{\hat{B}}(\mathbf{x}, \mathbf{s}; z)\Big|_{1/k=0} = \lim_{k\to\infty} \hat{\hat{B}}(\mathbf{x}, \mathbf{s}; z). \quad (4.50)$$

Equation (4.50) is the equation of radiative transfer in free space for the asymptotic radiance $\hat{\hat{B}}_0(\mathbf{x}, \mathbf{s}; z)$ corresponding to large k. Thus, in reply to the question posed in the beginning of the present section, we can conclude that *in the short-wavelength limit, the generalized radiance* $\hat{\hat{B}}(\mathbf{x}, \mathbf{s}; z)$ *defined by Eq. (4.29) remains invariant on propagation along the line through point* $\mathbf{x}$ *in the direction* $\mathbf{s}$*, i.e., it obeys the fundamental radiative transfer law of classical radiometry*.

Reverting to Eq. (4.46), one may hypothesize that for any finite k, the second term in its left-hand side corresponds to the fine spatial structure of the generalized radiance and, therefore, if the radiance is measured in such a way as to average out this detail, the result will satisfy Eq. (4.49). Then, the traditional radiance of classical radiometry, within the framework of the paraxial approximation, may be regarded as being an asymptotic short-wavelength limit of our generalized radiance (4.29).

4.5 Modal Radiometry of Gaussian Schell-Model Source

As an example of the application of the considered theory, we will calculate here the modal radiometric characteristics of the 1D Gaussian Schell-model source, whose coherent-mode representation was the subject of Section 1.6.1.

The coherent-mode structure of the 1D Gaussian Schell-model source is defined by Eqs. (1.54)–(1.61). For convenience, we recall it here, omitting the explicit dependence of the considered quantities on frequency ν as follows:

$$\varphi_n(x) = \left(\frac{2c}{\pi}\right)^{1/4} \frac{1}{\sqrt{2^n n!}} H_n\left(x\sqrt{2c}\right) \exp\left(-cx^2\right), \tag{4.51}$$

$$\lambda_n = S(0) \left(\frac{\pi}{a+b+c}\right)^{1/2} \left(\frac{b}{a+b+c}\right)^n, \tag{4.52}$$

where

$$a = \frac{1}{4\sigma_S^2}, \qquad b = \frac{1}{2\sigma_\mu^2}, \qquad c = \left(a^2 + 2ab\right)^{1/2}, \tag{4.53}$$

and H_n is the Hermite polynomial of order n. On making use of the relation[72]

$$\int_{-\infty}^{\infty} H_n(x) \exp\left(-\frac{x^2}{2}\right) \exp(\mathrm{i}ux)\,\mathrm{d}x = \mathrm{i}^n \sqrt{2\pi} H_n(u) \exp\left(-\frac{u^2}{2}\right), \tag{4.54}$$

one may readily find the 1D Fourier transform (4.25) with $u = ks/2\pi$ as

$$\widetilde{\varphi}_n\left(\frac{k}{2\pi}s\right) = (-\mathrm{i})^n \left(\frac{\pi}{2c}\right)^{1/4} \left(\frac{2}{2^n n!}\right)^{1/2} H_n\left(\frac{k}{\sqrt{2c}}s\right) \exp\left(-\frac{k^2}{4c}s^2\right). \tag{4.55}$$

Substituting for φ_n and $\widetilde{\varphi}_n$ from Eqs. (4.51) and (4.55), respectively, into 1D versions of Eqs. (4.29)–(4.31) with due regard for $s = \sin\theta$, we obtain the following expressions for modal radiometric characteristics of the 1D Gaussian Schell-model source:

$$\begin{aligned}\widehat{\widehat{B}}(x,\theta) = {} & \frac{k}{\pi} \exp\left(-2cx^2\right) \exp\left(-\frac{k^2}{2c}\sin^2\theta\right) \cos\theta \\ & \times \sum_n \frac{\lambda_n}{(2^n n!)^2} H_n^2\left(x\sqrt{2c}\right) H_n^2\left(\frac{k}{\sqrt{2c}}\sin\theta\right),\end{aligned} \tag{4.56}$$

$$\widehat{\widehat{J}}(\theta) = \frac{k}{\pi} \left(\frac{\pi}{2c}\right)^{1/2} \exp\left(-\frac{k^2}{2c}\sin^2\theta\right) \cos^2\theta \sum_n \frac{\lambda_n}{2^n n!} H_n^2\left(\frac{k}{\sqrt{2c}}\sin\theta\right), \tag{4.57}$$

$$\hat{\hat{E}}(x) = \frac{k}{\pi}\exp\left(-2cx^2\right)\sum_n \frac{\lambda_n}{2^n n!}H_n^2\left(x\sqrt{2c}\right) \times \int_0^1 \left(1-s^2\right)^{1/2} H_n^2\left(\frac{k}{\sqrt{2c}}s\right)\exp\left(-\frac{k^2}{2c}s^2\right)\mathrm{d}s, \qquad (4.58)$$

where λ_n are given by Eq. (4.52).

We performed a numerical calculation of the modal radiant intensity $\hat{\hat{J}}(\theta)$ and modal radiant emittance $\hat{\hat{E}}(x)$, given by Eqs. (4.57) and (4.58), for different values of the degree of global coherence γ of the source (see Section 1.6.1). In our calculations, we truncated the summation in the corresponding expressions by the effective number of coherent modes $\mathcal{N}$ given by Eq. (1.62). The results of this calculation are presented in Fig. 4.3. For comparison, the curves corresponding to a Lambertian source with Gaussian power spectrum are shown by dashed lines.

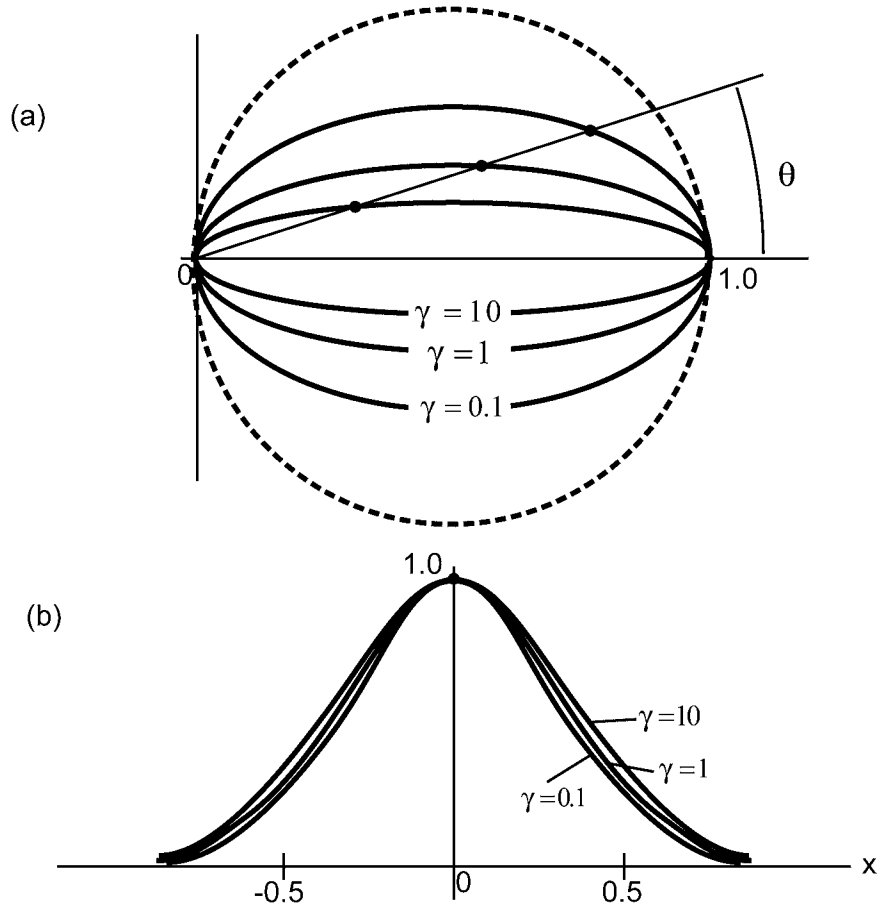

Figure 4.3 Normalized modal radiometric characteristics of Gaussian Schell-model source calculated for different values of the degree of global coherence γ: (a) modal radiant intensity; (b) modal radiant emittance.

As can be seen from Fig. 4.3(a), the more coherent is the source (the larger is γ), the more directional is its radiant intensity. At the same time, as can be seen from Fig. 4.3(b), the radiant emittance of the 1D Gaussian Schell-model source changes very slightly with variations of γ, taking on approximately a Gaussian form. These results are in complete agreement with the predictions of the theory.

4.6 Concluding Remarks

The coherent-mode representations considered in the present chapter express the radiometric quantities as superpositions of the corresponding elementary contributions produced by the coherent modes of the source, which makes them attractive from the standpoint of better understanding the physics of generating and propagating a partially coherent optical radiation. All of the modal radiometric characteristics are real positive quantities, which makes them attractive also from a standpoint of possible interpretation of the results of measurements in practical radiometry. Despite this, for inexplicable reasons, modal radiometric characteristics have not yet found their application. Nevertheless, we are sure they will gain their due place in optical science and practice. In confirmation of this, in particular, the modal radiance given by Eq. (4.29) will be efficiently used in the next chapter for constructing an alternative coherent-mode representation of a planar source with an unknown cross-spectral density function.

5

Alternative Coherent-Mode Representation of a Planar Source

5.1 Introduction

We recall the coherent-mode representation of the cross-spectral density function (1.18) and rewrite it for a planar secondary source, omitting an explicit dependence of the considered quantities on frequency ν, as follows:

$$W(\mathbf{x}_1, \mathbf{x}_2) = \sum_n \lambda_n \varphi_n^*(\mathbf{x}_1)\, \varphi_n(\mathbf{x}_2), \tag{5.1}$$

where λ_n are the eigenvalues and $\varphi_n(\mathbf{x})$ are the eigenfunctions of the Fredholm integral equation

$$\int_D W(\mathbf{x}_1, \mathbf{x}_2)\, \varphi_n(\mathbf{x}_1)\, d\mathbf{x}_1 = \lambda_n \varphi_n(\mathbf{x}_2). \tag{5.2}$$

The coherent-mode representation of the source is an essential tool in describing the processes and systems in optics. However, the practical value of this representation is essentially restricted. Really, in practice, the analytic expression for the cross-spectral density function $W(\mathbf{x}_1, \mathbf{x}_2)$, as a rule, is unknown and, hence, values λ_n and functions $\varphi_n(\mathbf{x})$ cannot be found as the solution of the Fredholm equation (5.2). Moreover, even when the cross-spectral density function is approximated by a certain analytic function, the solution of this equation in closed form may be obtained only for a very limited number of field models (see Section 1.6). Clearly, an alternative approach to the problem of the coherent-mode representation of the source, which does not involve the solution of the Fredholm equation (5.2), is desired. Here, we propose such an approach based on the replacement of an original source with an unknown cross-spectral density function by an alternative source with a cross-spectral density function that may be approximated according to the results of physical measurements.[126]

5.2 Alternative Source and its Coherent-Mode Structure

Owing to the nonlinear dependence of $B(\mathbf{x}, \mathbf{s})$ on eigenfunctions $\varphi_n(\mathbf{x})$, there may be found some *alternative radiatively equivalent source* that occupies the same

domain D in the plane $z = 0$, has another cross-spectral density function, but radiates into the half-space $z > 0$ with the same radiance function as does the original source. In order to describe such a source, we will introduce the function

$$\Psi(\mathbf{x}_1, \mathbf{x}_2) = \sum_{m=0}^{M-1} \mu_m \psi_m^*(\mathbf{x}_1)\, \psi_m(\mathbf{x}_2), \tag{5.3}$$

where μ_m are some arbitrary real positive values bounded from above, and $\psi_m(\mathbf{x})$ are some prescribed continuous functions that obey the orthonormality condition

$$\int_D \psi_n^*(\mathbf{x})\, \psi_m(\mathbf{x})\, \mathrm{d}\mathbf{x} = \delta_{nm}. \tag{5.4}$$

It may be readily shown that, in accordance with its construction, the function $\Psi(\mathbf{x}_1, \mathbf{x}_2)$ obeys the following conditions:

$$\iint_D |\Psi(\mathbf{x}_1, \mathbf{x}_2)|^2\, \mathrm{d}\mathbf{x}_1 \mathrm{d}\mathbf{x}_2 < \infty, \tag{5.5}$$

$$\Psi(\mathbf{x}_2, \mathbf{x}_1) = \Psi^*(\mathbf{x}_1, \mathbf{x}_2), \tag{5.6}$$

$$\iint_D \Psi(\mathbf{x}_1, \mathbf{x}_2)\, f^*(\mathbf{x}_1)\, f(\mathbf{x}_2)\, \mathrm{d}\mathbf{x}_1 \mathrm{d}\mathbf{x}_2 \geqslant 0, \tag{5.7}$$

where $f(\mathbf{x})$ is any square-integrable function. Conditions (5.5)–(5.7) imply that the function $\Psi(\mathbf{x}_1, \mathbf{x}_2)$ is square integrable, Hermitian, and nonnegative definite, respectively. These are just the same conditions that the cross-spectral density function of any steady state field obeys. Hence, the function $\Psi(\mathbf{x}_1, \mathbf{x}_2)$ may be considered as the cross-spectral density function $W_{\mathrm{A}}(\mathbf{x}_1, \mathbf{x}_2)$ of some alternative source, i.e.,

$$W_{\mathrm{A}}(\mathbf{x}_1, \mathbf{x}_2) = \sum_{m=0}^{M-1} \mu_m \psi_m^*(\mathbf{x}_1)\, \psi_m(\mathbf{x}_2). \tag{5.8}$$

Formally changing λ_n and $\varphi_n(\mathbf{x})$ in Eq. (4.29) for μ_m and $\psi_m(\mathbf{x})$, respectively, one may obtain the following expression for the radiance function of such an alternative source:

$$B_{\mathrm{A}}(\mathbf{x}, \mathbf{s}) = \left(\frac{k}{2\pi}\right)^2 \chi(\mathbf{x}) \cos\theta \sum_{m=0}^{M-1} \mu_m |\psi_m(\mathbf{x})|^2 \left|\widetilde{\psi}_m\left(\frac{k}{2\pi}\mathbf{s}_\perp\right)\right|^2, \tag{5.9}$$

where

$$\widetilde{\psi}_m\left(\frac{k}{2\pi}\mathbf{s}_\perp\right) = \int_{(z=0)} \psi_m(\mathbf{x}) \exp(-\mathrm{i}k\mathbf{s}_\perp \cdot \mathbf{x})\, \mathrm{d}\mathbf{x}. \tag{5.10}$$

Once the radiance function $B(\mathbf{x}, \mathbf{s})$ of the original source has been measured in a physical experiment, a good approximation of the alternative radiatively equivalent source may be obtained by solving the following problem of conditional optimization:

$$\int_{(2\pi)} \int_{(z=0)} [B(\mathbf{x}, \mathbf{s}) - B_{\mathrm{A}}(\mathbf{x}, \mathbf{s})]^2\, \mathrm{d}\mathbf{x}\mathrm{d}\Omega \longrightarrow \min_{\mu_m}, \qquad \mu_m > 0, \tag{5.11}$$

where $\mathrm{d}\Omega$ is the element of a solid angle around a direction specified by $\mathbf{s}$, and the first integral extends over the 2π solid angle subtended by a hemisphere in the half-space, into which the source radiates. Substituting from Eq. (5.9) and making use of the relations $\mathrm{d}\Omega = \mathrm{d}\mathbf{s}_\perp / \cos\theta$ and $\cos\theta = (1 - \mathbf{s}_\perp^2)^{1/2}$, one may rewrite the optimization problem (5.11) in the following explicit form:

$$\left\{ \frac{1}{2} \sum_{m=0}^{M-1} \sum_{l=0}^{M-1} \mu_m \mu_l P_{ml} + \sum_{m=0}^{M-1} \mu_m Q_m \right\} \longrightarrow \min_{\mu_m}, \qquad \mu_m > 0, \tag{5.12}$$

where

$$P_{ml} = \int_D |\psi_m(\mathbf{x})|^2\, |\psi_l(\mathbf{x})|^2\, \mathrm{d}\mathbf{x} \times \int_{(\mathbf{s}_\perp^2 \leqslant 1)} \left(1 - \mathbf{s}_\perp^2\right)^{1/2} \left|\widetilde{\psi}_m\left(\frac{k}{2\pi}\mathbf{s}_\perp\right)\right|^2 \left|\widetilde{\psi}_l\left(\frac{k}{2\pi}\mathbf{s}_\perp\right)\right|^2 \mathrm{d}\mathbf{s}_\perp, \tag{5.13}$$

$$Q_m = -\left(\frac{2\pi}{k}\right)^2 \int_{(\mathbf{s}_\perp^2 \leqslant 1)} \int_D B(\mathbf{x}, \mathbf{s})\, |\psi_m(\mathbf{x})|^2 \left|\widetilde{\psi}_m\left(\frac{k}{2\pi}\mathbf{s}_\perp\right)\right|^2 \mathrm{d}\mathbf{x}\mathrm{d}\mathbf{s}_\perp. \tag{5.14}$$

Problem (5.12) represents a classical quadratic programming problem, which may be solved by well-known methods.

As is well known, the only true physical quantity that can be observed (or measured) in the output plane of an optical system is the irradiance $\mathcal{E}(\mathbf{x}')$ defined as follows:

$$\mathcal{E}(\mathbf{x}') = \int_{(2\pi)} B(\mathbf{x}', \mathbf{s}) \cos\theta \mathrm{d}\Omega, \tag{5.15}$$

where

$$B(\mathbf{x}', \mathbf{s}) = \mathfrak{L}[B(\mathbf{x}, \mathbf{s})], \tag{5.16}$$

and $\mathfrak{L}$ is an operator describing the propagation of the primary source radiance function $B(\mathbf{x}, \mathbf{s})$ through an optical system. It is obvious that two primary sources with different cross-spectral density functions, e.g., $W(\mathbf{x}_1, \mathbf{x}_2)$ and $W'(\mathbf{x}_1, \mathbf{x}_2)$, but with the same radiance function, produce the same irradiance in the output plane of an optical system. Hence, when examining the processes going on in some optical system, an original source with cross-spectral density function $W(\mathbf{x}_1, \mathbf{x}_2)$ may be replaced in a good approximation by an alternative source with an appropriately chosen cross-spectral density function $W_{\mathrm{A}}(\mathbf{x}_1, \mathbf{x}_2)$. In this sense,

$$W_{\mathrm{A}}(\mathbf{x}_1, \mathbf{x}_2) = \sum_{m=0}^{M-1} (\mu_m)_{\mathrm{opt}} \psi_m^*(\mathbf{x}_1) \psi_m(\mathbf{x}_2), \tag{5.17}$$

with $(\mu_m)_{\mathrm{opt}}$ calculated as the solution of problem (5.12), may be accepted as the *alternative coherent-mode representation*of an original source.

5.3 Choice of the Alternative Modal Basis

As follows from the previous section, the only theoretical requirements that the alternative coherent-mode functions $\psi_m(\mathbf{x})$ must satisfy is that they have to be continuous and orthonormal in the plane $z = 0$. From the point of view of practice, we will also require that these functions permit calculation in the closed form of the Fourier transform (5.10). Below, we show how such functions may be constructed in two orthogonal bases, viz., *Hermitian basis* and *Bessel basis*.

5.3.1 Hermitian basis

If the original source has rectangular form, it is appropriate to choose the basis formed by the Hermitian polynomials $H_n(u)$ of the integral order n, which obey the orthogonality relation[72]

$$\int_{-\infty}^{\infty} \exp\left(-u^2\right) H_n(u) H_m(u)\, du = 2^n n! \sqrt{\pi} \delta_{nm}. \tag{5.18}$$

Comparing Eqs. (5.18) and (5.4), one finds that, in this case, the alternative coherent-mode functions must be chosen in the form

$$\psi_m(x, y) = \frac{1}{2^m m!} \left(\frac{ab}{\pi}\right)^{1/2} H_m(ax) H_m(by) \times \exp\left(-\frac{a^2 x^2}{2}\right) \exp\left(-\frac{b^2 y^2}{2}\right), \tag{5.19}$$

with scale factors a and b being discussed later. On making use of the well-known equality[71]

$$\int_{-\infty}^{\infty} H_n(u) \exp\left(-\frac{u^2}{2}\right) \exp(\mathrm{i}us)\,\mathrm{d}u = \mathrm{i}^n \sqrt{2\pi} H_n(s) \exp\left(-\frac{s^2}{2}\right), \tag{5.20}$$

one may readily find the Fourier transform

$$\widetilde{\psi}_m\left(\frac{k}{2\pi}s_x, \frac{k}{2\pi}s_y\right) = (-\mathrm{i})^{2m} \frac{2}{2^m m!} \left(\frac{\pi}{ab}\right)^{1/2} H_m\left(\frac{ks_x}{a}\right) H_m\left(\frac{ks_y}{b}\right) \times \exp\left(-\frac{k^2 s_x^2}{2a^2}\right) \exp\left(-\frac{k^2 s_y^2}{2b^2}\right). \tag{5.21}$$

In order to provide the best approximation in accordance with Eq. (5.11), it is necessary to match the effective area of the function $[\psi_0(x, y)]^2$ with the area of the characteristic source function $\chi(x, y)$, i.e.,

$$\int_{-\infty}^{\infty} \exp\left(-a^2x^2\right) dx \int_{-\infty}^{\infty} \exp\left(-b^2y^2\right) dy = XY, \tag{5.22}$$

where X and Y are linear dimensions of the source. Calculating the integrals in Eq. (5.22), one may find the following values of the scale factors a and b:

$$a = \frac{\sqrt{\pi}}{X}, \qquad b = \frac{\sqrt{\pi}}{Y}. \tag{5.23}$$

5.3.2 Bessel basis

If the original source possesses circular symmetry, it is appropriate to construct the mode functions in the basis formed by the Bessel functions of the first kind and integral order n, $J_n(r)$, which clearly obey the orthogonality relation

$$\int_0^R \int_0^{2\pi} \exp[\mathrm{i}(n-m)] J_n(r) J_m(r)\, r\,\mathrm{d}r\,\mathrm{d}\phi = 2\pi \int_0^R J_n^2(r)\, r\,\mathrm{d}r\,\delta_{nm}, \tag{5.24}$$

where (r, ϕ) are the polar coordinates in the (x, y) plane. In this case, the alternative coherent-mode functions must be chosen in the form

$$\psi_m(r, \phi) = \left[2\pi \int_0^R J_n^2(r)\, r\,\mathrm{d}r\right]^{-1/2} \exp(-\mathrm{i}n\phi) J_n(r). \tag{5.25}$$

It may be readily shown that

$$\widetilde{\psi}_m(\rho, \theta) = \mathrm{i}^{-m} \sqrt{2\pi} \left[\int_0^R J_n^2(r)\, r\,\mathrm{d}r\right]^{-1/2} \int_0^R J_m(r) J_m(2\pi\rho r)\, r\,\mathrm{d}r. \tag{5.26}$$

It should be noted that the integrals in Eqs. (2.25) and (2.26) can be easily calculated in closed form using the Lommel integrals[72]

$$\int_0^P J_m(ax)\, J_m(bx)\, x\,\mathrm{d}x = \frac{P}{a^2-b^2}\left[bJ_m(aP)\, J'_m(bP) - aJ'_m(aP)\, J_m(bP)\right] \tag{5.27}$$

and

$$\int_0^P J_m^2(ax)\, x\,\mathrm{d}x = \frac{P^2}{2}\left[J_m'^2(aP) + \left(1-\frac{m^2}{a^2P^2}\right)J_m^2(aP)\right], \tag{5.28}$$

where

$$J'_m(aP) = \left.\frac{\mathrm{d}}{\mathrm{d}(ax)}J_\beta(ax)\right|_{x=P}. \tag{5.29}$$

Indeed, on making use of Eq. (5.28) with due regard for recurrence relations,[72]

$$J_{m-1}(x) + J_{m+1}(x) = \frac{2m}{x}J_m(x) \tag{5.30}$$

and

$$J_{m-1}(x) - J_{m+1}(x) = 2J'_m(x), \tag{5.31}$$

one readily finds

$$\int_0^R J_n^2(r)\, r\,\mathrm{d}r = \frac{R^2}{2}\left[J_m^2(R) - J_{m-1}(R)\, J_{m+1}(R)\right]. \tag{5.32}$$

On making use of Eq. (5.27) with due regard for relation,[72]

$$\frac{\mathrm{d}}{\mathrm{d}x}\left[x^{-m}J_m(x)\right] = -x^{-m}J_{m+1}(x), \tag{5.33}$$

one readily finds

$$\int_0^R J_m(r)\, J_m(2\pi\rho r)\, r\,\mathrm{d}r = \left[\frac{1}{R}J_m(R) - \frac{1}{2}J_{m-1}(R) + \frac{1}{2}J_{m+1}(R)\right] \times \frac{J_m(2\pi R\rho)}{1-(2\pi\rho)^2} - 2\pi J_m(R)\,\frac{\rho J_{m+1}(2\pi R\rho)}{1-(2\pi\rho)^2}. \tag{5.34}$$

5.4 Numerical Simulation

To illustrate the proposed technique, we considered an example of constructing the alternative coherent-mode representation of the original source with a known radiance function. In this example, we considered the homogeneous 1D Lambertian source with the radiance function

$$B(x,s)=\begin{cases} Ck/2\pi, & \text{when} \quad |x|\leqslant X/2,\ |s|\leqslant 1,\\ 0, & \text{when} \quad |x|>X/2,\ |s|>1, \end{cases} \tag{5.35}$$

where C is a constant (further, for the sake of simplicity, we will equate it to unity). To construct the alternative coherent-mode representation of such a source, we used

$$\psi_m(x)=\frac{1}{(X2^m m!)^{1/2}}H_m\left(\frac{\sqrt{\pi}}{X}x\right)\exp\left(-\frac{\pi x^2}{2X^2}\right) \tag{5.36}$$

and

$$\widetilde{\psi}_m\left(\frac{k}{2\pi}s\right)=\mathrm{i}^m\left(\frac{2X}{2^m m!}\right)^{1/2}H_m\left(\frac{kX}{\sqrt{\pi}}s\right)\exp\left(-\frac{k^2X^2s^2}{2\pi}\right). \tag{5.37}$$

For this example, the coefficients of problem (5.12) given by Eqs. (5.13) and (5.14) take the following values:

$$P_{ml}=\frac{16}{k\,(2^m m!)^2\left(2^l l!\right)^2}\int_0^{\sqrt{\pi}/2}H_m^2(u)\,H_l^2(u)\exp\left(-2u^2\right)\mathrm{d}u$$
$$\times\int_0^{kX/\sqrt{\pi}}\left[1-\frac{\pi v^2}{(kX)^2}\right]^{1/2}H_m^2(v)\,H_l^2(v)\exp\left(-2v^2\right)\mathrm{d}v, \tag{5.38}$$

$$Q_m=-\frac{8}{k\,(2^m m!)^2}\int_0^{\sqrt{\pi}/2}H_m^2(u)\exp\left(-u^2\right)\mathrm{d}u\int_0^{kX/\sqrt{\pi}}H_m^2(v)\exp\left(-v^2\right)\mathrm{d}v. \tag{5.39}$$

We performed the numerical calculation of coefficients (5.38) and (5.39) and solved problem (5.12) using the modified gradient method. To simplify the calculations, we chose $kX=10$ (typically, this value may be of the order of 10^3 and larger). The obtained solutions for different values of M and the corresponding values of the relative error of approximation ε are given in Table 5.1. As can be seen from this table, the error of approximation decreases rapidly with the increase of M and, when $M=30$, it becomes less than 10%, which is quite admissible in the majority of practical applications. It is not out of place to add here that the considered example represents the most difficult case in the sense of approximation

accuracy. Indeed, as is known (see Section 1.6.3), the Lambertian source is very close to a completely incoherent source that contains an infinite number of coherent contributions in its modal representation. Hence, it is well grounded to expect that the alternative coherent-mode representation will be much more efficient for any other, non-Lambertian, partially coherent planar source.

Table 5.1 Results of calculations.

M	5	10	20	30
μ_0	0.2723	0.1335	0.0000	0.0000
μ_1	0.5899	0.2938	0.0000	0.0000
μ_2	1.0718	0.4544	0.0000	0.0000
μ_3	2.1906	0.6467	0.0000	0.0000
μ_4	3.0898	0.9426	0.0106	0.0000
μ_5	–	1.1818	0.0008	0.0000
μ_6	–	1.8589	0.0117	0.0000
μ_7	–	2.0979	0.0318	0.0000
μ_8	–	4.4068	0.0374	0.0000
μ_9	–	5.4077	0.1575	0.0000
μ_{10}	–	–	0.2035	0.0000
μ_{11}	–	–	0.5844	0.0000
μ_{12}	–	–	1.0153	0.2039
μ_{13}	–	–	2.1614	1.2738
μ_{14}	–	–	3.8866	2.7781
μ_{15}	–	–	6.2033	5.0672
μ_{16}	–	–	9.4392	7.667
μ_{17}	–	–	10.5465	8.9493
μ_{18}	–	–	11.0982	8.8142
μ_{19}	–	–	6.9331	5.1981
μ_{20}	–	–	–	1.1903
μ_{21}	–	–	–	0.0008
μ_{22}	–	–	–	1.6739
μ_{23}	–	–	–	5.2415
μ_{24}	–	–	–	5.2495
μ_{25}	–	–	–	1.5986
μ_{26}	–	–	–	0.0000
μ_{27}	–	–	–	1.9317
μ_{28}	–	–	–	4.8002
μ_{29}	–	–	–	3.1132
ε	0.6595	0.4586	0.1087	0.0993

5.5 Concluding Remarks

The coherent-mode representations considered in the previous chapters may be characterized as an approach based on the explicit use of a priori data about the

source, such as the knowledge of its cross-spectral density function. The approach considered in the present chapter is based on the use of a posteriori data about the source, namely, its radiance measured in a physical experiment. We have defined an alternative coherent-mode representation of the original plane source with unknown cross-spectral density function in terms of the coherent modes of some alternative source that generates radiation with nearly the same radiance function as does the original source. Such a representation may be obtained by approximating the measured radiance function of the original source by the modal radiance of an alternative source calculated in the prescribed orthonormal basis. We wish to stress that an alternative coherent-mode representation does not reproduce in any way the true coherent-mode structure of the original source, but may substitute it in practice when examining the processes going on in some optical system. We propose that this approach reveals a new and promising perspective for practical application of the coherent-mode representation of processes and systems in optics.

References

1. E. Wolf, "New theory of partial coherence in the space-frequency domain. Part I: spectra and cross-spectra of steady-state sources," *J. Opt. Soc. Am. A*, Vol. 72, No. 3, pp. 343–351 (1982).
2. E. Wolf, "New theory of partial coherence in the space-frequency domain. Part II: Steady-state fields and higher-order correlations," *J. Opt. Soc. Am. A*, Vol. 3, No. 1, pp. 76–84 (1986).
3. H. Gamo, "Matrix Treatment of Partial Coherence," in: *Progress in Optics III*, Chap. 3, E. Wolf, ed., North-Holland, Amsterdam, pp. 187–332 (1964).
4. L. Mandel and E. Wolf, *Optical Coherence and Quantum Optics*, Cambridge University Press, New York (1995).
5. A. Starikov, "Effective number of degrees of freedom of partially coherent sources," *J. Opt. Soc. Am. A*, Vol. 72, No. 11, pp. 1538–1544 (1982).
6. A. Starikov and E. Wolf, "Coherent-mode representation of Gaussian Schell-model sources and of their radiation fields," *J. Opt. Soc. Am.*, Vol. 72, No. 7, pp. 923–928 (1982).
7. F. Gori, "Collet-Wolf sources and multimode lasers," *Opt. Commun.*, Vol. 34, No. 3, pp. 301–305 (1980).
8. F. Gori, "Mode propagation of the field generated by Collett-Wolf Schelll-model sources," *Opt. Commun.*, Vol. 46, No. 3–4, pp. 149–154 (1983).
9. R. Simon, K. Sundar, and N. Mukunda, "Twisted Gaussian Schell-model beams. I. Symmetry structure and normal-mode spectrum," *J. Opt. Soc. Am. A*, Vol. 10, No. 9, pp. 2008–2016 (1993).
10. F. Gori, G. Guattari, and C. Padovani, "Modal expansion for J_0-correlated Schell-model sources," *Opt. Commun.*, Vol. 64, No. 4, pp. 311–316 (1987).
11. A. Starikov and A. T. Friberg, "One-dimensional Lambertian source and associated coherent-mode representation," *Appl. Opt.*, Vol. 23, No. 23, pp. 4261–4268 (1984).
12. A. Papoulis, *Systems and Transforms with Applications in Optics*, McGraw-Hill, New York (1968).
13. J. W. Goodman, *Introduction to Fourier Optics*, 2d ed., McGraw-Hill, New York (1996).
14. B. J. Thompson, "Image formation with partially coherent light," *Progress in Optics*, E. Wolf, ed., North-Holland, Amsterdam, Vol. 7, pp. 191–202 (1969).
15. M. Schetzen, *The Volterra and Wiener Theories of Non-Linear Systems*, Wiley, New York (1980).
16. V. Volterra, *Theory of Functionals and of Integral and Integro-Differential Equations*, Dover, New York (1959).

17. B. E. A. Saleh, "Optical bilinear transforms: General properties," *Opt. Acta*, Vol. 26, No. 6, pp. 777–799 (1979).
18. J. W. Goodman, *Statistical Optics*, Wiley, New York (1985).
19. E. C. Kintner, "Method for calculation of partially coherent imagery," *Appl. Opt.*, Vol. 17, No. 17, pp. 2747–2753 (1978).
20. S. Subramanian, "Rapid calculation of defocused partially coherent images," *Appl. Opt.*, Vol. 20, No. 10, pp. 1854–1857 (1981).
21. B. E. A. Saleh and M. Rabbani, "Simulation of partially coherent imagery in the space and frequency domains by modal expansions," *Appl. Opt.*, Vol. 21, No. 15, pp. 2770–2777 (1982).
22. R. Martínez-Herrero and P. M. Mejías, "Relation between the expansions of the correlation function at the object and image planes for partially coherent illumination," *Opt. Commun.*, Vol. 37, No. 4, pp. 234–238 (1981).
23. J. Duvernoy, "Volterra-Wiener partially coherent imaging systems: Three-dimensional objects and generalized *G* functionals," *J. Opt. Soc. Am. A*, Vol. 7, No. 5, pp. 809–819 (1990).
24. J. van der Gracht, "Simulation of partially coherent imaging by outer-product expansion," *Appl. Opt.*, Vol. 33, No. 17, pp. 3725–3731 (1994).
25. S. Withington, M. P. Hobson, and R. H. Berry, "Representing the behavior of partially coherent optical systems by using overcomplete basis sets," *J. Opt. Soc. Am. A*, Vol. 21, No. 2, pp. 207–217 (2004).
26. A. S. Ostrovsky, O. Ramos-Romero, and M. V. Rodríguez-Solís, "Coherent-mode representation of partially coherent imagery," *Opt. Rev.*, Vol. 3, No. 6B, pp. 492–496 (1996).
27. A. S. Ostrovsky, O. Ramos-Romero, and G. Martínez-Niconoff, "Fast algorithm for bilinear transforms in optics," *Proc. SPIE*, Vol. 4418, pp. 88–95 (2000).
28. A. S. Ostrovsky, G. Martínez-Niconoff, and J. C. Ramírez-San-Juan, "On the modal representation of partially coherent imagery," *Proc. SPIE*, Vol. 4419, pp. 431–434 (2001).
29. A. S. Ostrovsky, O. Ramos-Romero, G. Martínez-Niconoff, and J. C. Ramírez-San-Juan, "On the modal representation of partially coherent imagery," *Rev. Mex. Fís.*, Vol. 47, No. 5, pp. 404–407 (2001).
30. A. S. Ostrovsky, O. Ramos-Romero, G. Martínez-Niconoff, and J. C. Ramírez-San-Juan, "Modal theory of partially coherent imagery," *Proc. SPIE*, Vol. 4436, pp. 109–115 (2001).
31. A. S. Ostrovsky, O. Ramos-Romero, and G. Martínez-Niconoff, "Fast algorithm for bilinear transforms in optics," *Rev. Mex. Fís.*, Vol. 48, No. 3, pp. 186–191 (2002).
32. A. S. Ostrovsky, O. Ramos-Romero, G. Martínez-Niconoff, and J. C. Ramírez-San-Juan, "Fast algorithm for computer simulation of optical systems with partially coherent illumination," *WSEAS Trans. on Syst.*, Vol. 1, No. 1, pp. 149–153 (2002).

33. J. Durnin, "Exact solutions for nondiffracting beams. I. The scalar theory," *J. Opt. Soc. Am. A*, Vol. 4, No. 4, pp. 651–654 (1987).
34. F. Gori and G. Guattari, "Bessel-Gaussian beams," *Opt. Commun.*, Vol. 64, No. 6, pp. 491–495 (1987).
35. J. Durnin, J. J. Miceli, Jr., and J. H. Eberly, "Comparison of Bessel and Gaussian beams," *Opt. Lett.*, Vol. 13, No. 2, pp. 79–80 (1988).
36. G. Indebetouw, "Nondiffracting optical fields: some remarks on their analysis and synthesis," *J. Opt. Soc. Am. A*, Vol. 6, No. 1, pp. 150–152 (1989).
37. A. B. Valyaev and S. G. Krivoshlykov, "Mode properties of Bessel beams," *Sov. J. Quantum Electron.*, Vol. 19, pp. 679–680 (1989).
38. L. Vicari, "Truncation of non-diffracting beams," *Opt. Commun.*, Vol. 70, No. 4, pp. 263–266 (1989).
39. J. Ojeda-Castañeda and A. Noyola-Iglesias, "Nondiffracting wave fields in GRIN and free-space," *Microwave and Opt. Techn. Lett.*, Vol. 3, No. 12, pp. 430–433 (1990).
40. F. Bloisi and L. Vicari, "Comparison of nondiffracting laser beams," *Opt. Commun.*, Vol. 75, No. 5–6, pp. 353–357 (1990).
41. P. Szwaykowski and J. Ojeda-Castañeda, "Nondiffracting beams and the self-imaging phenomenon," *Opt. Commun.*, Vol. 83, No. 12, pp. 1–4 (1991).
42. S. R. Mishra, "A vector wave analysis of a Bessel beam," *Opt. Commun.*, Vol. 85, No. 2–3, pp. 159–161 (1991).
43. Z. Bouchal and M. Olivík, "Non-diffractive vector Bessel beams," *J. Modern Opt.*, Vol. 21, No. 8, pp. 1555–1566 (1995).
44. D. G. Hall, "Vector-beam solutions of Maxwell's wave equation," *Opt. Lett.*, Vol. 21, No. 1, pp. 9–11 (1996).
45. V. Kettunen and J. Turunen, "Propagation-invariant spot arrays," *Opt. Lett.*, Vol. 23, No. 16, pp. 1247–1249 (1998).
46. S. Chávez-Cerda and M. A. Meneses-Nava, "Interference of traveling non-diffracting beams, " *Opt. Lett.*, Vol. 23, No. 24, pp. 1871–1873 (1998).
47. R. Piestun and J. Shamir, "Generalized propagation-invariant wave fields," *J. Opt. Soc. Am. A*, Vol. 15, No. 12, pp. 3039–3044 (1998).
48. J. C. Gutiérrez-Vega, M. D. Iturbe-Castillo, and S. Chávez-Cerda, "Alternative formulation for invariant optical fields: Mathieu beams," *Opt. Lett.*, Vol. 25, No. 20, pp. 1493–1495 (2000).
49. S. Chávez-Cerda and G. H. C. New, "Evolution of focused Hankel waves and Bessel beams," *Opt. Commun.*, Vol. 181, No. 4–6, pp. 369–377 (2000).
50. J. Durnin, J. J. Miceli, Jr., and J. H. Eberly, "Diffraction-free beams," *Phys. Rev. Lett.*, Vol. 58, No. 14, pp. 1499–1501 (1987).
51. J. Turunen, A. Vasara, and A. T. Friberg, "Holographic generation of diffraction-free beams," *Appl. Opt.*, Vol. 27, No. 19, pp. 3959–3962 (1988).
52. A. Vasara, J. Turunen, and A. T. Friberg, "General diffraction-free beams produced by computer-generated holograms," *Proc. SPIE*, Vol. 311, pp. 85–89 (1989).

53. A. Vasara, J. Turunen, and A. T. Friberg, "Realization of general nondiffracting beams with computer-generated holograms," *J. Opt. Soc. Am. A*, Vol. 6, No. 11, pp. 1748–1754 (1989).
54. G. Scott and N. McArdle, "Efficient generation of nearly diffraction-free beams using an axicon," *Opt. Eng.*, Vol. 31, No. 12, pp. 2641–2643 (1992).
55. R. M. Herman and T. A. Wiggins, "Production and uses of diffractionless beams," *J. Opt. Soc. Am. A*, Vol. 8, No. 6, pp. 932–942 (1991).
56. J. Rogel-Salazar, G. H. C. New, and S. Chávez-Cerda, "Bessel-Gaussian beam optical resonator," *Opt. Commun.*, Vol. 190, No. 1–3, pp. 117–122 (2001).
57. G. Häusler and W. Heckel, "Light sectioning with large depth and high resolution," *Appl. Opt.*, Vol. 27, No. 24, pp. 5165–5169 (1988).
58. M. Florjanczyk and R. Tremblay, "Guiding of atoms in traveling-wave laser trap formed by axicon," *Opt. Commun.*, Vol. 73, No. 6, pp. 448–450 (1989).
59. K. M. Iftekharunddin and M. A. Karim, "Heterodyne detection by using a diffraction-free beam: tilt and offset effects," *Appl. Opt.*, Vol. 31, No. 23, pp. 4853–4856 (1992).
60. J.-Y. Lu and J. F. Greenleaf, "Nondiffracting X waves-exact solutions of free-space scalar wave equation and their finite aperture realizations," *IEEE Transactions on Ultrasonics, Ferroelectrics and Frequeny Control*, Vol. 39, No. 1, pp. 19–31 (1992).
61. Y. Ohtsuka, Y. Nozoe, and Y. Imai, "Acoustically modified spatial coherence in optical Fresnel diffraction region," *Opt. Commun.*, Vol. 35, No. 2, pp. 157–160 (1980).
62. Y. Ohtsuka, "Non-modified propagation of optical mutual intensity in the Fresnel diffraction region," *Opt. Commun.*, Vol. 39, No. 5, pp. 283–286 (1981).
63. J. Turunen, A. Vasara, and A. T. Friberg, "Propagation invariance and self-imaging in variable-coherence optics," *J. Opt. Soc. Am. A*, Vol. 8, No. 2, pp. 282–289 (1990).
64. A. S. Ostrovsky, G. Martínez-Niconoff, and J. C. Ramírez-San-Juan, "Coherent-mode representation of propagation-invariant fields," *Opt. Commun.*, Vol. 195, No. 1–4, pp. 27–34 (2001).
65. A. S. Ostrovsky, G. Martínez-Niconoff, and J. C. Ramírez-San-Juan, "Coherent-mode structure of propagation-invariant fields," *Proc. SPIE*, Vol. 4419, pp. 427–430 (2001).
66. A. S. Ostrovsky, G. Martínez-Niconoff, and J. C. Ramírez-San-Juan, "Exact solutions for coherent modes of propagation-invariant optical fields," *WSEAS Trans. on Systems*, Vol. 1, pp. 144–149 (2002).
67. A. S. Ostrovsky, G. Martínez-Niconoff, and J. C. Ramírez-San-Juan, "Generation of light string and light capillary beams," *Opt. Commun.*, Vol. 207, No. 1–6, pp. 131–138 (2002).
68. A. S. Ostrovsky, G. Martínez-Niconoff, and J. C. Ramírez-San-Juan, "Propagation-invariant fields of the third kind," *Proc. SPIE*, Vol. 4829, pp. 253–255 (2003).

69. A. S. Ostrovsky, G. Martínez-Niconoff, and J. C. Ramírez-San-Juan, "Generation of light string and light capillary beams," *Proc. SPIE*, Vol. 4829, pp. 255–257 (2003).
70. A. S. Ostrovsky, G. Martínez-Niconoff, and J. C. Ramírez-San-Juan, "Propagation-invariant fields of the third kind and their optical generation," *J. Opt. A: Pure and Appl. Opt.*, Vol. 5, pp. 276–279 (2003).
71. I. S. Gradshteyn and I. M. Ryzhik, *Table of Integrals, Series, and Products*, 5th ed., Academic Press, New York (1994).
72. G. Arfken, *Mathematical Methods for Physicists*, 5th ed., Academic Press, New York (2001).
73. G. N. Watson, *A Treatise of the Theory of Bessel Functions*, 2d ed., Cambridge University Press, Cambridge (1966).
74. A. S. Ostrovsky and E. Hernández-García, "Modulation of spatial coherence of optical field by means of liquid crystal light modulator," *Rev. Mex. Fís.*, Vol. 51, No. 5, pp. 442–446 (2005).
75. A. Walther, "Radiometry and coherence," *J. Opt. Soc. Am.*, Vol. 58, No. 9, pp. 1256–1259 (1968).
76. Yu. N. Barabanenkov, "On the spectral theory of radiation transport equations," *Sov. Phys. JETP*, Vol. 29, pp. 679–684 (1969).
77. G. V. Rozenberg, "The statistical-electrodynamic content of photometric quantities and the basic concepts of radiation-transfer theory," *Opt. Spectrosc.* (USSR), Vol. 28, pp. 210–213 (1970).
78. G. I. Ovchinnikov and V. I. Tatarskii, "On the problem of the relationship between coherent theory and the radiation-transfer equation," *Radiophys. Quantum Electron.*, Vol. 15, pp. 1087–1089 (1972).
79. E. W. Marchand and E. Wolf, "Angular correlation and far-zone behavior of partially coherent fields," *J. Opt. Soc. Am.*, Vol. 62, No. 3, pp. 379–385 (1972).
80. A. Walther, "Radiometry and coherence," *J. Opt. Soc. Am.*, Vol. 63, No. 12, pp. 1622–1623 (1973).
81. G. V. Rozenberg, "Coherence, observability and the photometric aspects of beam optics, " *Appl. Opt.*, Vol. 12, No. 12, pp. 2855–2862 (1973).
82. E. W. Marchand and E. Wolf, "Radiometry with sources of any state of coherence," *J. Opt. Soc. Am.*, Vol. 64, No. 9, pp. 1219–1226 (1974).
83. E. W. Marchand and E. Wolf, "Walther's definition of generalized radiance," *J. Opt. Soc. Am.*, Vol. 64, No. 9, pp. 1273–1274 (1974).
84. A. Walther, "Reply to Marchand and Wolf," *J. Opt. Soc. Am.*, Vol. 64, No. 9, p. 1275 (1974).
85. W. Carter and E. Wolf, "Coherence properties of Lambertian sources," *J. Opt. Soc. Am.*, Vol. 65, No. 9, pp. 1067–1071 (1975).
86. W. Carter and E. Wolf, "Coherence and radiometry with quasihomogeneous planar sources," *J. Opt. Soc. Am.*, Vol. 67, No. 6, pp. 785–796 (1977).
87. A. S. Marathay, "Radiometry of partially coherent fields I," *Opt. Acta*, Vol. 23, pp. 785–794 (1976).

88. A. S. Marathay, "Radiometry of partially coherent fields II," *Opt. Acta*, Vol. 23, pp. 795–798 (1976).
89. G. V. Rozenberg, "The light ray (Contribution to the theory of the light field)," *Sov. Phys. Usp.*, Vol. 20, pp. 55–79 (1977).
90. E. Collet, J. T. Foley, and E. Wolf, "On an investigation of Tatarskii into the relationship between coherence theory and the theory of radiative transfer," *J. Opt. Soc. Am.*, Vol. 67, No. 4, pp. 465–477 (1977).
91. E. Wolf, "Coherence and radiometry," *J. Opt. Soc. Am.*, Vol. 68, No. 1, pp. 6–17 (1978).
92. E. Wolf, "The radiant intensity from planar sources of any state of coherence," *J. Opt. Soc. Am.*, Vol. 68, No. 11, pp. 1597–1605 (1978).
93. A. T. Friberg, "On the question of the existence of nonradiating primary sources of finite extent," *J. Opt. Soc. Am.*, Vol. 68, No. 11, pp. 1281–1283 (1978).
94. A. Walther, "Propagation of generalized radiance through lenses," *J. Opt. Soc. Am.*, Vol. 68, No. 11, pp. 1606–1610 (1978).
95. H. P. Baltes, J. Geist, and A. Walther, "Radiometry and Coherence," Chap. 5 in *Inverse Source Problems in Optics*, H. P. Baltes, ed., Springer-Verlag, Berlin (1978).
96. A. T. Friberg, "On the existence of a radiance function for finite planar sources of arbitrary state of coherence," *J. Opt. Soc. Am.*, Vol. 69, No. 1, pp. 192–198 (1979).
97. A. T. Friberg, "Radiation from partially coherent sources," *Proc. SPIE*, Vol. 194, pp. 71–83 (1979).
98. A. T. Friberg, "Effects of coherence in radiometry," *Proc. SPIE*, Vol. 194, pp. 55–70 (1979).
99. R. L. Fante, "Relationship between radiative transport theory and Maxwell's equations in dielectric media," *J. Opt. Soc. Am.*, Vol. 71, No. 4, pp. 460–468 (1980).
100. A. T. Friberg, "On the generalized radiance associated with radiation from a quasihomogeneous source," *Opt. Acta*, Vol. 28, pp. 261–277 (1981).
101. W. Carter, "Statistical radiometry," *Radio Sci.*, Vol. 18, p. 144 (1983).
102. R. Martínez-Herrero and P. M. Mejías, "Radiometric definitions of partially coherent sources," *J. Opt. Soc. Am. A*, Vol. 1, No. 5, pp. 556–558 (1984).
103. L. A. Apresyan and Yu. A. Kravtsov, "Photometry and coherence: wave aspects of the theory of radiation transport," *Sov. Phys. Usp.*, Vol. 27, pp. 301–313 (1984).
104. J. T. Foley and M. Nieto-Vesperinas, "Radiance functions that depend nonlinearly on the cross-spectral density," *J. Opt. Soc. Am. A*, Vol. 2, No. 9, pp. 1446–1447 (1985).
105. J. T. Foley and E. Wolf, "Radiometry as a short-wavelength limit of statistical wave theory with globally incoherent sources," *Opt. Commun.*, Vol. 55, No. 4, pp. 236–241 (1985).

106. R. Martínez-Herrero and P. M. Mejías, "Radiometric definitions from second-order coherence characteristics of planar sources," *J. Opt. Soc. Am. A*, Vol. 3, No. 7, pp. 1055–1058 (1986).
107. A. T. Friberg, "Energy transport in optical system with partially coherent light," *Appl. Opt.*, Vol. 25, No. 24, pp. 4547–4556 (1986).
108. R. Winston and X. Ning, "Constructing a conserved flux from plane waves," *J. Opt. Soc. Am. A*, Vol. 3, No. 10, pp. 1629–1631 (1986).
109. M. Nieto-Vesperinas, "Classical radiometry and radiative transfer theory: a short-wavelength limit of a general mapping of cross-spectral densities in second-order coherence theory," *J. Opt. Soc. Am. A*, Vol. 3, No. 9, pp. 1354–1359 (1986).
110. W. Welford and R. Winston, "Generalized radiance and practical radiometry," *J. Opt. Soc. Am. A*, Vol. 4, No. 3, pp. 545–547 (1987).
111. G. S. Agarwal, J. T. Foley, and E. Wolf, "The radiance and phase-space representations of the cross-spectral density operator," *Opt. Commun.*, Vol. 62, No. 2, pp. 67–72 (1987).
112. K. Kim and E. Wolf, "Propagation law for Walther's first generalized radiance function and its short-wavelength limit with quasihomogeneous sources," *J. Opt. Soc. Am. A*, Vol. 4, No. 7, pp. 1233–1236 (1987).
113. R. Winston and X. Ning, "Generalized radiance of uniform Lambertian sources," *J. Opt. Soc. Am. A*, Vol. 5, No. 4, pp. 516–519 (1988).
114. R. Winston, "Analogy between Fresnel diffraction and generalized radiance," *J. Opt. Soc. Am. A*, Vol. 6, No. 1, pp. 145–149 (1988).
115. H. M. Pedersen, "Exact geometrical theory of free-space radiative energy transfer," *J. Opt. Soc. Am. A*, Vol. 8, No. 1, pp. 176–185 (1991).
116. H. M. Pedersen, "Propagation of generalized specific intensity in refracting media," *J. Opt. Soc. Am. A*, Vol. 9, No. 9, pp. 1623–1625 (1992).
117. A. T. Friberg, G. S. Agarwal, J. T. Foley, and E. Wolf, "Statistical wave-theoretical derivation of the free-space transport equation of radiometry," *J. Opt. Soc. Am. B*, Vol. 9, No. 8, pp. 1386–1393 (1992).
118. R. G. Littlejohn and R. Winston, "Corrections to classical radiometry," *J. Opt. Soc. Am. A*, Vol. 10, No. 9, pp. 2024–2037 (1993).
119. R. G. Littlejohn and R. Winston, "Generalized radiance and measurements," *J. Opt. Soc. Am. A*, Vol. 12, No. 12., pp. 2736–2743 (1995).
120. K. Yoshimori and K. Itoh, "An operator method of the theory of optical coherence and radiometry," *Opt. Rev.*, Vol. 7, No. 1, pp. 34–43 (2000).
121. H. Arimoto, K. Yoshimori, and K. Itoh, "Interferometric three-dimensional imaging based on retrieval of generalized radiance distribution," *Opt. Rev.*, Vol. 7, No. 1, pp. 25–33 (2000).
122. A. S. Ostrovsky, "Paraxial approximation of modern radiometry for beamlike wave propagation," *Opt. Rev.*, Vol. 3, No. 2, pp. 83–88 (1996).
123. A. S. Ostrovsky and M. V. Rodríguez-Solís, "Free-space propagation of the generalized radiance defined in terms of the coherent-mode representation of cross-spectral density function," *Opt. Rev.*, Vol. 7, No. 2, pp. 112–114 (2000).

124. R. W. Boyd, *Radiometry and the Detection of Optical Radiation*, Wiley, New York (1983).
125. S. Chandrasekhar, *Radiative Transfer*, Dover, New York (1960).
126. A. S. Ostrovsky, A. M. Zemliak, and E. Hernández-García, "Alternative coherent-mode representation of a planar source," *Opt. Commun.*, Vol. 249, pp. 1–6 (2005).

Index to Referenced Authors

Subject Index

About the author

Andrey S. Ostrovsky, born in 1944 in Russia, is at present a resident of Mexico. *Degrees*: M.Sc. in Electrical Engineering, Ph.D. in Technical Cybernetics, D.Sc. in Optics; all of them from the National Technical University of Ukraine. *Titles*: Professor of Technical Cybernetics at the National Technical Universirty of Ukraine, Elected Member of the National Academy of Engineering of Ukraine, National Researcher of Mexico. *Appointments*: Assistant Professor, Professor, Head of Optical Engineering Department, at the National Technical University of Ukraine, 1970–1993; Professor of Physics and Mathematics Department at the Autonomous University of Puebla, Mexico, 1994–present. *Scientific areas*: Fourier optics and optical data processing, statistical optics and coherence theory. *Publications*: More than 100 scientific and technical articles in professional journals and books, 12 patents of Russian Federation. *Tutorships*: 12 Ph.D. and 58 M.Sc. theses. *Memberships*: OSA, Optical Societies of Ukraine, Russia and Mexico.